Unlocking Flexibility in Electricity Distribution Networks

Saman Nikkhah

Supervisors: **Prof. Damian Giaouris**
Dr. Adib Allahham
Dr. Charalampos Patsios

School of Engineering
Newcastle University

A Thesis submitted for the award of the degree of
Doctor of Philosophy

April 2023

Abstract

Climate change is a global challenge which has affected the decision-making process in various sectors including energy systems. Different approaches have been proposed to decrease carbon emission in energy systems. A vital tool in the transformation of energy systems towards Net-Zero emission is flexibility. The literature suggests different ways in enabling flexibility in an energy system, such as demand, distributed energy resources (DER), and network flexibilities. This thesis investigates the role of flexibility in the energy networks through demand, DER, and network flexibilities.

In the first part of this thesis, demand flexibility is studied through disaggregating the demand response to the building as the source of providing flexibility. Due to the high percentage of demand consumption by dwellings (e.g. 36% in the UK), this thesis developed different approaches in unlocking building flexibility (BF). Firstly, a systematic literature review is performed to explore the challenges and opportunities in enabling BF. Then, in order to improve the robustness of existing control methods in face of uncertainty of input data (e.g. weather forecast), a robust rolling horizon method is introduced. Finally, novel building-to-building (B2B), and building-for-grid (B4G) strategies are developed along with optimal energy management of dwellings to optimise BF while considering energy bill and occupants' comfort as the objective functions simultaneously. This part also investigates the participation of electric vehicles in B2B and building energy management and their role in activating BF. The proposed controller was shown to decrease computational time by 76% compared to the conventional methods, with occupants comfort having a considerable effect on the robustness of controller (e.g. 1.3% decrease in occupants comfort increased the robustness in face of uncertainty by 10%). The electric vehicles participation in the energy management strategy decreased the energy bill by 44%.

The second part of this thesis studies the flexibility in distribution networks through network reconfiguration, conservation voltage reduction, and DER as the means of flexibility in the network, load, and DERs respectively. A risk- and security-constrained model predictive control is developed to improve the security of islanded microgrid considering mentioned flexibility measures. The computational efficiency of the proposed hierarchical control system in terms of accuracy and processing time is guaranteed through a mixed integer conic programming model. Then, the role of different flexibilities in the distribution level is studied for coordination of distribution networks with the transmission system. The use of conservation voltage reduction and network reconfiguration as the flexibility options decreased the emergency load curtailment in case of contingency by 3.8% and 19% respectively.

Acknowledgements

My gratitude first extends to my supervisors Prof. Damian Giaouris, Dr. Adib Allahham, and Dr. Haris Patsios for their guidance and support throughout my time at Newcastle, and for the freedom they gave me to pursue my interests. I would like to particularly thank Prof. Janusz Bialek and Prof. Sara Walker, who have helped me a lot to understand the quality of research. All of these people have put in many hours of work to help me develop as a researcher, and for that I am very grateful.

This work was made possible through funding from Newcastle University and Engineering and Physical Sciences Research Council grant EP/S016627/1: Active building Centre.

I am indebted to the many friends and colleagues who have supported me by providing feedback on my work, including Ilias, Matt, Arman, and Hamid. Particular thanks go to Dr. Mohammad Royapoor who has always been there and provided me with his support.

Special thanks to Malcolm Hill for his help and support during my studies, and for his heroic efforts in proofreading my works. I am grateful for my teachers and friends Dr. Abbas Rabiee and Alireza Soroudi who taught me the basics of research and the ethics of research world.

Finally, I am grateful for the love and support of my family. My parents Sharif and Khadijah have supported me in so many ways through all of my studies. Special thanks to love and support of my brothers, Soran, Saywan, and Mobin.

List of Publications

Within this doctorate program, the candidate has published the research works listed below.

Publications in international peer-reviewed journals

1. **Nikkhah S**, Allahham A, Royapoor M, Bialek JW, Giaouris D "Optimising Building-to-Building and Building-for-Grid Services Under Uncertainty: A Robust Rolling Horizon Approach," *IEEE Transactions on Smart Grid,* 2021. DOI: 10.1109/TSG.2021.3135570

2. **Nikkhah S**, Sarantakos I, Zografou-Barredo NM, Rabiee A, Allahham A, Giaouris D "A Joint Risk-and Security-Constrained Control Framework for Real-Time Energy Scheduling of Islanded Microgrids" *IEEE Transactions on Smart Grid,* 2022. DOI: 10.1109/TSG.2022.3171816

3. **Nikkhah S**, Allahham A, Bialek JW, Walker SL, Giaouris D, Papadopoulou S "Active Participation of Buildings in the Energy Networks: Dynamic/Operational Models and Control Challenges" *Energies,* 2021. DOI: 10.3390/en14217220

4. **Nikkhah S**, Rabiee A, Soroudi A, Allahham A, Taylor PC, Giaouris D "Distributed Flexibility to Maintain Security Margin through Decentralised TSO-DSO Coordination," *International Journal of Electrical Power & Energy Systems,*. DOI: 10.1016/j.ijepes.2022.108735

International peer-reviewed conference papers

1. **Nikkhah S**, Allahham A, Royapoor M, Bialek JW, Giaouris D "A Community-Based Building-to-Building Strategy for Multi-Objective Energy Management of Residential Microgrids," *International Renewable Engineering Conference (IEEE),* 2021. DOI: 210.1109/IREC51415.2021.9427816
2. **Nikkhah S**, Allahham A, Giaouris D, Bialek JW, Walker S "Application of Robust Receding Horizon controller for Real-Time Energy Management of Reconfigurable Islanded Microgrids," *IEEE Madrid PowerTech,* 2021. DOI: 10.1109/PowerTech46648.2021.9494926

Also, the following journal papers were under review as a result of this doctorate program at the time of submission:

1. **Nikkhah S**, Allahham A, Patsios H, Taylor PC, Walker SL, Giaouris D "Building-to-Building Energy Trading under the Influence of Occupant Comfort. Energy and Buildings," *International Journal of Electrical Power & Energy Systems* 2023.

Contents

Abbreviations

AB Active Building. 4

B2B Building-to-building. 49

B4G Building-for-grid. 49

BEIS Business, Energy and Industrial Strategy. 2

BEMS Building energy management system. 26

BES Battery energy storage. 5

CHP Combined heat and power. 22

CoBs Cluster of buildings. 23

COP Current operation point. 114

CVaR Conditional value at risk. 156

CVR Conservation voltage reduction. 104

DER Distributed energy resources. 3

DG Distributed generation. 5

DR Demand response. 3

DSO distribution system operator. 104

DU Dispatchable unit. 152

EV Electric vehicle. 25

FIMG Flexible islanded microgrid. 141

HVAC Heating ventilating and air conditioning. 22

MICP Mixed-integer conic programming. 149

MILP Mixed integer linear programming. 31

MINLP Mixed integer non-linear programming. 31

MPC Model Predictive Control. 37

OFGEM Office of Gas and Electricity Markets. 2

OPF Optimal power flow. 115

PV Photovoltaic. 5

RA Risk averse. 172

RES Renewable Energy Source. 2

RMG Residential microgrid. 49

RN Risk neutral. 172

RRH Robust rolling horizon. 53

RSC-MPC Risk- and security-constrained model predictive control. 141

SLP Security limit point. 114

TSO Transmission network operator. 104

WT Wind turbines. 152

Nomenclature

Indices

ψ	Index for voltage-dependent load model. $\psi \in \{$*residential, commercial, industrial*$\}$ load model.
b, m	Index of transmission or distribution system buses.
d	Index of parallel distribution feeders connected to a specific transmission bus.
i	Index of tasks
j	Index of buildings
o	Operation period of building appliances
t	Index of time periods

Sets

$\mathcal{B}_b$	Set of distribution network buses.
$\mathcal{B}_S$	Set of distribution network substations.
Ω_b	Set of transmission system buses.
Ω_b^m	Set of buses that are not connected to the upstream network
Ω_b^s	Set of buses connected to the upstream network

$\Omega_b^{f/c}$ Set of responsive/curtailable loads

$\Omega_{g/w/e}$ Set of DU/WT/BES installed buses

Ω_s Set of scenarios

Chapter 3

ψ_i Set of tasks

ψ_n Set of linearisation intervals

ψ_t Set of time periods

$\psi_{t_j}^{oc}$ Set of occupied periods of building j

ψ_j Set of buildings

Parameters

Chapter 3

$\hat{P}_{j,t}^{PV_F}$ Predicted photovoltaic unit output [kW]

$\hat{T}_t^{out}$ Predicted outdoor temperature [°C]

$\hat{V}_t^N$ Predicted outdoor illuminance level [lux]

$T_{j,t}^{Set}$ Temperature set point [°C]

$V_{j,t}^{Set}$ Illumination set point [lux]

β Tolerable value of robustness

Δt Duration of time periods [hour]

$\eta_I^{u/m}$ Utilization/maintenance factor of lightening devices

$\hat{\lambda}_t^{I/E}$ Predicted electricity import/export price[$£/kWh$]

κ_j Number of lightening devices in building j

A_j	Illuminated space in building j [m^2]
B	Total number of buildings
D_j^{th}	Thermal capacitance of building j [°C/kWh]
$E_{u/l}^{ESS}$	Maximum/minimum state of charge of energy storage [kWh]
f_j	Source flux value of building j
$P_{j,i,o}^{Ap}$	Power consumption of each task [kW]
P_u^G	Maximum power exchange rate with the main grid [kW]
$P_u^{ESS_{c/d}}$	Maximum charge/discharge rate of each building [kW]
R_j^{th}	Thermal reactance of building j [°C/kW]
T_j^{oc}	Total occupied periods of building j
$T_{j,t}^{B_{u/l}}$	Maximum/minimum temperature inside building j [°C]
$V_{j,t}^{B_{u/l}}$	Maximum/minimum Illuminance level [lux]
$\omega_{j,t}^{V/T}$	Visual/thermal weight factors
Chapter 4	
$\eta_{ev}^{C/D}$	Charging/discharging efficiency of EV battery
$\Delta D_{j,t}^{EV}$	Travel distance of EV
η_{ev}^{t}	Driving efficiency of EV
$E_j^{EV_{Max/min}}$	Maximum/minimum state of charge of EV
$P_j^{C/D_{ev}^{\max}}$	Maximum/minimum Charging/discharging power of EV
$P_{j,t}^{T_{ev}}$	EV Power consumption in transport vector
Chapter 5	

$(\alpha/\beta)^{\psi}_{b,d}$ The active/reactive exponent of load type ψ at Bus b of the d-th parallel distribution bus b.

$(\hat{P/Q})^{D}_{b}$ Active/reactive power demand in b-th bus of transmission system at SLP.

$(\overline{p/q})^{D}_{b,d}$ Initial active/reactive power demand of b-th bus in the d-th parallel distribution feeder.

$(g/b)_{bm,d}$ Conductance/susceptance of the line connecting buses b and m in the d-th parallel distribution feeder.

$(kp/kq)^{\psi}_{b,d}$ Active/reactive power share of load type ψ at Bus b of the d-th parallel distribution bus.

$(P/Q)^{D}_{b}$ Active/reactive power demand in b-th bus of transmission system at COP.

$(P/Q)^{G_{\max\,/\,\min}}_{b}$ Maximum/minimum limits of $(P/Q)^{G}_{b}$.

$(p/q)^{S_{\max\,/\,\min}}_{b,d}$ Maximum/minimum value of $(p/q)^{S}_{b,d}$.

$(p/q)^{LC,max}_{b}$ Maximum limit of $(p/q)^{LC}_{b}$.

$(Y/\phi)_{bm}$ Magnitude/angle of bm-th element of the transmission system's admittance matrix.

Λ^{D}_{b} Increment rate of the transmission system load.

Λ^{G}_{b} Increment rate of active power output of generation units.

λ_{des} Desired loading margin.

$\overline{v}_{b,d}$ Initial voltage magnitude of b-th bus in the d-th parallel distribution feeder.

$\pi^{dg}_{b,d}$ Available DG output.

$\pi_{b,d}^{(p/q)}$ Active/reactive power share of d-th parallel feeder connected to the transmission Bus b.

$i_{bm,d}^{\max}$ Maximum limit of $i_{bm,d}$.

N_b Total number of parallel distribution feeders connected to the b-th transmission bus.

$S_{bj}^{\max}$ Maximum limit of S_{bm}.

$V_b^{\max\,/\,\min}$ Maximum/minimum limits of V_b.

$v_{b,d}^{\max\,/\,\min}$ Maximum/minimum limits of $v_{b,d}$.

Chapter 6

$(G/B)_{bm}^{\ell/Sh}$ Series/Shunt conductance/susceptance of the line between buses b and m [pu]

$(P/Q)_{b,\max\,/min}^{G}$ Maximum/minimum active/reactive power capacity of DUs [kW]

β Weighting factor

$\chi_{b,t}^{G}$ Parameter indicating the on/off status of DUs

γ_t^m Energy price [$/kWh]

π_s^W The probability of falling to each wind scenario [%]

$\psi_{b,s}^{WT}$ Available wind power at each scenario

ρ CVaR confidence layer [%]

$I_{\max}^{\ell}$ Maximum current capacity of branch ℓ [pu]

L_i^{Cur} Value of loss load [$/kWh]

$P_{b,t,s}^{D_0}$ Base active load [kW]

P_R^{WT} Rated power of WTs [kW]

$R_b^{U/D}$ Ramp up/down limits of DUs [kW]

RT Repair time of distribution lines [hour]

$SOC_{\max/min}^{BES}$ Maximum minimum state of charge of BES [kWh]

$V_b^{\max/min}$ Maximum/minimum voltage magnitude [pu]

Δt Duration of time periods [hour]

Variables

Chapter 3

$(G/D)_t^{RMG}$ Total generation/demand capacity of RMG [kW]

$\alpha^{w/p}$ Weather related/market price robustness degree

$\chi_{j,i,t}^{Ap}$ Binary variable denoting the ON/OFF status of building appliances

$\chi_{j,t}^{G}$ Binary variable denoting the import/export power from main grid

$\chi_{j,t}^{ESS_{c/d}}$ Charging/discharging binary variables of energy storage

E_t^{ESS} State of charge of energy storage [kWh]

$H_{j,t}^{HP}$ Output power of heat pump for heating purpose [kW]

$P_{j,t}^{I}$ Power consumption rate of each lighting device in building j [kW]

$P_{j,t}^{B2B}$ Active power of building j at time period t under B2B strategy [kW]

$P_{j,t}^{B4G}$ Active power of building j at time period t under B2B strategy [kW]

$P_{j,t}^{buy/sell}$ Buying/selling power inside RMG [kW]

$P_{j,t}^{ESS_{c/d}}$ Charge/discharge power of each building from/to energy storage [kW]

$P_{j,t}^{PV/HP}$ Output power of photovoltaic/heat pump [kW]

$P_{j,t}^{G_{I/E}}$ Imported/exported power from/to main grid [kW]

$T_{j,t}^{B}$ Indoor temperature of building j [°C]

$V_{j,t}^{B}$ Illuminance level of building j [lux]

$V_{j,t}^{T}$ Total illuminance level of building j [lux]

Chapter 4

$B_{j,t}^{C/D_{ev}}$ Binary variables indicating the charge/discharge status of EV

$E_{j,t}^{EV}$ State of charge of EV

$P_{j,t}^{C/D_{ev}}$ Charging/discharging power of EV

Chapter 5

$(\hat{P/Q})_{b}^{G}$ Active/reactive power output of generation unit of Bus b at the SLP.

$(\hat{V/\theta})_{b}$ Voltage magnitude/angle of b-th bus of transmission system at the SLP.

$(P/Q)_{b}^{G}$ Active/reactive power output of generation unit of Bus b at the COP.

$(P/Q)_{b}^{LC}$ Active/reactive load curtailment at b-th transmission bus.

$(p/q)_{b,d}^{S}$ Active/reactive power injection at b-th bus of the d-th parallel distribution feeder.

$(p/q)_{b,d}^{dg}$ Active/reactive DG output.

$(p/q)_{bm,d}$ Active/reactive power flowing through the line connecting buses b and m in the d-th parallel distribution feeder.

$(p/q)_{b}^{LC}$ Active/reactive load curtailment in the b-th bus in the d-th parallel distribution feeder.

$(V/\theta)_{b}$ Voltage magnitude/angle of b-th bus of transmission system at the COP.

$(v/\theta)_{b,d}$ Voltage magnitude/angle of b-th bus in the d-th parallel distribution feeder.

$\chi_{bm,d}^{l}$ Binary variable indicating the on/off status of line l connecting buses b and m in the d-th parallel distribution feeder.

λ Loading margin of the transmission network.

$\tau_{bm,d}$ Tap level of the voltage regulator on the line between buses b and m in the d-th parallel distribution feeder.

$i_{bm,d}$ Current flowing through the line connecting buses b and m in the d-th parallel distribution feeder.

$S_{bm}/\hat{S}_{bm}$ Power flow between transmission buses b and j at COP/SLP.

Chapter 6

$(P/Q)_{b,t,s}^{D}$ Active/reactive load demand [kW/kVAr]

$(P/Q)_{b,t,s}^{G}$ Active/reactive power output of DUs [kW/kVAr]

$(P/Q)_{b,t,s}^{UN}$ Active/reactive power imported from upstream network [kW/kVAr]

$(P/Q)_{b,t,s}^{WT}$ Active/reactive power output of WTs [kW/kVAr]

$(P/Q)_{bm,t,s}^{\ell}$ Active/reactive power flow between buses b and m [kW/kVAr]

$(R/T)^{\ell}_{bm,t,s}$	Variables associated with the line between buses b and m in MICP model [pu]
$\alpha^{\ell}_{mb,t,s}$	Binary variable specifying the parent bus [=1 if bus b is the parent of bus m, =0 otherwise]
$\beta^{res}_{b,t,s}$	Degree of flexibility of responsive loads [%]
$\lambda^{Ch/DCh}_{b,t,s}$	Binary variables indicating the charge/discharge status of BES [0,1]
σ	Auxiliary variable indicating the value of CVaR [$]
$\theta_{bm,t,s}$	Voltage angle between buses b and m [pu]
φ_s	ExcBES of the cost in each scenario over expected cost [$]
$\vartheta^{\ell}_{bm,t,s}$	Binary variable representing the status of line between buses b and m [0-1]
$P^{Ch/DCh}_{b,t,s}$	Charge discharge power of BESs [kW]
$P^{C}_{b,t,s}$	Load curtailment [kW]
$SOC^{BES}_{b,t,s}$	State of charge of BES [kWh]
$U_{b,t,s}$	Variable associated with bus i in the MICP model [pu]
$U^{\ell}_{bm,t,s}$	Variable associated with the line between buses b and m in MICP model [pu]
$V_{b,t,s}$	Voltage magnitude of bus i [pu]

List of Figures

List of Tables

1

General Introduction

The topic of this thesis is broken down into answering the following research questions:

1. How to enable higher levels of building flexibility in the distribution networks?
2. To what extent flexibility can improve the electricity distribution network characteristics?

This chapter includes a general introduction to briefly cover the problem statement, motivation, and focus of the main topic. The main contributions of the thesis to knowledge is given in this chapter. Additionally, a short description of each chapter's content is included to provide a generic outlook of the thesis for the reader.

1.1 Motivation: Flexibility & Decarbonisation

The industrial revolution was a transition at which oil, gas, and coal were used to power vehicles, warm our houses and energise the economy. However, the catastrophic effects of climate change in recent decades is becoming a serious threat to our planet which requires rapid shift from fossil fuels to green energy resources. As for the energy grid, this means that we need to shift from coal-fired plants to renewable energy sources (RESs) such as wind power and hydrogen. Energy grids are also required to electricify their demand which brings about the necessity of electricifying the transport and heat sectors.

This transformation has been followed by the UK government in different world-leading plans. Shifting the RESs and electricifying the transport and heat sectors have been followed by grand-stand plans. The UK government plans include increasing the wind power generation to 40GW by 2030 [1], banning the sale of new petrol and diesel cars by 2030 [2], and increasing the number of heat pumps installed each year to 600,000 by 2028 [3]. The whole government plan is to achieve a Net-Zero economy by 2050.

These transitions, however, mean that an exponential amount of extra generation and demand (from electricifying heat and transport sector) will be added to the electricity system over the upcoming decades. The added generation will be mainly from variable energy sources, and dependent of different weather conditions. The variability of these energy resources is a challenging issue for system operators and planners. On the demand side, the Department for Business, Energy and Industrial Strategy (BEIS) white paper [1] indicates that the demand will be doubled by 2050. Therefore, the variability of RESs and the twofold increase in the demand together will be even more challenging.

All of these challenges require a solid plan which ensures the integration of new technologies into the system while making sure the supply and demand are balanced. The BEIS and Office of Gas and Electricity Markets (OFGEM) report on 2021 [4] introduced flexible energy networks as one of the main

solutions to aforementioned challenges. As directly indicated from this report [4]: *"a smart and flexible system is one which uses smart technologies to provide flexibility to the system, to balance supply and demand and manage constraints on the network"*. The flexibility can be enabled by different technologies of the network [4, 5]:

- Distributed energy resources (DER) flexibility: the DER flexibility can be provided by using the storage technologies along with RESs to store excess generation and discharged when needed.
- Demand flexibility: this type of flexibility is applied by shifting demand between peak hours and off-peak hours. The demand flexibility has been playing its part in the energy network as demand response (DR)[6] where the demand consumption pattern is changed based on the price signals.
- Grid flexibility: this type of flexibility can be provided by benefiting from topology of the network and the use of smart technologies.

The use of different flexibility methods in the energy grid can be a vital plan for decarbonisation. For example, by utilising the storage technologies to capture extra renewable generation, higher contribution from RESs can be added to the energy grid. On the demand side, demand flexibility can be pivotal by shifting the demand to the hours of high RES penetration. The mixed utilisation of these methods can increase the share of green generating and decrease the carbon footprint.

1.2 Objectives: Investigating Flexibility

Fig. 1.1 which is taken from Future Energy Scenarios [7] shows that around 60Gw of flexibility is provided by different sources in 2020. At the same time, the BEIS analysis indicates that flexibility can provide £10bn cost saving per year in 2050 [4]. These statistics altogether show the significance of flexibility in achieving the Net-Zero goals. Therefore, this thesis investigates flexibility in different technologies.

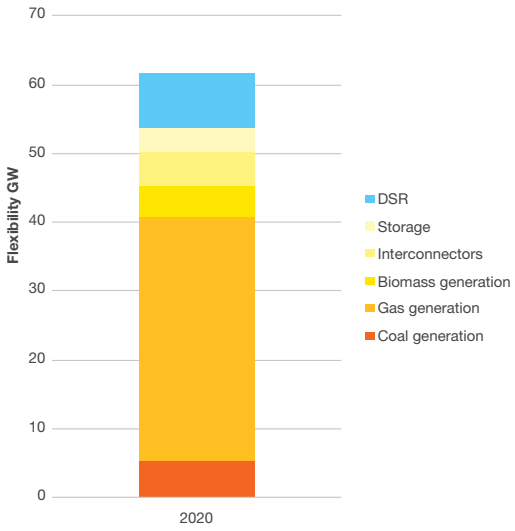

FIGURE 1.1: Flexibility provided by different sources in 2020 [7].

Although Fig. 1.1 shows a higher amount of flexibility provided in 2020, the share of demand response (or demand flexibility) is not considerable. Therefore, enabling higher levels of flexibility in the demand can be a critical step towards Net-Zero goals. To do so, this thesis disaggregates the demand flexibility to its source: buildings. As the end-users of the energy networks, buildings are responsible for 30% of the global energy consumption, excluding the construction industry, which consumes 6% of total energy [8]. At the same time, the proportion of carbon dioxide (CO_2) emission caused by the building sector is about 38% worldwide [8]. These statistics clearly indicate potential flexibility that can be enabled by active participation of buildings in the energy network. The flexibility in the buildings side can be enabled by adding small-scale generation [9] and/or controlling their demand [10].

The first part of this thesis investigates the challenges and opportunities in enabling flexibility in the buildings. Then, different approaches are developed for enabling flexibility in active buildings (ABs). ABs are defined as the dwelling units which benefit from renewable generation to supply their load, store the excess generation to meet their own needs, and are cooperating with the main grid intelligently by exchanging data and energy. This paradigm

shift enables integrated co-operation of buildings and the energy grid, and has multiple advantages [11]: 1) It can bring about lower energy bill for buildings, 2) the investment on the generation and transmission can be delayed, 3) grid resources can be used more efficiently, 4) grid operators can develop plans for the ancillary services that can be provided by buildings, and 5) in-site small-scale generation (e.g. photovoltaic (PV)) and storage (e.g. battery energy storage (BES)) units can be integrated into the grid more efficiently. The other levels of flexibility in the ABs can be unlocked by developing the energy transaction frameworks between dwellings.

The second part of this thesis investigates the flexibility in the DER and network topology. Distribution-level DERs can play a vital role in providing flexibility for the transmission network [12]. The DER flexibility is investigated in this thesis by designing control methods for microgrids with the DERs being the main sources of supply. These microgrids are supplied by different BES and distributed generation (DG) units. Another form of flexibiltiy is studied in this part by using the voltage regulators in the distribution level, as the demands are voltage-dependent. This scheme is widely known as conservation voltage reduction (CVR) [13]. The network flexibility studied by investigating the role of network reconfiguration, which has been used to improve different techno-economic characteristics of distribution grid separately [14]. The collaborative effect of DER, demand and network flexibility on improving the system security as an important characteristics of smart energy networks is studied in this part of the thesis.

1.3 Main Contributions of the Thesis

The key contributions to knowledge from this research are as follows:

Contribution 1 (Chapter2)

A systematic literature review is conducted which studies the challenges and opportunities for unlocking the building flexibility. This chapter introduces a

graphical method to analyse the citation network of research related to enabling flexibility in the ABs.

Results based on this contribution are published in the following paper:

- *Nikkhah S, Allahham A, Bialek JW, Walker SL, Giaouris D, Papadopoulou S. Active Participation of Buildings in the Energy Networks: Dynamic/Operational Models and Control Challenges. Energies. 2021 Nov* 2;14(21):7220.

Contribution 2 (Chapter3-I)

A multi-level mixed integer linear programming optimisation model is proposed for residential microgrids, with consideration for occupant comfort and appliance/task constraints. Compared to current mixed integer linear programming models, the proposed solution allows greater asset/building participation using a linear robust controller that does not require excessive processing power (as opposed to the mixed integer non-linear programming predecessors). It also pursues multiple goals in achieving an optimal energy management.

Results based on this contribution are published in the following papers:

- *Nikkhah S, Allahham A, Royapoor M, Bialek JW, Giaouris D. Optimising Building-to-Building and Building-for-Grid Services Under Uncertainty: A Robust Rolling Horizon Approach. IEEE Transactions on Smart Grid. 2021 Dec 15;13(2):1453-67.*
- *Nikkhah S, Allahham A, Royapoor M, Bialek JW, Giaouris D. A Community-Based Building-to-Building Strategy for Multi-Objective Energy Management of Residential Microgrids. In2021 12th International Renewable Engineering Conference (IREC) 2021 Apr 14 (pp. 1-6). IEEE.*

Contribution 3 (Chapter3-II)

Introducing a robust rolling horizon controller to maximise the robustness of real-time energy management systems against prediction uncertainties at a lower computational time (compared to conventional controllers) while accounting for partial knowledge of input parameters. The controller takes into account the effect of multiple sources of uncertainty on the local energy markets, while exploring the role of building occupants in improving residential microgrid robustness.

Results based on this contribution are published in the following paper:

- *Nikkhah S, Allahham A, Royapoor M, Bialek JW, Giaouris D. Optimising Building-to-Building and Building-for-Grid Services Under Uncertainty: A Robust Rolling Horizon Approach. IEEE Transactions on Smart Grid. 2021 Dec 15;13(2):1453-67.*

Contribution 4 (Chapter3-III)

Proposing building-to-building and building-for-grid strategies to oversee the peer-to-peer energy trading in residential microgrid level while valuing the occupants comfort, and appliance settings under an uncertain environment. The former strategy facilitates the power exchange between dwellings using flexibility in in-site generation capacity, while the latter deconstructs the demand-side response to its sources of sensitivity to alterations of comfort level and timing- ON/OFF status – or load adjustment of home appliances.

Results based on this contribution are published in the following paper:

- *Nikkhah S, Allahham A, Royapoor M, Bialek JW, Giaouris D. Optimising Building-to-Building and Building-for-Grid Services Under Uncertainty: A Robust Rolling Horizon Approach. IEEE Transactions on Smart Grid. 2021 Dec 15;13(2):1453-67.*

Contribution 5 (Chapter 4)

The effect of electrification of transport on the building flexibility will be

studied through adding corresponding electric vehicle model to the energy balance model.

Results based on this contribution are published in the following paper:

- *Nikkhah S, Allahham A, Giaouris D, Bialek JW, Walker S. Application of Robust Receding Horizon controller for Real-Time Energy Management of Reconfigurable Islanded Microgrids. In2021 IEEE Madrid PowerTech 2021 Jun 28 (pp. 1-6). IEEE.*
- *Nikkhah S, Allahham A, Royapoor M, Bialek JW, Giaouris D. A Community-Based Building-to-Building Strategy for Multi-Objective Energy Management of Residential Microgrids. In2021 12th International Renewable Engineering Conference (IREC) 2021 Apr 14 (pp. 1-6). IEEE.*

Contribution 6 (Chapter 5-I)

Distributed optimal conservation voltage reduction and network reconfiguration are adopted as the flexibility measures preserving the security of transmission and distribution systems' coordination with minimum physical load curtailment. In the upper level, the transmission system operator ensures the minimum loading margin for the transmission network considering the critical components of the power flow model. In the lower-level distributed optimisation models, distribution system operators aim at minimising the actual load curtailment, using the available flexibility options. Each distribution system operator provides a different level of flexibility in the proposed distributed framework. However, the total flexibility provided comply with the requirements of the transmission system operator.

Results based on this contribution are published in the following paper:

- *Nikkhah S, Rabiee A, Soroudi A, Allahham A, Taylor PC, Giaouris D. Distributed Flexibility to Maintain Security Margin through Decentralised TSO-DSO Coordination. International Journal of*

Electrical Power & Energy Systems, Volume 146, March 2023, 108735

Contribution 7 (Chapter 5-II)

A decentralised control framework is introduced for transmission and distribution systems' coordination with the least information exchange between them. In this method, distribution system operators use their available flexibility measures or/and load curtailment to comply with the requirements of the transmission system operator. The proposed method benefits from short computational time spans and achieves the required convergence degree with a small number of iterations. The transmission network's loadability constraint is considered as the main security margin influencing the transmission and distribution systems' coordination. This index can be utilised as a measure for evaluating the degree of security of transmission and distribution systems' coordination.

Results based on this contribution are published in the following paper:

- *Nikkhah S, Rabiee A, Soroudi A, Allahham A, Taylor PC, Giaouris D. Distributed Flexibility to Maintain Security Margin through Decentralised TSO-DSO Coordination. International Journal of Electrical Power & Energy Systems, Volume 146, March 2023, 108735*

Contribution 8 (Chapter 6-I)

Proposing a multi-layer mixed integer conic programming model for multi-objective energy scheduling of islanded microgrids. The introduced model is computationally efficient and can provide an accurate representation of the power flow model for inclusion in the risk and security constrained model predictive controller. Also, developing a min-max-min risk and security constrained model predictive controller framework which considers the uncertainty of predicted data and the risk associated with them. The DER and network flexibility are deployed in this controller to improve system

security. The introduced control model allows the inclusion of uncertainties in real-time energy scheduling of islanded microgrids while accounting for structural changes in the network topology.

Results based on this contribution are published in the following papers:

- *Nikkhah S, Sarantakos I, Zografou-Barredo NM, Rabiee A, Allahham A, Giaouris D. A Joint Risk and Security Constrained Control Framework for Real-Time Energy Scheduling of Islanded Microgrids. IEEE Transactions on Smart Grid. 2022 May 2.*
- *Nikkhah S, Allahham A, Giaouris D, Bialek JW, Walker S. Application of Robust Receding Horizon controller for Real-Time Energy Management of Reconfigurable Islanded Microgrids. In2021 IEEE Madrid PowerTech 2021 Jun 28 (pp. 1-6). IEEE.*

Contribution 9 (Chapter 6-II)

Building time-varying security constraints based on a mixed integer conic programming power flow model. The proposed framework takes into account the real-time disruptions which change over the grid zones. This framework allows the inclusion of more realistic contingency conditions.

Results based on this contribution are published in the following paper:

- *Nikkhah S, Sarantakos I, Zografou-Barredo NM, Rabiee A, Allahham A, Giaouris D. A Joint Risk and Security Constrained Control Framework for Real-Time Energy Scheduling of Islanded Microgrids. IEEE Transactions on Smart Grid. 2022 May 2.*

Contribution 10 (Chapter 6-III)

Developing a corrective real-time network reconfiguration model as the network flexibility option which improves system security, while guaranteeing the network radiality over uncertainty scenarios (i.e. stochastic network reconfiguration). This framework enables the system controller to change the

system configuration so as to prevent load curtailment caused by real-time contingency, while considering the uncertainty.

Results based on this contribution are published in the following papers:

- *Nikkhah S, Sarantakos I, Zografou-Barredo NM, Rabiee A, Allahham A, Giaouris D. A Joint Risk and Security Constrained Control Framework for Real-Time Energy Scheduling of Islanded Microgrids. IEEE Transactions on Smart Grid. 2022 May 2.*
- *Nikkhah S, Allahham A, Giaouris D, Bialek JW, Walker S. Application of Robust Receding Horizon controller for Real-Time Energy Management of Reconfigurable Islanded Microgrids. In2021 IEEE Madrid PowerTech 2021 Jun 28 (pp. 1-6). IEEE.*

1.4 Outline of the Thesis

Chapter 1

This chapter includes a general introduction to briefly cover the problem statement, motivation, and focus of the main topic. The main objectives defined at the beginning of the research as a roadmap are also listed. Additionally, a short description of each chapter's content is included to provide a generic outlook of the thesis for the reader.

Chapter 2

The aim of this chapter is to investigate the role of building flexibility in the energy networks. Accordingly, different research works have been explored to analyse the current issues of disaggregating the demand flexibility to the active buidlings, and the way that a single building or cluster of buildings communicate effectively either together or with the grid(s), focusing on the challenges that can be brought about by integration of such grids. A citation network overview is provided by Gepghi software and analysed using

"ForceAtlas2" and "Yifan Hu Proportional" algorithms so as to discuss and explore the future challenges in the area.

Chapter 3

This chapter attempts to propose a multi-level real-time energy management for a community of buildings, in order to investigate different flexibility measures in the dwellings. A rolling horizon based method is adopted to receive real-time weather and energy price data, while the robustness in each consecutive dispatch time interval is increased using the notion of information gap decision theory. The proposed residential microgrid controller exploits flexibility in AB loads (through interruptible loads and building inertia) and shared distributed energy resources to introduce building-to-building and building-for-grid strategies. The mid-market rate approach is adopted in the building community level to create a local pricing market. The proposed model is multi-level and multi-objective. While the latter makes a trade-off between energy bill and occupants comfort, the former can guarantee the preference/benefits of active buildings in the local energy market. The proposed architecture is an mixed integer linear programming model which can be solved by commercial solvers. The performance of the proposed controller is benchmarked against a conventional controller, and also tested under atypical operational characteristics such as COVID-19 related lock-down condition in 2020 which further highlighted the critical nature of modern power systems planning.

Chapter 4

This chapter attempts to adopt a mathematical model for the electric vehicles that is affected by the driving pattern. The effect of electrification of transport on the building flexibility will be studied through adding corresponding electric vehicle model to the energy balance model studied in Chapter 3. Furthermore, the effect of electric vehicles on the occupant comfort is studied. Finally, the model investigates the effect of electric vehicles on the building-to-building. Therefore, this chapter is the continuation of the previous chapter by adding the electric vehicles as a

mobile storage that can be effected by occupants decisions.

Chapter 5

This chapter investigates the practical flexibility options at the distribution level for preventing load curtailment in an emergency condition. A decentralised control architecture is proposed for optimising the critical components of the power flow model (i.e. active/reactive power, and voltage magnitude) in the interface between transmission and distribution networks. To ensure secure coordination, the proposed model considers the loading margin as the security measure. This measure should be satisfied under different circumstances. The transmission system operator optimises the system operation while preserving the system security. The desired values of power exchange and voltage level in the interface are sent to the distribution system operators. To respond to the required set-point given by the transmission system operator, the distributed distribution system operator optimisers try to benefit from available network flexibility options while respecting the integrity of their internal constraints. The first promising flexibility option is the use of voltage regulators in the distribution level, as the demands are voltage-dependent. The next network flexibility option is the reconfiguration of the distribution network, which has been used to improve different techno-economic characteristics of distribution grid separately. The solutions of distribution system operator optimisers are sent to the interface and compared with the requirement of transmission system operator. This process is repeated by optimisers until a degree of convergence is achieved. If the distribution system operators fail in satisfying the required boundary points, they would apply the load curtailment to preserve the security of the whole system. This paradigm highlights the role of distribution system operators in providing flexibility measures for preserving the transmission and distribution systems' coordination. This framework can converge with a small number of iterations and with a short computational time (only seconds), which enables it as a suitable practical transmission and distribution systems' coordination scheme for research and industry.

Chapter 6

This chapter proposes a tri-layer min-max-min joint risk and security constrained model predictive controller framework for real-time energy scheduling of islanded microgrids and different flexibility options under the influence of uncertainty and real-time time-varying contingency conditions. The control philosophy starts from first layer cost optimisation, which applies the preventive measures based on the predicted data. The preventive security measures in this layer are adopted through optimal pre-scheduling of DERs, and applying the demand flexibility program. The second layer aims at identifying the worst-case contingency conditions by maximising the load curtailment and the mismatch between the pre-scheduling energy procurement cost (i.e. first layer) and that of real-time (i.e. second layer). Convex time-varying security constraints are developed for the risk and security constrained model predictive controller in the second layer, which consider changeability in the location of disruptions over different zones of the islanded microgrids. Finally, in the third layer, the controller develops a convex real-time network reconfiguration as a corrective flexibility measure against the contingency conditions, while re-scheduling the islanded microgrids with a trade-off decision making (i.e. making compromise between energy procurement cost and risk of uncertainty in the predicted data). Note that solving the model without the first two layers results in an optimistic decision making which neglects contingency condition or risk of uncertainty. The proposed model benefits from a mixed integer conic programming which is computationally efficient in terms of accuracy and processing time. These developments allow the inclusion of risk and security measures in the real-time energy management of microgrids that have to operate in islanded mode.

Chapter 7

Lastly, this chapter covers the conclusions and summarises the achievements of this PhD research followed by suggested opportunities for continuation of this research as future work.

2

Background and Challenges

The following research question has been answered in this chapter:

What are the flexibility approaches in buildings for providing various grid services? Furthermore, what are the main challenges?

New advances in small-scale generation and consumption technologies has shifted conventional buildings' functionality towards energy-efficient active buildings (ABs). Such developments drew the attention of researchers all around the world, resulting in a variety of publications, including several review papers. However, a comprehensive literature survey, investigating the flexibility of ABs in the energy networks through analytical control and optimisation methods while addressing dynamic/operational modelling challenges, is missing. This chapter conducts a systematic literature review so as to analyse the concepts/factors enabling active participation of buildings (i.e. buidling flexibility) in the energy networks. To do so, a relatively large number of publications devoted to the subject are identified, introducing the taxonomy of control and optimisation methods for the ABs. Then, a study selection methodology is proposed to nominate potential literature that have investigated the role of ABs in the energy networks. The modelling

approaches in enabling flexible ABs are identified, while the potential challenges have been highlighted. Furthermore, the citation network of included papers is illustrated by Gephi software and analysed using "ForceAtlas2" and "Yifan Hu Proportional" algorithms so as to analyse the insights and possibilities for future developments. The survey results provide a clear answer to the research question around the potential flexibility that can be offered by ABs to the energy grids, and highlights possible prospective research plans, serving as a guide to research and industry.

Sections of this chapter have been published by the candidate as in the following journal paper:

Nikkhah S, Allahham A, Bialek JW, Walker SL, Giaouris D, Papadopoulou S. Active Participation of Buildings in the Energy Networks: Dynamic/Operational Models and Control Challenges. Energies. 2021 Nov 2;14(21):7220.

Chapter roadmap: Section 2.1 gives a short description of the chapter. Section 2.2 explains the research methodology. Section 2.3 presents the results. The citation network overview is provided and analysed in Section 2.4. Discussion and future challenges are given in Section 2.5. Finally, Section 2.6 concludes the study.

2.1 Introduction

The aim of this chapter is to investigate the role of AB flexibility in the energy networks. Accordingly, different research works have been explored to analyse the current issues of ABs, and the way that a single building or cluster of buildings communicate effectively either together or with the grid(s), focusing on the modelling challenges that can be brought about by unlocking the flexibility in the dwellings. A citation network overview is provided by Gepghi software and analysed using "ForceAtlas2" and "Yifan Hu Proportional" algorithms so as to discuss and explore the future challenges in the area. Generally, the main question that would be investigated in this chapter is:
What are the flexibility approaches in buildings for providing various grid services? Furthermore, what are the main challenges?

2.2 Review Methodology

In this chapter, a systematic review is carried out which mainly focuses on activating flexibility through control and optimisation of single/multiple ABs. Generally, a systematic literature review should aim at identifying, evaluating, and interpreting specific issue in a particular field of study [15]. Thus, this thesis focuses on controlling and optimising of the ABs operation and their energy/information exchange with the grid.

2.2.1 Search Strategy

The key-terms, related to the subject area and review question are used for searching available research in different databases. The following search terms have been used: "smart/active building/home", "flexibility","nanogrid", "energy service", "application for the network", "virtual power plant", "review", "prosumer", "sustainable/smart cities", "electricity/heat/cooling consumption", " emission", "operation", "optimisation and control", and

"energy management". It is noteworthy that the mentioned keywords are used in various combinations.

Furthermore, the methodology of [16], known as backward and forward search, is used in some cases; to further identify the papers which were recognised as high quality publications. Several related keywords are selected, and the search has been conducted based on them; then, the key-terms that have not resulted in more related materials are removed and search re-started with new terms.

2.2.2 Eligibility Criteria

Eligibility criteria are introduced in this thesis for selecting the final research works for inclusion in the review. Based on such criteria, a framework is suggested for study selection in the review, shown in Fig. 2.1. The first round enquiry results in selecting all available publications based on the search strategy. These studies are evaluated by three subsequent rounds, at which some articles are extracted due to the designed filters for each round. The extracting process starts from the second round, in which the general criteria are applied to total publications. At first, the language of all manuscripts is evaluated; then, in the next level, the extraction is continued by screening the title of research works. The third round screens the title and abstract of the papers, while in a more precise process, round four screens the whole text of the papers that are included in this stage. This process is followed step-by-step, until the fifth round at which the total included papers have been classified.

2.2.3 Classification and Research Analysis

For the classification process, different perspectives highlighted by the available research works have been investigated. Then, their concepts presented in various categories, while the possible pathways for prospective research have been indicated. Note that the classification criteria have been reviewed several times, and the included studies analysed in different categories. In-depth review is carried out to cover all required data, such as:

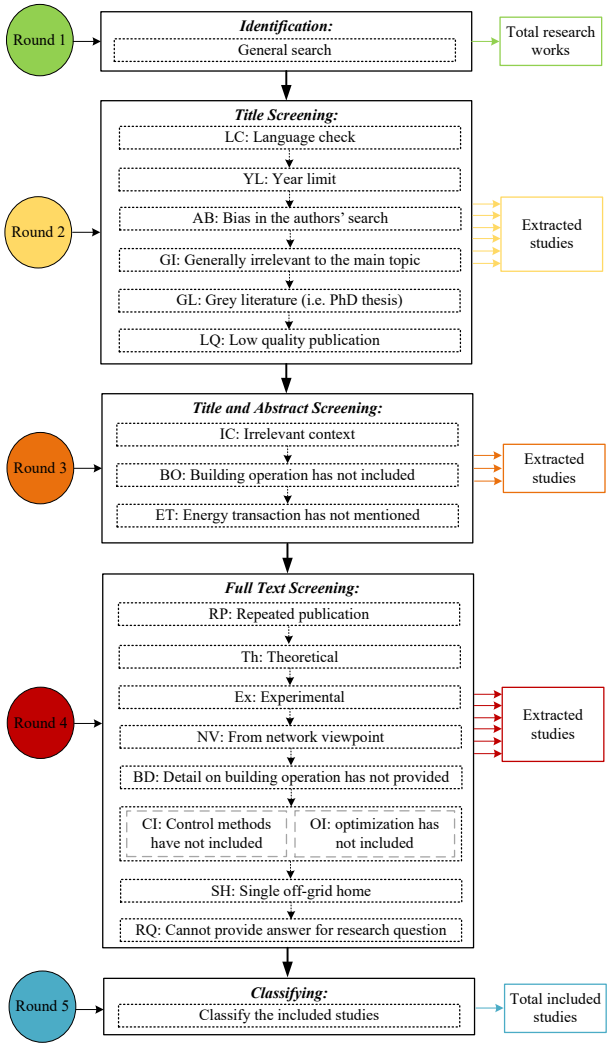

FIGURE 2.1: The proposed search and classification flowchart.

journal, year of publication, aims and objectives, model, test systems, solver, results, and references.

2.3 Results

The mentioned study selection criteria have been applied to all research works. 446 publications have been selected in the first enquiry, consisting of 325 journal papers, 10 books, 101 conference papers, and 10 grey literature.

The titles of all publications have been screened in the second round, resulting in the exclusion of 186 cases by different measures. The summary of the first and second review process is given in Table 2.1. The main factor for extracting such papers in the second level is the fourth criterion, in which the publications that were generally irrelevant to the main topic of the survey have been removed. It is worth mentioning that the main reason for applying the year limit is the recognition that the key developments have taken place in building technologies over the last decade. Consequently, the publications before the year 2010 have been removed in this step.

A total of 208 papers have been progressed to the third round, of which 81 papers were removed by screening their title and abstract. During the extraction process, 32 publications have been removed since they mainly focused on other concepts in the AB; 35 research works have been deleted since the operation of AB (either autonomous or grid-connected) was not evident in their study description; the energy conservation/consumption criterion is another filter for extraction of 14 publications. The summary of this level is given in Table 2.2.

The fourth round of the evaluation process was more critical since all parts of the papers have been analysed. To do so, the included papers in this level

TABLE 2.1: Summary of first and second rounds' study selection.

Publication	Round 1	Round 2						
	Selected	Included	Excluded					
			LC*	YL	AB	GI	GL	LQ
Journal paper	325	173	6	10	34	44	-	13
Conference paper	101	39	4	6	8	11	-	33
Book	10	3		1	1	5	-	
Grey literature	10	-	1				9	

* Detail of each abbreviation can be found in Fig. 2.1.

TABLE 2.2: Extracted papers in the third Round.

Publication	Included	Excluded		
		IC*	BO	ET
Journal paper	112	22	29	10
Conference paper	19	10	6	4
Book	3			

* Detail of each abbreviation can be found in Fig. 2.1.

have been evaluated by various conceptual measures. In the first criterion, the publications that were presented by the same authors and were similar in methodology have been removed. Then, the papers that were mainly focused on the theory of AB have been excluded, while the experimental papers have been removed since they fail to comply with the research question, and their authors mainly investigate the technical aspects. The research works that considered flexibility from a grid viewpoint have not been considered for the next level. Since the evaluation of building operation requires detailed information, those papers that have not provided enough detail on this issue have been removed. The control and optimisation criteria were another important factor. The papers that have not focused on the operation of an AB and its energy optimisation have been excluded in this level. In the final level of study extraction, the papers that marginally covered the research question have been removed.

Finally, in the fifth round, the included papers have been classified. 54 papers are included in the final round and processed from different viewpoints, based on the concept-based survey. The included papers are analysed in two dependent phases. In the first phase, the selected papers are analysed by various concepts, while the second phase of analysis presented a citation network so as to organise various concept-based clusters of the first phase and highlight the future investigation paths. In the following, a general overview of the selected papers is given; then, the main concept of flexibility is discussed based on the system structures and building assets enabling flexibility.

2.3.1 General Overview of Selected Articles

A wide range of terms have been utilised to distinguish the ABs from the conventional passive ones. For example, in [17], the term *"nanogrid"* has been used, while *"smart building"* and *"smart home"* are other popular terms that have been widely used separately [18, 19], or interchangeably [20]. 72% of selected papers either used *"smart building"* or *"smart home"*. In a different terminology, Borou *et al* [21] introduced the term *"domotic home"*, meaning *"automation of the various facilities of the house and the application of automation techniques for the comfort and security of its dwellers"*. The main keyword in the majority of these papers is the term *"smart"* which has been utilised with different building types such as *"commercial"* [22], and *"office"* [23].

Although the term *" smart"* is a suitable keyword for identifying the new buildings from the conventional ones, it cannot clearly show the role of buildings and can misinterpret the application. Therefore, this thesis utilises the term *"Active Building (AB)"* to highlight the role of buildings in the energy network, which means that they can actively exchange energy and information with the main grid.

2.3.2 System Structure and Flexibility Services

The overview of selected articles shows that two structures have been utilised to integrate AB flexibility into the grid. These structures are shown in Fig. 2.2. The first group (Fig. 2.2-(a)) mainly focused on the operation and energy management of the buildings. In this framework, different small-scale generation assets (e.g. photovoltaic (PV) and combined heat and power (CHP) units) are considered along with different controllable appliances (e.g. washing machine, and dishwasher) for the ABs, while they are able to send/receive energy and information to/from grid(s). The grid structure has been neglected in this type of architecture and the main focus is on the energy management of building(s). Also, the heating ventilating and air conditioning (HVAC) loads are mainly concerned with heat demand (without consideration

for temperature set points) in this group. This layout has been utilised by 81.5% (e.g. references [24–26]) of selected studies. This group will be referred as *"Building-Oriented Structure"* in the rest of this chapter. The second architecture (Fig. 2.2-(b)), which accounts for 18.5% of selected publications, has mainly focused on a grid that aggregates the different types of loads including AB loads. In the majority of articles in this category, an AB [27] or a cluster of buildings (CoBs) [19] has been connected to the distribution network. However, references [18] and [28] neglected the distribution network and connected the CoBs to the transmission system. The on-site capacity of ABs has been neglected, and the HVAC loads are the only controllable assets in this category. This group will be referred to as *"Grid-Tied Structure"*.

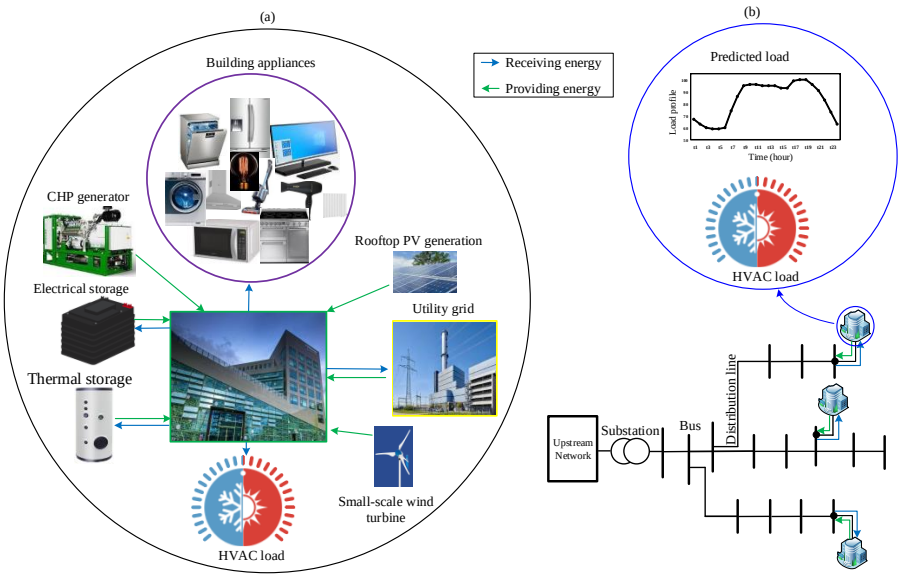

FIGURE 2.2: Different architectures in integration of ABs into the grid: a) building-oriented, and b) grid-tied structures.

In both structures, the main goal is to analyse different flexibility services that could be enabled by the ABs. Fig. 2.3 shows various flexibility services that could be provided for the grid by ABs based on the selected articles. As can be seen in this figure, in addition to the economic benefits for the ABs, these units can provide several services for the grid. The cost in this figure can be energy bill reduction or even generation and transmission investment cost in

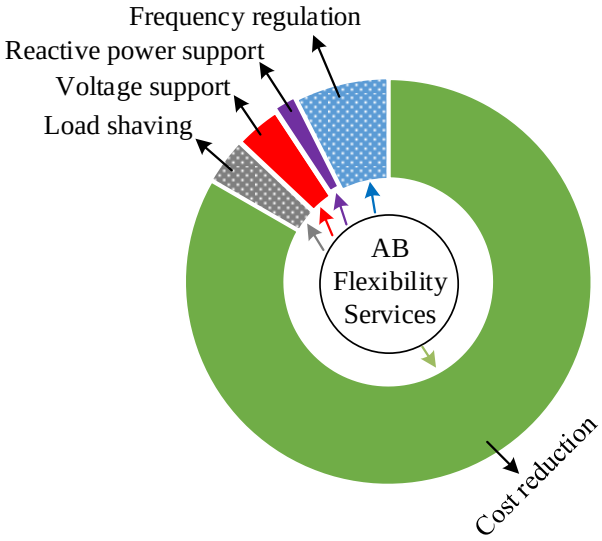

FIGURE 2.3: Various building flexibility services for the grid.

the grid side. This is the major point of flexibiltiy according to this figure, which has been investigated in the operational [29] and investment costs of the grid [11]. This major advantage of building flexibility is achieved by energy exchange between the grid and ABs. The other services have mainly focused on the technical characteristics of the grid such as frequency regulation and other ancillary services.

The building flexibility services can be divided into two groups: a) slow services, which are enabled through building thermal capacity and can affect the operational cost of the grid as a slow demand response (DR), and b) fast services, which can provide both technical and economical services for the

TABLE 2.3: Technologies in the AB.

Battery energy storage	[17, 20, 23, 25, 27, 30–57]
Thermal energy storage	[20, 21, 32, 36, 49, 54, 57–59]
Wind turbine	[20, 25, 26, 33, 41, 51, 53–55, 58, 60]
PV	[17, 20–23, 25–27, 30–51, 53–56, 58, 59, 61–64]
CHP	[20, 21, 29, 32, 36, 40, 44, 54, 56–58, 65]
Boiler	[20, 21, 23, 32, 36, 40, 54, 57, 61, 62, 65]
Controllable loads	[18–21, 23–51, 53–59, 61–70]

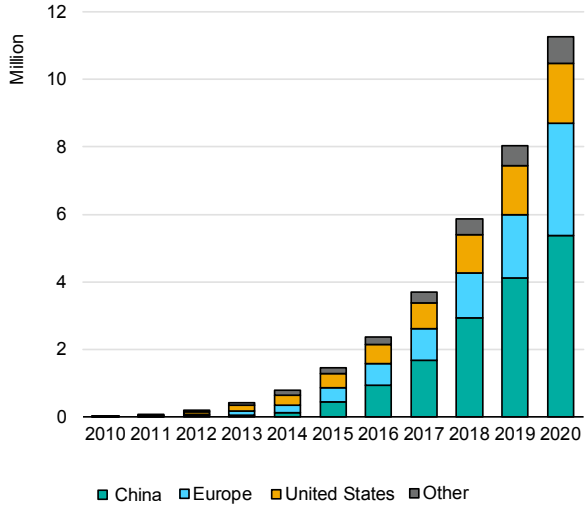

FIGURE 2.4: Worldwide EV investment [71].

grid. Enabling the flexibility in the latter group can be done through controlling various AB assets. Table 2.3 summarises the main technologies that have been utilised to actualise flexibility in the ABs. The internal AB components are mainly supervised by a controller that optimises the energy transaction based on the available data transfer. According to Table 2.3, the means of flexibility based on the technology is mainly enabled through controlling demand, especially those which have considered large-scale integration of ABs into the grid. This table also shows the importance of storage devices in enabling different types of flexibility. However, the potential of on-site generation capacity of ABs cannot be neglected. They can provide more flexibility and postpone the need for new generation investments [11].

Similarly, electric vehicles (EVs) can be a proactive player in the control and optimisation of buildings, as the consumer or even as the service provider for the building or grid. According to the recent global EV outlook (see Fig. 2.4), a significant increase in the number of EVs is observed over a year, passing 10 million in 2020, an increase of 41% from the previous year regardless of the pandemic issues [71]. In 2018, total electricity consumption of EVs was 58 terawatt-hours, worldwide, which is similar to the total electricity demand

of Switzerland in 2017 [72]. Furthermore, EVs can also provide energy for the network, with their discharging properties, enabling them to be a service provider in a small scale, say as a microgrid, consisting of smart home or a community of buildings. This characteristics of the EVs along with other available smart technologies, existing in ABs, enable the concept of flexibility for the building energy management system (BEMS) [30]. This characteristics will be highlighted in Section 4.1.

2.3.3 Dynamic Modelling Approaches for Flexible ABs

Based on their structure, the flexibility in ABs is investigated by two different approaches. In the building-oriented structures (i.e. Fig. 2.2-(a)), the main focus is on the controlling of different assets and tasks. The grid-tied structures (i.e. Fig. 2.2-(b)), however, focused on AB behaviour in the grid. According to [27], three modelling approaches can be utilised for investigating the AB behaviour, namely, data-driven models, high fidelity physical formulation, and thermodynamic models. While the first group provides good operation data, they fail in giving accurate results outside the trained set. Also, the size and complexity of physical models is a stumbling block, regardless of their accuracy, especially in real-time methods, which require reliable and frequent processing of the model in a short period of time. Therefore, the thermodynamic models enjoy a considerable popularity among the literature thanks to their simplified performance and accurate evaluation of system states. This section discusses the system dynamics, operation mode, and control variables which are three important concepts that define the flexibility of ABs in the modelling approaches.

2.3.3.1 System Dynamics

In order to analyse the integration of ABs into the energy grids, it is of utmost importance to build a dynamic model for both sides. The model should cover vital perspectives of energy transactions, with consideration for important constraints that limit such interactive energy scheduling. Such mathematical models are mainly assembled around one or a set of objective

functions. The outcome of this optimisation problem defines the decision variables that control the system elements. As aforementioned, the modelling approaches of flexible ABs can be discussed based on their structure. The building-oriented models (i.e. Fig. 2.2-(a)) mainly focus on the operational characteristics, while grid-tied models (i.e. Fig. 2.2-(b)) are concerning AB and the grid dynamics simultaneously.

The building-oriented operational models mainly proposed an optimisation problem that considered flexibility in the AB tasks (depending on the type of building) and small-scale generation units such as roof-top PVs. In the selected papers (e.g. [20, 31]), the AB demand and generation has been modelled as follows:

$$\sum_{t} \chi_{i,t}^{Ap} P_{i,t}^{Ap} = \sum_{o} P_{i,o}^{Ap} \tag{2.1}$$

$$\sum_{i} \chi_{i,t}^{Ap} P_{i,t}^{Ap} = P_{t}^{AB} \tag{2.2}$$

$$0 \leq P_{t}^{Gen} \leq P_{t}^{G_{\max}} \tag{2.3}$$

where constraint (2.1) is mainly used for controlling the AB tasks based on their operation (i.e. cooking, washing, heating etc). By optimally controlling the on/off status of each building appliance (i.e. $\chi_{i,t}^{Ap}$) at time period t, the controller can create flexibility in each AB's load. The optimal load of each AB (i.e. P_{t}^{AB}) can be obtained in (2.2) based on the consumption power of each building appliance (i.e. $P_{i,t}^{Ap}$). Constraint (2.3) shows the capacity limits of AB-installed generation units. As aforementioned, flexibility in the AB side is defined by controlling the generation and load of each building. This flexibility can be provided by introducing load balance in each building, defined by [57]:

$$P_{t}^{AB} = P_{t}^{Gen} + P_{t}^{import} - P_{t}^{Export} \tag{2.4}$$

where the variables P_t^{import} and P_t^{export} respectively show the imported and exported power from/to the utility grid at time period t. The interaction between different forms of energy, such as heating and electricity, can be applied through consideration of technologies such as heat pumps that convert energy from one form (electricity) to another (heat) [44]. Note that in the selected papers, the electrical sector plays the main part in control and optimisation, as electricity can be converted to other forms of energy for supplying demand and creating flexibility in all energy sectors. Generally, the imported and exported power are the main control variables that enable flexibility from the ABs. These control actions are mainly applied through definition of a binary variable (e.g. χ_t^{Grid}) as follows [54]:

$$P_t^{import} \leq P_{Max}^{Grid} \times \chi_t^{Grid} \tag{2.5}$$

$$P_t^{Export} \leq P_{Max}^{Grid} \times (1 - \chi_t^{Grid}) \tag{2.6}$$

However, it has been shown in [19] that neglecting the energy grid constraints in building-oriented operational models can create critical challenges for the energy grids, such as affecting the voltage profile of distribution networks. This problem has been addressed in the building-integrated dynamic models by considering the grid constraints through optimal power flow method [29]. The grid dynamics are mainly modelled as follows:

$$\sum_{nm} P_{nm,t}^f - \sum_{nm} \left(P_{mn,t}^f + R_{nm} I_{nm,t}^2 \right) = P_t^{AB} + P_t^L \tag{2.7}$$

$$\sum_{nm} Q_{nm,t}^f - \sum_{nm} \left(Q_{mn,t}^f + X_{nm} I_{nm,t}^2 \right) = P_t^{AB} \sqrt{\frac{1}{fp^2} - 1} + Q_t^L \tag{2.8}$$

where $P_{mn,t}^f$ and $Q_{mn,t}^f$ are active and reactive power flow at time period t through the grid feeder connecting the n, and m buses. The energy system load

consists of the building demand (i.e. P_t^{AB}) and the feeder demand (i.e. P_t^L). These constraints are supported by other physical and operational limits of the electricity grid such as voltage and feeder limits. Consideration of reactive power in this form of optimisation is another positive aspect in relation to the scope of work undertaken in the literature. The non-linear nature of these equations, however, can create computational challenge. In this regards, the majority of selected studies have scarified the accuracy by simplifying the model [28, 29]. The important grid constraints, such as voltage profile of electricity grid, has been neglected in some papers [18].

In the building-integrated dynamic models, $P_t^{AB} = P_t^{HVAC} + P_t^{fix}$ represents the active power consumption of ABs, consisting of the fixed load of each building P_t^{fix} and the power consumed by HVAC units P_t^{HVAC}. The latter is mainly obtained based on the thermodynamics of the ABs, which is basically modelled by a resistance and capacitance network as follows [27, 28, 36]:

$$T_{t+1}^B = T_t^B + \frac{\Delta t}{R^{th} D^{th}} \left(\hat{T}_t^{out} - T_t^B \right) + \frac{\Delta t}{D^{th}} H_t^{th} \tag{2.9}$$

where, in (3.4), the thermal load can be modelled as $H_t^{th} = COP \times P_t^{HVAC}$, in which COP is the coefficient of performance of HVAC systems. R^{th} (in $^\circ C/kW$) and D^{th} (in $^\circ C/kWh$) respectively represent the thermal reactance and capacitance of of ABs. These parameters are defined for each individual building based on the thermal resistance and capacitance of rooms, walls,and windows [18].

In order to summarise the important characteristics of mathematical models, Table 2.4 is provided, which gives a taxonomy of selected articles based on the properties of their mathematical models, including objective function, constraints, model type, and solvers. The main observations are:

(i) It is a well-known fact that customers are concerned about their bills and the economic perspectives of their controller. Accordingly, 100% of the papers considered cost/profit-based objective functions for their model. In the majority of research works, economic aspects of the

energy exchange, which includes the cost of energy imported from the main grid and the income from selling energy back to grid, has been taken into account as the main part of any cost minimisation function, highlighting the key-role of optimised energy transaction with the grid, and re-emphasising the concept of ABs as the active players of energy optimisation.

(ii) Based on Table 2.4, whether considering or not considering the grid constraints is an important denominator of the models. Meanwhile, the similarity in both types of optimisation problems (i.e. those which consider the gird constraints and those which do not account for grid constraints) is the flexibility that can be activated in the ABs through the optimal control of their assets. This flexibility has been reflected in the variable that defines the exported power to the main grid. In addition to the exported power to the main grid, however, new load control mechanisms can be applied to the ABs. For instance, the consumption pattern of AB appliances (i.e. $P_{i,t}^{Ap}$ in Eq. (2.1)) can be considered as a variable rather than a parameter. Considering it as a variable allows the controller to adjust the building load based on desired control objectives. This can add more flexibility to the AB loads in addition to the shifting mechanism that is controlled by on/off status of each task. Meanwhile, interaction among the ABs needs more investigation (See Section 3.1). This idea can be adopted based on the concept of peer to peer energy markets [73]. However, the occupants' preferences should not be neglected in such a paradigm. Thus, the control models should be modified to make trade-off between cost and occupants' comfort (See Section 3.1).

(iii) Only a small proportion of the papers considered other objective functions rather than the operational cost, such as occupants' comfort or/and environmental aspects (See Section 3.1). In [64], the authors have integrated different goals in the formulation of one objective function, and the problem has been solved as a single-objective optimisation. In some cases [25], focusing on the comfort level, the economic factors in the objective function are considered for the energy transaction between building and grid, which limits the energy exchange

based on the comfort level. Despite the importance of the economic targets, there is a need to consider other aspects in the objective function(s) and solve the model as a multi-objective optimisation. Of the selected papers, only 18.5% of them have solved the models as a multi-objective; almost all have used the weighted sum method [74] for handling the problem as a multi-objective. However, the weighted sum method cannot sufficiently handle non-convex optimisation problems [75].

(iv) The majority of articles focusing on the operation of ABs have proposed a mixed integer linear programming (MILP) model, which is a common practice for control and optimisation purposes in the building sector [76, 77]. This kind of optimisation model can be solved by commercial solvers, like CPLEX. Meanwhile, 42.5% of the papers proposed mixed integer non-linear programming (MINLP) models. It is generally a difficult task to obtain a global optimal solution from such typically NP-hard problems. The types of solvers that have been used for each optimisation problem is given in Table 2.4, which have been applied using GAMS, MATLAB, Python, Julia, and EnergyPlus software packages.

TABLE 2.4: Mathematical model characteristics of selected articles.

Objective function	Reference number																	
	[54]	[30]	[17]	[18]	[19]	[20]	[21]	[22]	[23]	[24]	[25]	[26]	[27]	[28]	[29]	[31]	[32]	[33]
Economical	✓	✓	✓	✓	✓	✓	✓	✓	✓	✓	✓	✓	✓	✓	✓	✓	✓	✓
Operational					✓													
Comfort										✓								
Environmental	✓																	
Grid constraints				✓	✓					✓			✓	✓	✓			
Building constraints	✓	✓	✓	✓	✓	✓	✓	✓	✓	✓	✓	✓	✓	✓	✓	✓	✓	✓
Model type	MILP	MILP	MILP	MILP	MINLP	MILP	MILP	MINLP	MILP	MINLP	MINLP	MILP	MILP	MILP	MILP	MINLP	MILP	MINLP
Solver	CPLEX	CPLEX	CPLEX	CPLEX	YALMIP	CPLEX	X-Press	GA[I]	CPLEX	PSO[II]	PSO	CPLEX	CPLEX	CPLEX	CPLEX	NAA[III]	YALMIP	GA
Objective function	Reference number																	
	[34]	[35]	[36]	[37]	[38]	[39]	[40]	[41]	[42]	[43]	[44]	[45]	[46]	[47]	[48]	[49]	[50]	[51]
Economical	✓	✓	✓	✓	✓	✓	✓	✓	✓	✓	✓	✓	✓	✓	✓	✓	✓	✓
Operational																		
Comfort					✓													✓
Environmental							✓									✓		
Grid constraints		✓																
Building constraints	✓	✓	✓	✓	✓	✓	✓	✓	✓	✓	✓	✓	✓	✓	✓	✓	✓	✓
Model type	MILP	MINLP	MINLP	MINLP	MILP	MINLP	MINLP	MILP	MINLP	MINLP	MILP	MINLP	MILP	MILP	MILP	MILP	MILP	MILP
Solver	YALMIP	EP[IV]	LO-M[V]	IPM[VI]	CPLEX	M-S[VII]	SQP	GUROBI	M-S	PSO	CPLEX	M-T [VIII]	GUROBI	CPLEX	CPLEX	CVX	CPLEX	YALMIP
Objective function	Reference number																	
	[52]	[53]	[55]	[56]	[57]	[58]	[59]	[60]	[61]	[62]	[63]	[64]	[65]	[66]	[67]	[68]	[69]	[70]
Economical	✓	✓	✓	✓	✓	✓	✓	✓	✓	✓	✓	✓	✓	✓	✓	✓	✓	✓
Operational																		
Comfort				✓		✓						✓						✓
Environmental													✓					
Grid constraints	✓																	
Building constraints	✓	✓	✓	✓	✓	✓	✓	✓	✓	✓	✓	✓	✓	✓	✓	✓	✓	✓
Model type	MINLP	MILP	MINLP	MINLP	MILP	MILP	MILP	MILP	MILP	MINLP	MILP	MINLP	MILP	MINLP	MILP	LP	MINLP	MINLP
Solver	GA	CPLEX	M-S	GA	CPLEX	GUROBI	GUROBI	CPLEX	SCIP	M-S	CPLEX	CSA[IX]	CPLEX	CSA[XII]	CVX	PATH	M-S	M-S

I: Genetic algorithm, II: particle swarm optimisation, III: natural aggregation algorithm, IV: EnergyPLus, V: Lyapanov optimisation-MATLAB, VI: Interior point method, VII: MATLAB-SIMULINK, VIII MATLAB-TOMLAB, IX: Competitive swarm optimisation.

2.3.3.2 Operation mode

As previously stated, the energy and data transaction with the main grid is the most important feature of AB flexibility. Accordingly, their flexibility is mainly defined based on their connection with the grid. The summary of operation mode (off-grid, grid connected) and the involvement of multi-energy carriers in the selected papers is given in Table 2.5. This table clearly shows that all available works studied the operation mode as grid connected. Although the off-grid characteristic could be a significant feature for buildings, it has not been considered in the literature to any depth. This option can add more resilience characteristics to the ABs. Being able to operate in off-grid mode is regarded as an important characteristic of well-managed ABs [17]. It has been shown in [26] that the building can benefit from the available installed wind and solar capacity efficiently in both on- and off-grid modes, and it has been shown that the majority of building load is supplied by RESs in both situations. In [46], an economic analysis is performed to show the effect of electricity tariffs on the decision of the home owner to stay connected with the grid or operate in off-grid mode.

As shown in Table 2.5, another important characteristic of ABs is their capability to deal with various energy carriers. Despite the importance of the multi-carrier energy concept [78], in a wide range of papers, there is no evidence of dealing with other forms of energy except for electricity. The majority of those articles which have investigated different forms of energy, belong to the first architecture of integration, which has been shown in Fig. 2.2-(a). However, those which have concerned the grid dynamics mainly focused on the electric networks and neglected the potential of other energy systems in enabling more flexibility. It has been shown in Reference [29] that more flexibility can be provided by ABs through coupling the heating and electricity systems.

2.3.3.3 Control Variables

In both types of building-oriented operational and grid-tied dynamic models, providing the flexibility is actualised based on the decision variables that are

TABLE 2.5: Operation modes and energy carrying in included papers.

Ref	Operation mode		Energy carrying		Ref	Operation mode		Energy carrying	
	off-grid	on-grid	multiple	single		off-grid	on-grid	multiple	single
[54]		✓	✓		[43]		✓		✓
[30]		✓		✓	[44]		✓	✓	
[17]	✓	✓		✓	[45]		✓		✓
[18]		✓		✓	[46]	✓	✓		✓
[19]		✓		✓	[47]		✓		✓
[20]		✓	✓		[48]		✓		✓
[21]		✓	✓		[49]		✓	✓	
[22]		✓		✓	[50]		✓		✓
[23]		✓		✓	[51]		✓	✓	
[24]		✓		✓	[52]		✓		✓
[25]		✓		✓	[53]		✓		✓
[26]	✓	✓		✓	[55]		✓		✓
[27]		✓		✓	[56]		✓		✓
[28]		✓		✓	[57]		✓	✓	
[29]		✓		✓	[58]		✓	✓	
[31]		✓		✓	[59]		✓		✓
[32]		✓	✓		[60]		✓		✓
[33]		✓		✓	[61]		✓	✓	
[34]		✓		✓	[62]		✓	✓	
[35]		✓		✓	[63]		✓		✓
[36]		✓	✓		[64]		✓		✓
[37]		✓	✓		[65]		✓	✓	
[38]		✓		✓	[66]		✓		✓
[39]		✓		✓	[67]		✓	✓	
[40]		✓		✓	[68]		✓		✓
[41]		✓	✓		[69]		✓		✓
[42]		✓		✓	[70]		✓		✓

sent by the controller to the ABs or CoBs. The share of various control variables in enabling energy exchange with the main grid is shown in Fig. 2.5. This figure clearly shows that controlling the energy interaction between the grid and ABs accounts for 100% of the selected papers, putting emphasise on the significance of the flow of energy between the main grid and buildings. Note that the double-headed arrows demonstrate the energy exchange with the grid, based on the control signals. It is evident from Fig. 2.5 that the main control signal in enabling flexibility is general load control, accounting for 90.7% of selected articles. With 74% of share, the second in this list is energy storage, which can enable energy transaction with the grid through charge and discharge mechanism. However, a lower percentage (e.g. 31%) of the articles focused on enabling flexibility through home appliances. Besides, despite the importance of on-site generation units in enabling flexibility, this group accounts for the lowest proportions of interests among the selected studies, with 11.1%.

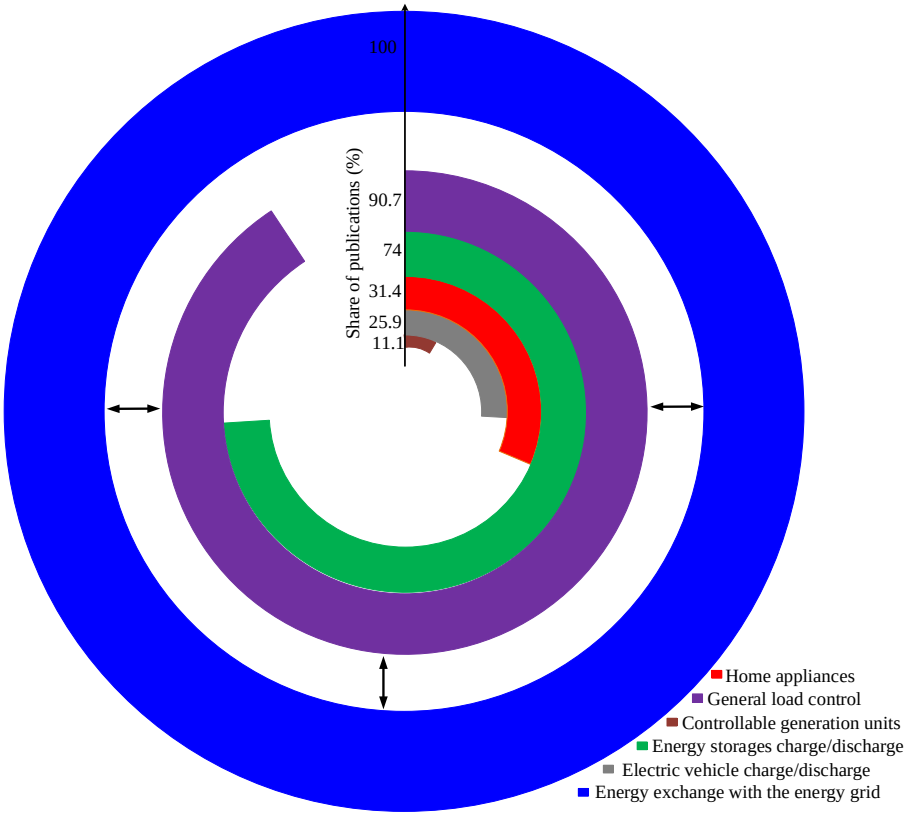

FIGURE 2.5: Share of differnet control variables in enabling flexibility.

2.3.4 Flexibility Challenges

Energy systems have been enjoying a centralised control mechanism for a long period of time. Enabling the flexibility in the ABs requires the decentralisation of control architectures. Decentralising the control mechanisms and embedding control systems in the conventionally passive buildings can not be an easy task and brings about several challenges. Regardless of technical and operational challenges, three important issues should be considered precisely. The first challenge is how to integrate millions of buildings into the energy systems. Designing a control mechanism that can handle the time-scale discrepancy is the second issue, while the variability of input data which are under the influence of external factors is the third in the list. This section discusses these

three issues, and investigates the main approaches in the selected articles for dealing with them.

2.3.4.1 Scalability of integration

Despite the importance of data-driven methods in predicting the building load demand [79], it is of utmost importance to investigate the dynamics of building integration to the grid through a precise analytical method rather than a prediction method. To do so, a critical question arises here, which is how to achieve an optimal control decision for a relatively large number of ABs?

Table 2.6 shows the proportion of various number of ABs in the case study of selected articles. As can be seen in this figure, the majority of articles focused on a small number of ABs and tried to investigate the concept of flexibility. Different types of load and generation control techniques are evident in these papers [22, 23]. However, it has been shown in [80] that increasing the number of ABs affects the quantified participation of buildings in the grid. In Table 2.6 the papers that have concerned the large-number integration models are mainly grouped as the building-tied structures (i.e. Fig. 2.2-(b)). Some of the articles benefited from data driven methods for their integration [41, 43, 46], and focused on the exploring of different scenarios of flexibility that could be provided by ABs. The other group [29] utilised the thermodynamic models for large-scale integration. They have simplified their model in two ways so as to achieve acceptable computational efficiency. Firstly, they have simplified the dynamics of the grid, which brought about neglecting important measures such as voltage profile of electricity grid [18, 28]. On the AB side, as shown in Fig. 2.2-(b), they have only focused on the thermal loads and considered other building loads as a constant parameter. The thermal loads are modelled with thermodynamic load model given in Equation (3.4). Those which have considered the other characteristics of ABs have mainly focused on a small proportion of properties [19, 27].

TABLE 2.6: The number of ABs in the integration models of selected articles.

Number of ABs	Popularity (%)
1	50
$1-9$	22.3
$10-99$	16.7
$100-999$	4
≥ 1000	7

2.3.4.2 Time-scale discrepancy

The issue of time-scale discrepancy is another major challenge in activating the building flexibility. In order to tackle this issue, the existing literature suggested the utilisation of hierarchical control methodologies, and benefiting from the real-time control algorithms. Through this method, the time-steps of energy grid are resided in those of ABs through real-time energy management techniques [28]. The popularity of real-time and day-ahead techniques among the selected studies is illustrated in Fig. 2.6. Despite the importance of time-scale discrepancy, this figure shows lower interest among the selected literature for solving the integration problems as a real-time optimisation. Nonetheless, this issue can clearly affect the results of energy management strategies, as it has been demonstrated in [27], by solving the energy management strategy with and without real-time simulation. Therefore, it is of utmost importance to concern the time-scale discrepancy in the integration models and benefit from a real-time control approach.

Fig. 2.6 also shows the share of different control algorithms is dealing with the real-time optimisation problems. Among the selected studies which have concerned the real-time controlling, the look-ahead algorithms, which mainly operate based on the idea of the model predictive controller (MPC) [47, 60], are enjoying considerable popularity. Another efficient approach to deal with time-scale discrepancy is to proceed an online dynamic simulation, which has been utilised in several articles [42, 62, 66], as shown in Fig. 2.6.

Regardless of the efficiency of the real-time control approaches, there are several important issues that should be taken into account. Firstly, these approaches

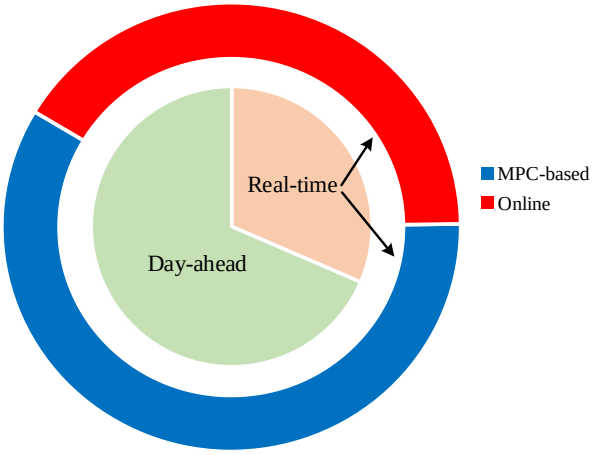

FIGURE 2.6: Popularity of different control mechanisms among the selected studies.

should be able to deal with large-scale integration of ABs. The importance of this issue has been explained in the preceding section. Secondly, increasing the simulation resolution (i.e. decreasing the time-scale to seconds) increases the computational time exponentially, especially for large-scale problems. This can demand powerful processing and creates substantial challenge for control designs (See Section 3.1). The data-driven methods can be utilised to tackle this challenge. Finally, the input data is the last but not the least in the potential challenges of the control systems. The real-time data transfer between different parts requires the involvement of the concept of internet of things [81] in this process. Besides, the uncertainty in the prediction of future data for processing look-ahead control signals creates substantial challenges (See Section 3.1) . The influence of uncertainty on the flexibility will be explained in the next section.

2.3.4.3 Uncertainty of input data

Similar to any other analytical methods, the control and optimisation methods that are suggested for the AB flexibility require data handling. Regardless of control mechanism (i.e. real-time or day-ahead), the acquisition of data into the simulation is another challenge for enabling grid-aware buildings. Although the data-driven methods, which mainly operate based on

machine learning approaches [82], have been proven as an efficient approach, the issue of uncertainty in the prediction cannot be ignored. In the selected literature, different sources of uncertainty such as renewable energy resources [17, 30], market price [20, 50], and system demand [23, 63] have been taken into consideration. As shown in [22], however, there is some possibility of violation between actual and real-time input data, even for real-time methods. These algorithms are less capable of predicting sudden changes in generator output, and therefore, can have possible prediction errors. The issue of uncertainty can influence the flexibility of ABs, which is the main target of this thesis. To show the significance of uncertainty in control and optimisation of ABs, the main results obtained from uncertainty management in the selected papers are summarised in Table 2.7. According to this table, it is clear that a key factor that could be affected by uncertainty is optimal cost of transaction with the main grid. Therefore, in the ABs, in which the energy/information transaction with the main grid would happen, it is of great importance to account for uncertainty and its effect on decision making (See Section 3.1).

TABLE 2.7: Effect of uncertainty on the flexibility based on the selected literature.

Ref No.	Main results
[54]	There is a need to raise operation cost to improve the system robustness.
[30]	Expected operation cost is higher in stochastic environment.
[17]	More investment cost for ESS planning is required in an uncertain environment.
[20]	Energy bill of building increased so as to improve the robustness of system.
[22]	Operation cost is affected by uncertainty.
[23]	Expected energy cost is increased.
[26]	Total operation cost needs to be increased.
[38]	Demand uncertainty affects forecast errors.
[48]	Cost saving is more usual in the winter season.
[49]	Considerable difference between buying energy from grid with and without consideration for uncertainty.
[50]	The scheduling pattern of home appliances' usage is changed
[53]	Operation cost would increase in uncertain environment.
[58]	The CHP should increase its generation capacity
[60]	Operation cost increased.
[63]	Importing power from main grid is more likely to be affected compared with the exported power.

2.4 Citation Network Overview

To further analyse the included papers and provide a visual overview, a citation network is illustrated in this section. Such a visualisation tool, builds a graph based on the layout and modularity algorithms, showing the existing path between relevant references and demonstrating the possible community structures that could be designed. The citation network is built based on the included papers, and they have been considered as the core of citation network, while their structure is developed based on the backward and forward methods [16] in Scopus citation database. Accordingly, the papers that cited the included papers as well as those which have been cited by the core nodes are added to the network. Gephi software package [83] is used in building the database, and the graph layout is analysed by "ForceAtlas2" [84] and "Yifan Hu Proportional" [85] algorithms, which provide a spatial mapping of the citation network. Fig. 2.7 represents the citation network overview, which was actual for May 2021.

Different communities are observed in Fig. 2.7, which have been shown with various colours. The connection nodes that drew a path between nodes of the same concept-based community are larger in the graph, which demonstrate how a specific concept is directed by other research works. Following each community is more likely to result in a research direction. The graph is explained in three layers as follows:

First layer: Regarded as the core layer of the graph, since the basic concepts are mainly taken into account in this layer. It accounts for the publications that mainly solved the model in day-ahead mode, with ABs connected to the main grid. These two concepts, that are mainly observed in the core layer, could be considered as the starting point of developing the optimisation and control of the AB operation. Consequently, the articles in this layer, Ref. [62] for instance, are connected to several nodes in the middle, and even outer layers. In addition, there are considerable interconnections between nodes of this layer. For instance, Reference [54], is connected to several of the nodes in the core layer, meaning that backward and forward citations of this work are mainly constructed based on the core concepts.

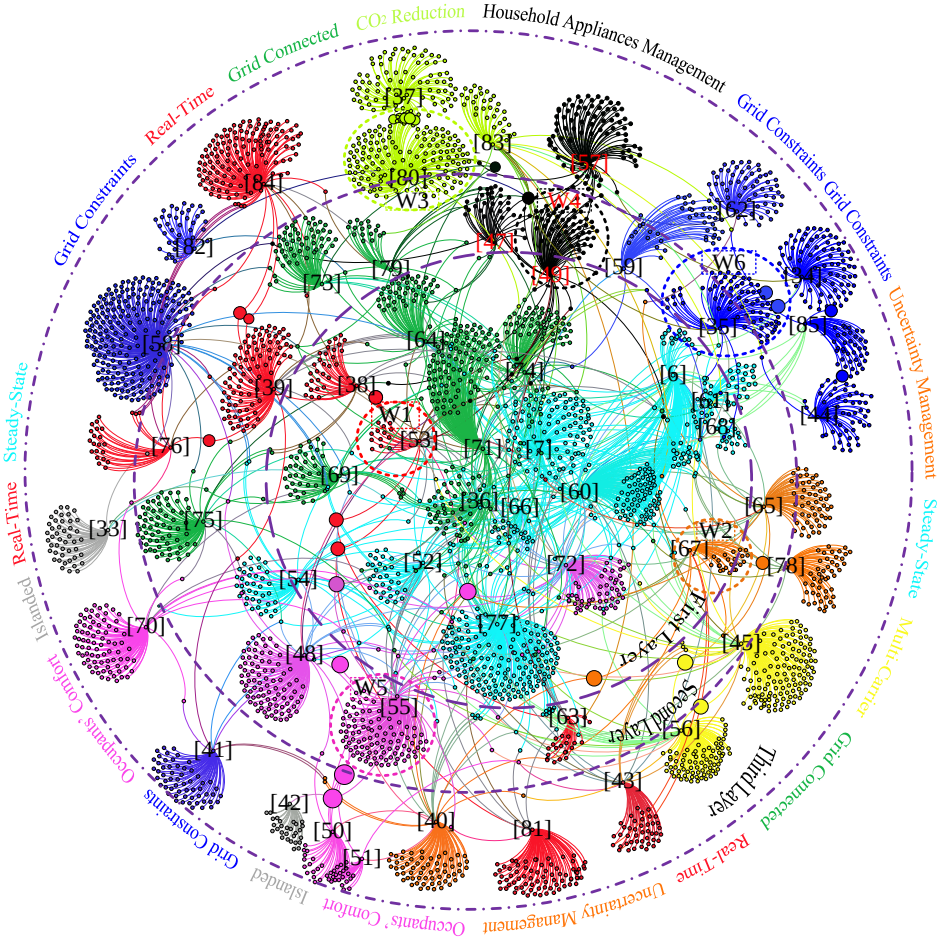

FIGURE 2.7: Citation network overview of selected papers based on the challenges and opportunities highlighted in this chapter.

Second layer: This layer, the middle layer, mainly consists of significant works that have been developed from the core layer, and could be regarded as the starting points of a wide variety of important subjects, such as occupants' comfort, real-time simulation, and islanded operation of ABs. Note that the majority of core nodes, separated by circular windows in the graph, are located in this layer. Therefore, the middle layer could be considered as the starting point of the developments that have taken place in the third layer.

Third layer: This layer, which is the outer part of the graph, shows the less

developed subjects that could be worthy of further research. It is evident from this graph that real-time models have been developed in recent years and could be continued. Also, papers which considered the grid constraints are a key part of the upper layer, demonstrating the significance of this concept in recent years. Examining the operation of ABs in off-grid mode is another development which has been investigated and could be extended through further research. Finally, the concept of multi-carrier ABs has been developed in several directions in the graph, mainly in the outer layer. Note that the interconnection between nodes from different clusters in this layer demonstrates the idea of combining various concepts for future investigations.

Based on the citation network graph overview, it is recommended that the basic concepts be investigated in six windows as:
W1: This window, which is located in the core layer, continued the path of those works which solved the model in day-ahead, by solving the model in real-time. This idea has been explored in several articles, such as references [47], [69], and [66] which are directed by connection nodes (i.e. large red nodes) to the basic node.
W2: As aforementioned, decision making under uncertainty is a critical issue in the operation and control of ABs. Accordingly, the node captured in this window investigated this subject, which has been followed by other works in this area (e.g. [24], and [63]), into the outer upper layer.
W3: It has been shown in the previous phase that carbon footprint reduction has not been widely investigated in the literature. This window shows that the work on this issue, presented in [65], has been continued by some new articles recently, proving the importance of the issue for further work.
W4: Optimal scheduling of household appliances is a basic concept, which has been captured in this window, that started from the first layer, and was continued by [31] and in the middle and outer layers respectively. The interconnection point in this window (i.e. large black node) is directed to many nodes, with various subjects in the outer layer.
W5: The idea of occupant's comfort is developed in this window, in [39], which has been connected to significant works in the outer layer. In addition to those works from the same cluster, this window includes other issues such as operation in islanded mode [26] and adding the grid constraints to the

model [25].

W6: The idea of this window is around grid-tied ABs. The core of this window is Reference [19], which has been continued by other articles in [28]. These references show the importance of including grid constraints in the model.

2.5 Discussion

The research works that have been reviewed in this thesis demonstrated that ABs can play a decisive role in the energy network. The literature review shows the potential value of this area of research. Nonetheless, the role of this concept in research and industry can be more crucial in the future. This chapter presents the challenges in enabling the role of ABs in the energy networks. These challeges will be studied in this thesis.

2.5.1 Overview of Future AB-Integrated Architectures

Different forms of technologies and structures can be linked to the ABs. For instance, adding EVs into the AB design can be a promising solution for improving flexibility. The mobility is a complex challenge when considering EVs for providing energy services for the grid. However, the challenges of integrating the transport structure into available systems should be studied and analysed.

2.5.2 Enabling More Flexible ABs

Changing the role of conventional passive building towards energy efficient ABs can create a wide range of services that can be provided to associated energy networks. Despite the significance of data-driven models [86] in exploring the behaviour of ABs, analytical methods are essential in studying the flexibility of ABs in the energy networks, especially when considering grid constraints. This requires use of the state of the art analytical methods such as the optimal power

flow. In an integrated grid and AB model, there will be several challenges that need exploration.

Objective function: in an integrated AB and grid model, the grid operator and AB objectives are more likely to affect each other inversely. Consequently, the objective function(s) of such optimisation problem should be defined based on grid and AB goals simultaneously. Also, in addition to economic models, there are other important criteria for controlling the buildings' operation, such as environmental objectives of reduction in carbon dioxide emissions.

Load aggregation: in the majority of previous literature, the interaction between ABs and the utility grid is studied with a small number of AB units. However, the aggregation of a large number of ABs in a big city or concentrated across a small area of energy network could be a challenging issue.

Occupants' comfort: the operation of ABs is highly influenced by occupants, and it is essential to consider occupant comfort either as a problem constraint or an objective function. Available comfort models mostly consider three main indices, which are visual, thermal, and air quality factors, while more lifestyle related measures can also be added to this category (See Section 3.1).

Services: creating the flexibility in the ABs can enable a wide range of services to be provided to the utility grids. Consideration for reactive power flow in the grid side creates different challenges and opportunities for activating reactive power support from the AB side. Also, enabling resilient ABs can create the possibility of providing resilience/security/reliability services in critical conditions.

Model type: the type of mathematical models applied in the research is an important point in defining the practical application of ABs. For example, for cost reasons, an AB controller should not demand an expensive powerful processor. Therefore, the MILP mathematical models should be developed for the AB controllers. Such models can be solved by commercial solvers and do not demand expensive processors.

Operation mode and energy vectors: integrating and communicating with different energy networks should be enabled in future ABs efficiently. Also,

the ABs should have the ability to co-operate with each other in grid-connected and autonomous modes. The latter mode can be crucial in contingency conditions when the distribution grid is disconnected from the upstream network.

2.6 Summary and Conclusion

Buildings as the end-users of energy networks are responsible for a sizeable amount of energy consumption and environmental pollution. Therefore, it is crucial to revise their role in the energy networks. A large number of publications have been delivered in the past decade, investigating the alternative tools in enabling flexibility in the buildings. This has engaged the various researchers and industries from different fields of engineering and science so as to find alternative control, optimisation, management, communication, and construction approaches for activating grid-aware buildings. This chapter presents work undertaken to identify and analyse relevant literature in the area of control and optimisation of ABs, through a systematic review. Firstly, all available research materials are obtained. Then, a sequential study selection criteria is introduced to identify potential literature which can comply with the research question. The included papers are evaluated based on a conceptual process so as to specify the current knowledge in the area and suggest future challenges for research and industry. Finally, a citation network is illustrated based on the included papers and backward/forward methods so as to show the interconnection between various papers and highlight the possible research pathways.

To conclude, mathematical models that will be developed for AB flexibility should be computationally efficient, while considering the occupants' comfort as an indispensable criteria in the integration of ABs into the energy networks. The control variables that are defined for technologies and devices within the building could be subject to the type of buildings (i.e. residential, commercial, or industrial), with consideration for the main lifestyle criteria, weather-related changes, and seasonal patterns. Available control models, explored in this chapter, can be adopted by real-life experiences and data-driven approaches. Therefore, the adaptation of data-driven models in defining this real-life information can help in developing the analytical models.

Based on this systematic literature review, Chapter 3 of this thesis fills the following gaps:

- The possibility of energy exchange between buildings while also managing occupants' thermo-visual comfort and his/her expressed preferences for domestic tasks (in the form of a schedule).
- Deconstructing the demand flexibility to its sources of sensitivity to alterations of comfort level and timing- ON/OFF status – or load adjustment of home appliances.
- Considering the effect of uncertainty on the model predictive control based rolling horizon methods, as suggested in [87], while improving the robustness of this method against uncertainty. The uncertainty can influence the energy exchange between buildings and overall comfort level. Furthermore, role of building occupants in improving robustness in face of uncertainty needs more exploration.

Also, Chapter 4 of this thesis fills the following gaps:

- Electrification of transport sector can influence the energy network and consequently local energy trading. Therefore, it is necessary to investigate the effect of multiple-energy vector optimisation on the local energy trading.
- Although the role of EVs on the economic perspectives has been studied, occupants comfort can have its influence on the decision making process. The EVs' participation can be affected by the users' preference.
- The papers that have considered EV in energy management strategies have not taken into account EV's driving patterns. This is a simplistic modelling of EV behaviour since the power that is consumed in driving mode of these units is an important factor in definition of their state of charge.

It is worth mentioning that the gaps observed in chapters 5 and 6 will be presented in their associated chapters.

This chapter reviewed the challenges and opportunities in activating building flexibility. The next chapter investigates the building flexibility based on the challenges discussed in this chapter.

3

Multi-Objective Energy Management of Building Flexibility

The following research question has been answered in this chapter:

How to optimise energy transaction between buildings as well as with the main grid so as to unlock their flexibility while accounting for uncertainty of weather forecast and market price?

Energy systems are undergoing radical changes that have resulted in buildings being regarded as proactive players with the potential to contribute positively to energy networks by enabling higher levels of flexibility. Achieving such a goal, however, requires a paradigm shift in the optimal management of building assets (i.e. building appliances and generation/storage capacity), occupants comfort and local energy exchange. As discussed in Chapter 2, achieving higher levels of flexibility in the buildings is subject to satisfaction of occupants. In order to deal with this challenge, a control framework is required which supervises buildings and their communally-shared portfolio of

assets, while exploiting the possibility of energy exchange between buildings and/or with the utility grid. This chapter proposes a multi-objective energy management strategy for a group of ABs that form a residential microgrid (RMG), making a trade-off between energy bill and comfort level of occupants. Such multi-objective control method could be compared against conventionally thermostat controlled buildings. Furthermore, different forms of AB flexibility is investigated by introducing a building-to-building (B2B) strategy for energy exchange between residential units, as well as a building-for-grid (B4G) model by exploiting the demand flexibility of RMG. These advanced flexibility measures could enable different opportunities for local grids. The mid-market rate mechanism is adopted to produce local market price signals at RMG level. Finally, due to the influence of various sources of uncertainty on the building energy management, a robust rolling horizon controller is developed for real-time energy management of the RMG. This control philosophy can improve the robustness of the RMG in face of uncertainty in the weather and energy price prediction errors. The repercussions of COVID-19 induced power consumption resulting from changing lifestyle and building occupancy profile is analysed by the proposed method as a case study. The efficiency of the proposed method is validated by simulation results. The simulation results demonstrate the significance of the proposed B2B and B4G strategies in enabling higher levels of flexibility. Besides, the results show a much improved efficiency of the proposed control strategy compared to existing conventional methods. The role of building users in unlocking the higher levels of flexibility is evident in the results.

Sections of this chapter have been published by the candidate as in the following journal paper:

Nikkhah S, Allahham A, Royapoor M, Bialek JW, Giaouris D. Optimising Building-to-Building and Building-for-Grid Services Under Uncertainty: A Robust Rolling Horizon Approach. IEEE Transactions on Smart Grid. 2021 Dec 15;13(2):1453-67.

Sections of this chapter have been published by the candidate as in the following conference paper:

Nikkhah S, Allahham A, Royapoor M, Bialek JW, Giaouris D. A Community-Based Building-to-Building Strategy for Multi-Objective Energy Management of Residential Microgrids. In2021 12th International Renewable Engineering Conference (IREC) 2021 Apr 14 (pp. 1-6). IEEE.

Sections of this chapter is under review in the following journal paper:

Nikkhah S, Allahham A, Patsios H, Taylor PC, Walker SL, Giaouris D. Building-to-Building Energy Trading under the Influence of Occupant Comfort. International Journal of Electrical Power & Energy Systems. 2023

Chapter roadmap: Section 3.1 describes the motivation and the research gap covered by this chapter. Section 3.2 illustrates the concept of RMG. Section 3.3 outlines formulation of problem. Section 3.4 explains different stages of the proposed multi-level control scheme. The framework description and simulation setup are introduced in Section 3.5. Simulation results are discussed in Section 3.6 and Section 3.7 concludes the chapter.

3.1 Introduction

Building's relationship to energy systems are evolving due to onsite generation, smart appliances and demand-side response. 36% of global energy consumption is attributed to building's embodied and operational energy use [88]. One way to reduce building's environmental impact is optimal scheduling and control of building loads that can enable them to become active agents within the wider energy system. Such ABs can also exchange energy and information locally to form a RMG [89]. This plan can enable them to unlock higher levels of flexibility. These dynamic characteristics have become crystallised in the concept of smart local energy systems that include a broad range of soft (i.e. digital and cyber) and hard (i.e. distributed generation) infrastructure components, and additionally underline the concept of peer-to-peer energy trading [73] within a cluster of ABs. As well as cost and carbon saving, AB flexibility models should seek to facilitate greater user choice, enable the possibility of energy transaction between ABs and maximising the use of distributed energy resources (DERs).

This requires a paradigm shift in the management of occupant comfort, maximising self-consumption and autonomy (in RMG), and maintaining virtual inertia and integrity (in the whole system). These requirements present two distinct opportunities for AB flexibility controller that supervises a community of ABs and their incorporated assets; first optimising the use of its communally-shared portfolio of energy resources, and second exploiting the possibility of energy exchange between buildings and/or with the utility grid. Following these goals can create a coordinated paradigm between ABs and energy networks, while facilitating the creation of community markets. These strategies supported by advanced telecommunication to enable real-time energy scheduling could be an efficient replacement for conventional load shedding [90]. To realise this, a RMG controller needs to overcome several challenges, namely real-time data processing of advanced metering infrastructure, catering for occupant preferences, and satisfying a set of techno-economic constraints. RMG controllers should also be

computationally (i.e. processing power/speed) and economically viable for a residential application.

As stated in Chapter 2, the current literature provided valuable evidence on effectiveness of BMES when activating AB flexibility. However, enabling energy exchange between buildings, while considering the occupants preferences requires more investigation. Also, the effect of uncertainty on the real-time BMES is another critical aspect which should be studies in more depth. In summary, this chapter examines the following research gaps that has been observed in existing literature:

(i) The possibility of energy exchange between buildings while also managing occupants' thermo-visual comfort and his/her expressed preferences for domestic tasks (in the form of a schedule) (Ass highlighted in 2.3.3.1).

(ii) Deconstructing the demand-side response to its sources of sensitivity to alterations of comfort level and timing- ON/OFF status – or load adjustment of home appliances (Ass highlighted in Sections 2.3.3.1 and Sections 2.5.2).

(iii) Considering the effect of uncertainty on the model predictive control based rolling horizon methods, as suggested in [87], while improving the robustness of this method against uncertainty. The uncertainty can influence the energy exchange between buildings and overall comfort level. Furthermore, role of building occupants in improving robustness in face of uncertainty needs more exploration (Ass highlighted in Sections 2.3.4.3).

(iv) Achieving [i]-[iii] through a computationally efficient control method that could be utilised in a residential sector and does not require investment for an expensive processor (Ass highlighted in Sections 2.3.4.2).

Hence, this chapter attempts to address this gap by proposing a multi-level real-time energy management for a community of buildings [1] which can actively co-operate to unlock flexibility. A rolling horizon based method is

[1] In this chapter, building refers to a generic UK type family house

adopted to receive real-time weather and energy price data, while the robustness in each consecutive dispatch time interval is increased (referred to as RRH hereafter) using the notion of information gap decision theory. The proposed RMG controller exploits flexibility in AB loads (through interruptible loads and building inertia) and shared distributed energy resources to introduce B2B and B4G strategies as advanced methods of flexibility. The mid-market rate approach is adopted in the AB community level to create a local pricing market. The proposed model is multi-level and multi-objective. While the latter makes a trade-off between energy bill and occupants comfort, the former can guarantee the preference/benefits of ABs in the local energy market. The proposed architecture is an mixed integer linear programming (MILP) model which can be solved by commercial solvers. The performance of the proposed controller is benchmarked against a conventional controller, and also tested under atypical operational characteristics such as COVID-19 related lock-down condition in 2020 which further highlighted the critical nature of modern power systems planning. The main contributions of this chapter are:

- A multi-level MILP optimisation model is proposed for AB flexibility, with consideration for occupant comfort and appliance/task constraints. Compared to current MILP models, the proposed solution allows greater asset/building participation using a linear robust controller that does not require excessive processing power (as opposed to the mixed integer non-linear programming (MINLP)) predecessors). It also pursues multiple goals in achieving an optimal energy management.
- Introducing an RRH controller to maximise the robustness of real-time energy management systems against prediction uncertainties at a lower computational time (compared to conventional controllers) while accounting for partial knowledge of input parameters.
- Proposing B2B and B4G strategies to oversee the peer-to-peer energy trading in RMG level while valuing the occupants comfort, and appliance settings under an uncertain environment. The former strategy facilitates the power exchange between dwellings using flexibility in in-site generation capacity, while the latter deconstructs the DR

response to its sources of sensitivity to alterations of comfort level and timing- ON/OFF status – or load adjustment of home appliances.

- Taking into account the effect of multiple sources of uncertainty on the local energy markets, while exploring the role of building occupants in improving AB flexibility robustness.

3.2 Overview of Residential Microgrid Controller

3.2.1 The Residential Microgrid (RMG) Structure

A bidirectional transaction framework is required for successful data and energy exchange in an RMG. This concept is summarised in Fig. 3.1. Each AB is equipped with an individual photovoltaic unit and a heat pump, while energy storage units are shared between the entire community given their high capital cost. The controller communicates internally with all ABs, the shared energy storage and externally with a weather forecast platform (e.g. website queries) and the grid. The controller is assumed to access occupant preferences through digital media (i.e. mobile phone apps) to receive [I] day-ahead scheduled time for home tasks, [II] the preferred zone comfort thresholds, and [III] occupancy profile. This is augmented by real-time energy prices and weather-related data.

Based on this data platform, the controller performs a multi-level real-time optimisation of scheduled tasks within the RMG, and communicates subsequent control signals to each building, while the amount of energy that is required from the upstream network or the flexibility provided is sent to the distribution grid controller. The optimal starting time of each task, cost and comfort level, the output of building level (photovoltaic unit and heat pump) and community level (energy storage) assets, and the value of B2B/B4G transactive tasks is then communicated by the controller. Cloud computing is assumed to enable real-time communication and control signal processing, while observing privacy issues. Therefore:

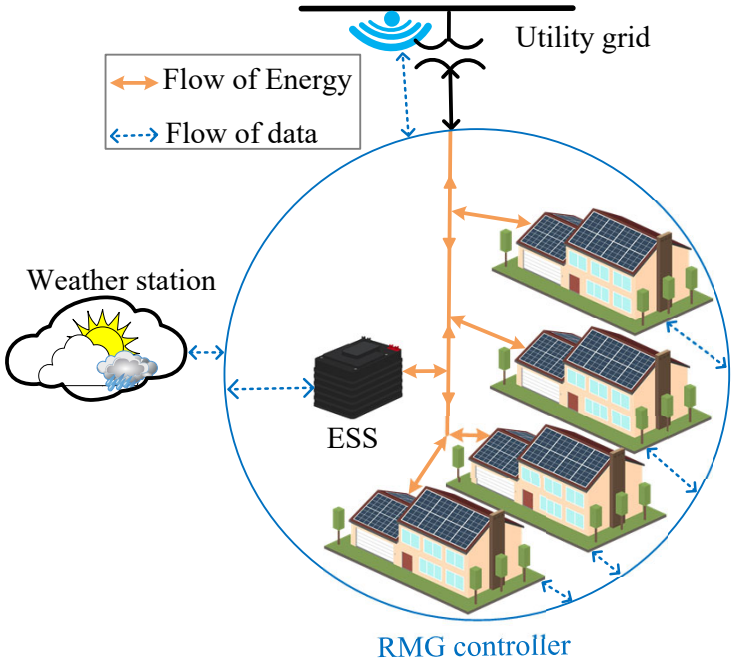

FIGURE 3.1: The conceptual illustration of RMG.

- Real-time communication is assumed and a delay has not been considered.
- The RMG controller is in charge of the entire RMG asset-base and all AB asset data.
- RMG is connected to the main grid at point of integration.
- The energy sources within each building (e.g. photovoltaic unit) are controlled by RMG controller.

3.2.2 Robust Rolling Horizon (RRH) Controller

The rolling horizon approach, which is based on the concept of model predictive control, can be used for real-time energy management of RMGs. This method uses real-time data for each discrete time interval to solve the optimisation over a nominal control horizon while also accounting for future time-slots. Therefore at time period t_1, the input data for upcoming intervals

(i.e. $t_2 ... t_n$) are forecasted, so the optimised results are defined based on a predicted path. Forecast data uncertainty (especially for parameters prone to wide fluctuation) results in a simulation error (i.e. the difference between predicted and actual value). To reduce error, the conventional methods use smaller time intervals (i.e. reducing optimisation interval from 30min to 5min). However, this requires high computational time and power which may present difficulties when performing real-time controls. Additionally, smaller time intervals cannot solve the issue of future uncertainty. To address these issues, an information gap decision theory based technique has been proposed in this paper to increase the robustness of rolling horizon method. This method does not require excessive information on input parameters, and needs lower computational time compared to stochastic methods [91], making it suitable for dealing with input data with unknown behavioural patterns such as weather forecast. This method has been explained in Section 3.4.3.

Figure 3.2 attempts to illustrate this approach. In the conventional method (Fig. 3.2-a) [19] and at time instance t_1, the forecast error for a future instance of time (e.g. t_m) propagates into a simulation error. The proposed RRH method (Fig. 3.2-b) introduces a robustness degree for those input data that

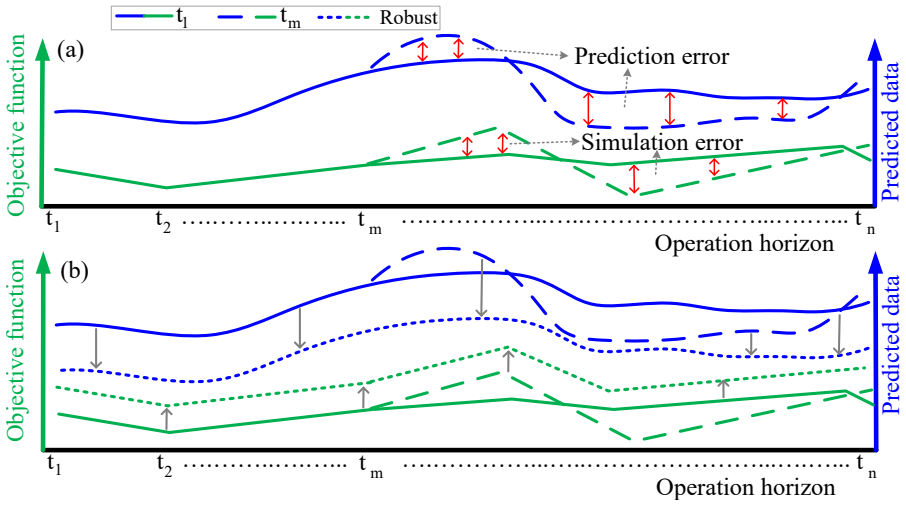

FIGURE 3.2: Comparison of a) conventional rolling horizon, and b) the proposed RRH controllers.

are more likely to change over operational horizon. As it can be seen in this figure, in the conventional methods, solving the model at time period t_1 is more likely to have an unrealistic result if the forecasted data change in the following intervals, especially those which occur in a longer period of time (i.e. t_{1+m}). This means based on Fig. 3.2-a, the prediction error (shown with broken blue line) can result in a simulation error (i.e. a pessimistic result) as shown by green broken line in Fig. 3.2-a. By maximising the degree of robustness, the erroneous effect of the changeable forecasts on the control action is reduced. It should be noted that the optimal value of robustness is related to its tolerable value. The tolerable value of robustness is a parameter defined by the decision maker and increases the value of the objective function. This increase in cost is called cost of robustness. The bigger the tolerable value of robustness, the greater the system robustness. Therefore, in Fig. 3.2-b, the optimal value of dotted green line is related to the amount of increase in the objective function (i.e. from the solid green line to the dotted green line in Fig. 3.2-b).

3.3 Problem Formulation

The proposed mathematical model describes optimal operation of multiple ABs, and shared energy sources, which form an RMG, while they can communicate with the utility grid, and locally together. The flexibility in these ABs is activated by increasing the value of local energy exchange or the power exchange with the main grid. It is worth mentioning that the power exchange with the main grid can be affected by local grid, yet is considered as a form of flexibility since ABs dependency on the main grid is improved. In the following, the technical and operational constraints of RMG are introduced. Then, the AB flexibility strategies are discussed.

3.3.1 Objective Functions

In the proposed optimisation, the controller follows two conflicting objective functions, namely energy bill and occupants comfort index, defined as:

$$\min \left(\zeta = \Delta t \sum_{t \in \psi_t} \sum_{j \in \psi_j} \hat{\lambda}_t^{G_I} P_{j,t}^{G_I} - \hat{\lambda}_t^{G_E} P_{j,t}^{G_E} \right) \tag{3.1}$$

$$\max \left(\Xi = \frac{1}{B} \sum_{t \in \psi_{t_j}^{oc}} \sum_{j \in \psi_j} \frac{1}{T_j^{oc}} \left(\omega_{j,t}^{V} I_{j,t}^{V_{com}} + \omega_{j,t}^{T} I_{j,t}^{T_{com}} \right) \right) \tag{3.2}$$

where, Eq. (3.1) represents the energy bill, in which the first and second terms are cost and income of importing/exporting power from/to the main grid, respectively. As discussed in Chapter 2, energy bill is one of the critical objective functions in investigating the flexibility, which shows itself in a higher level in terms of cost. The objective function given in (3.2) represents the comfort index of all ABs in the community (i.e.B) over the occupied period (i.e.T_j^{oc}) of each dwelling unit, which is obtained by multiplying the weighting factors $\omega_{j,t}^{V}$ and $\omega_{j,t}^{T}$ by virtual (i.e. $I_{j,t}^{V_{com}}$) and thermal (i.e. $I_{j,t}^{T_{com}}$) comfort indices respectively. While in predominant thermal comfort codes (i.e. BS EN ISO 7730, ASHRAE or Bedford) normally a 7 point approach is used to represent a 'too cold' to 'too hot' thermal spectrum, here for equation development this bidirectional band is translated into a single index of 0 to 1. Thermal neutrality (i.e. highest degree of comfort) is represented by 1 and degrees of departure from it (i.e. the space being too hot or too cold) moves the comfort index towards 0.

3.3.2 Operation of Different Tasks in Unlocking Flexibility

Optimal BMES strategies aim at controlling the operation of AB assets so as to enable flexibility. Operational characteristics of AB appliances can be categorised into different groups, as outlined below.

Comfort-Providing Tasks: the consumption of these tasks is defined based on the preferred comfort level. Visual and thermal comfort-providing tasks are categorised into this group. Power consumption of these tasks is defined as:

$$V_{j,t}^{B} = \frac{\kappa_j P_{j,t}^{I} f_j \eta_I^u . \eta_I^m}{A_j} \tag{3.3}$$

$$T_{j,t+1}^{B} = T_{j,t}^{B} + \frac{\Delta t}{R_j^{th} D_j^{th}} \left(\hat{T}_t^{out} - T_{j,t}^{B} \right) + \frac{\Delta t}{D_j^{th}} H_{j,t}^{th} \tag{3.4}$$

where, in (3.3), $P_{j,t}^{I}$ is the amount of power consumed by lighting devices to provide visual comfort (i.e. $V_{j,t}^{B}$). Eq.(3.4) is widely referred to as building resistance and capacitance thermodynamic model [36], in which $H_{j,t}^{th}$ denotes the amount of power that is consumed for providing thermal comfort.

Fixed Power Consumption Tasks (i.e. ψ_i^F): set of tasks which operate in a specific period (i.e. $\psi_{t_{op}}^{Ap}$) with a fixed power consumption rate (e.g. cooker hob). Based on the preferred time window of these tasks, which is defined between their starting time (i.e.$\psi_{t_{st}}^{Ap}$) and ending time (i.e. $\psi_{t_{end}}^{Ap}$), their operation is described as:

$$\sum_{t=\psi_{t_{st}}^{Ap}}^{\psi_{t_{end}}^{Ap} - \psi_{t_{op}}^{Ap}} \chi_{j,i,t}^{Ap} = 1 \quad , \forall i \in \psi_i^F \tag{3.5}$$

Variable Power Consumption Tasks (i.e. ψ_i^V): these tasks operate with a variable consumption rate, such as washing machine and dishwasher. Constraints (3.5) should be modified so as to describe the operation of these tasks, as follows:

$$\sum_{t=\psi_{t_{st}}^{Ap}}^{\psi_{t_{end}}^{Ap}} \chi_{j,i,t}^{Ap} P_{j,i,t}^{Ap} = \sum_{o=\psi_{t_{op}}^{Ap}} P_{j,i,o}^{Ap} \quad ,\forall i \in \psi_i^V \tag{3.6}$$

According to constraint (3.6), the ON/OFF status of each task (i.e. $\chi_{j,i,t}^{Ap}$) controls the required power at each period (i.e. $P_{j,i,t}^{Ap}$) so as to satisfy the variable power consumption at each operational period (i.e. $P_{j,i,o}^{Ap}$).

3.3.3 Comfort Constraints

The comfort indices are related to comfort related tasks as explained in (3.3)-(3.4). In addition to internal comfort providing technologies, outdoor illumination and temperature are considered as external factors which can affect the occupants comfort. These indices and their corresponding constraints are:

$$I_{j,t}^{V_{com}} = 1 - \left(\frac{V_{j,t}^T - V_{j,t}^{Set}}{V_{j,t}^{Set}} \right)^2 \tag{3.7}$$

$$V_{j,t}^T = V_{j,t}^B + \hat{V}_t^N \tag{3.8}$$

$$\begin{cases} V_j^{B_l} \leq V_{j,t}^T \\ V_{j,t}^B \leq V_j^{B_u} \end{cases} \quad ,\forall t \in \psi_{t_j}^{oc} \tag{3.9}$$

$$I_{j,t}^{T_{com}} = 1 - \left(\frac{T_{j,t}^B - T_{j,t}^{Set}}{T_{j,t}^{Set}} \right)^2 \tag{3.10}$$

$$T_j^{B_l} \leq T_{j,t}^B \leq T_j^{B_u} \tag{3.11}$$

where, (3.7) is the visual comfort index, while (3.8) shows the total illuminance level within each building, which is equal to the sum of natural illumination and that of lighting devices. Equation (3.9) limits the illuminance level. Besides,

(3.10) represents the thermal comfort index, while (3.11) limits the buildings' indoor temperature. The quadratic term in (3.7) is linearised as follows:

$$\Omega_{j,t}^{V_+} + \Omega_{j,t}^{V_-} = \sum_{n=1}^{N} \theta_{j,t,n}^{V} \tag{3.12a}$$

$$0 \leq \theta_{j,t,n}^{V} \leq \theta_{j}^{V_u} \tag{3.12b}$$

$$V_{j,t}^{T} - V_{j,t}^{Set} = \Omega_{j,t}^{V_+} - \Omega_{j,t}^{V_-} \tag{3.12c}$$

$$\theta_{j}^{V_u} = \frac{V_{j}^{B_u} - V_{j}^{B_l}}{N} \tag{3.12d}$$

$$\gamma_{j,n}^{V} = (2n-1)\theta_{j}^{V_u} \tag{3.12e}$$

$$I_{j,t}^{V_{com}} = 1 - \left(\frac{\sum\limits_{n \in \psi_n} \gamma_{j,n}^{V} \theta_{j,t,n}^{V}}{\left(V_{j,t}^{Set}\right)^2} \right) \tag{3.12f}$$

where, N is the number of linearisation intervals. The value of $\theta_{j,t,n}^{V}$ is limited by constraint (3.12b), and controlled by positive variables $\Omega_{j,t}^{T_+}$ and $\Omega_{j,t}^{T_-}$ which take their value from Equation (3.12c). The upper value of each linearised interval is obtained by (3.12d), while the linear function of each segment is defined by (3.12e). Finally, summing the multiplication of the length of each piece and linearised function of each segment is obtained in (3.12f), which is identical to the non-linear arc. The same strategy could be applied for linearising $I_{j,t}^{T_{com}}$ in Equation (3.10). Based on the piecewise linearisation technique, the parabolic curve $(V_{j,t}^{T} - V_{j,t}^{Set})^2$ is approximated by variable $\theta_{j,t,n}^{V}$.

3.3.4 Energy Balance Constraints

In the designed RMG, heating and electricity energy demand of ABs is supplied by internal (e.g. heat pump and photovoltaic units) and external (e.g. electricity grid). The following energy balance constraints are introduced for the model.

$$\begin{aligned}&\sum_{i\in\psi_i}\left(\chi^{Ap}_{j,i,t-o}P^{Ap}_{j,i,o}\right)+P^{I}_{j,t}+P^{ESS_c}_{j,t}+P^{G_E}_{j,t}\\&=P^{G_I}_{j,t}+P^{HP}_{j,t}+P^{PV}_{j,t}+P^{ESS_d}_{j,t}+P^{B2B}_{j,t}\end{aligned}\tag{3.13}$$

$$H^{th}_{j,t}=H^{HP}_{j,t}\tag{3.14}$$

where, (3.13) is the electric power balance, consisting of the consumption of different tasks and generation of various sources, while (3.14) represents the heating balance. The terms given in these equations are limited by their technical and operational constraints. The heat pump is the linking asset between heating and electricity.

3.3.5 RMG Asset Constraints

The central and individual energy providers of the RMG which are integrated to supply ABs load demand are limited by the following constraints.

$$H^{HP}_{j,t}\leq P^{HP}_{j,t}COP\tag{3.15}$$

$$E_t^{ESS} - E_{t-1}^{ESS} = \Delta t \left(\sum_{j \in \psi_j} \eta_{ess}^{c} P_{j,t}^{ESS_d} - \sum_{j \in \psi_j} \left[\frac{P_{j,t}^{ESS_d}}{\eta_{ess}^{d}} \right] \right) \tag{3.16}$$

$$E_l^{ESS} \leq E_t^{ESS} \leq E_u^{ESS} \tag{3.17}$$

$$0 \leq P_{j,t}^{ESS_c} \leq \chi_{j,t}^{ESS_d} P_u^{ESS_d} \tag{3.18}$$

$$0 \leq P_{j,t}^{ESS_d} \leq \chi_{j,t}^{ESS_c} P_u^{ESS_c} \tag{3.19}$$

$$\chi_{j,t}^{ESS_c} + \chi_{j,t}^{ESS_d} \leq 1 \tag{3.20}$$

$$\sum_{t \in \psi_t} P_{j,t}^{ESS_d} \leq \sum_{t \in \psi_t} P_{j,t}^{ESS_c} \tag{3.21}$$

$$0 \leq P_{j,t}^{PV} \leq \hat{P}_{j,t}^{PV_F} \tag{3.22}$$

Constraint (3.15) limits the output power of heat pump based on coefficient of performance (COP). The proposed model for heat pump is based on an operational formulation, which has been introduced for the proposed energy management scheme and does not require physical description of this technology. Equations (3.16)-(3.21) describe the energy storage model, in which (3.16) denotes the total state of charge of energy storage, while it is limited by (3.17). In order to prevent net accumulation, the state of charge of battery at the end of the period (i.e. t_{end}) should be equal to its initial value at the beginning of the period (i.e. t_{st}). The charge and discharge of each building from the central storage is limited by (3.18) and (3.19) respectively. Note that the $P_u^{ESS_{c/d}}$ is also the maximum allowable charge/discharge of all ABs. Constraint (3.20) is a limiting logic based on the binary variables $\chi_{j,t}^{ESS_d}$ and $\chi_{j,t}^{ESS_c}$ which prevent simultaneous charge and discharge. Constraint

(3.21) represents that the amount of discharged power for each AB is limited by the value of charged power. This means that AB j can utilise the power from energy storage if it has contributed to its charging before. Finally, constraint (3.22) represents the output power of rooftop photovoltaic units based on the predicted output.

3.3.6 Utility Grid

The RMG can receive and send electrical power from/to the utility grid. Enabling flexibility in the ABs through the BMES affects the power exchange with the main grid and consequently flexibility. These limits are represented in the following constraints:

$$P_{j,t}^{G_I} \leq P_u^G \times \chi_{j,t}^G \tag{3.23}$$

$$P_{j,t}^{G_E} \leq P_u^G \times (1 - \chi_{j,t}^G) \tag{3.24}$$

where, binary variable $\chi_{j,t}^G$ prevents the simultaneous import and export from/to the main grid.

3.3.7 Advanced Active Building Flexibility Strategies

Active building strategies advance the role of dwellings in the energy network by introducing flexibility measures, while taking into account critical denominators such as users' comfort. These strategies can be divided to those which serve the AB community and those which provide services for the grid. The former is referred to as B2B strategy while the latter deconstructs the idea of demand flexibility into its source and is called B4G strategy.

Building-to-Building Strategy: this strategy is developed based on the idea of peer-to-peer energy trading [73]. According to this framework, buildings can participate in a local market based on their available generation capacity and

demand flexibility. However, participating in peer-to-peer energy trading for an AB is subject to maintaining the techno-economic constraints and satisfying the occupant comfort. Furthermore, enrolling in B2B should bring about profit for each individual AB. This profit can be reflected in the energy bills. Finally, such a framework should not create security problems for the utility grid. The following equations represent the B2B strategy based on these criteria.

$$P_{j,t}^{B2B} = P_{j,t}^{buy} - P_{j,t}^{sell} \tag{3.25a}$$

$$0 \leq P_{j,t}^{buy} \leq P_{j,t}^{AB_D} - P_{j,t}^{AB_G} \tag{3.25b}$$

$$0 \leq P_{j,t}^{sell} \leq P_{j,t}^{AB_G} - P_{j,t}^{AB_D} \tag{3.25c}$$

$$0 \leq P_{j,t}^{buy} \leq (1 - \chi_{j,t}^{b2b}) \times M \tag{3.25d}$$

$$0 \leq P_{j,t}^{sell} \leq \chi_{j,t}^{b2b} \times M \tag{3.25e}$$

$$\sum_{j \in \psi_j} P_{j,t}^{B2B} = 0 \tag{3.25f}$$

The value of B2B for each AB and its role (i.e. buyer or seller) in the local market is defined by (3.25a). Each AB can specify its role as buyer (i.e. when $P_{j,t}^{B2B}$ takes its value from $P_{j,t}^{buy}$) or seller (i.e. when $P_{j,t}^{B2B}$ takes its value from $P_{j,t}^{sell}$) in the B2B framework by managing its generation capacity (i.e. $P_{j,t}^{AB_G}$) and demand (i.e. $P_{j,t}^{AB_D}$) as indicated by constraints (3.25b) and (3.25c) respectively. Constraints (3.25b) and (3.25c) also ensure that the energy exchange would happen based on the RMG internal capacities. Note that, the generation and demand of each individual AB are obtained in the energy balance equations. Based on constraints (3.25d) and (3.25e) each

building can be a buyer or a seller in each time period. The variable $P_{j,t}^{B2B}$ is also added to the power balance equations in (3.13).

Building-for-Grid Strategy: for the B4G strategy, a positive variable is defined (i.e. $L_{j,i,t}^{flex}$) to tolerate the power consumption of the adjustable power consumption tasks, through multiplying it by the building appliances' power usage (i.e. $L_{j,i,t}^{flex} \times \chi_{j,i,t-o}^{Ap} \times P_{j,i,o}^{Ap}$). However, this will change the model to a non-linear one. Thus, the term $\chi_{j,i,t-o}^{Ap} P_{j,i,o}^{Ap}$ in (3.13) is replaced by $L_{j,i,t}^{flex} P_{j,i,o}^{Ap}$, while the following linear model is defined for B4G.

$$\chi_{j,i,t-o}^{Ap} \times L_{l}^{flex} \leq L_{j,i,t}^{flex} \leq \chi_{j,i,t-o}^{Ap} \tag{3.26}$$

$$P_{j,t}^{B4G} = \sum_{i \in \psi_i^v} P_{j,i,o}^{Ap} \times \left(\chi_{j,i,t-o}^{Ap} - L_{j,i,t}^{flex} \right) \tag{3.27}$$

where, constraint (3.26) introduces the upper and lower limits on the variable $L_{j,i,t}^{flex}$ based on the binary variable $\chi_{j,i,t-o}^{Ap}$ which has been defined in (3.5) for ON/OFF status of appliances. If a building appliance is on (i.e. $\chi_{j,i,t-o}^{Ap} = 1$), the upper value of $L_{j,i,t}^{flex}$ will be one, while the minimum value is defined by parameter L_{l}^{flex}. Constraint (3.27) represents the value of B4G which is non-zero if the flexibility variable would take a value less than one. The willingness of an AB to participate in this program depends on the market prices. Based on this strategy, ABs can respond to the price signal by turning appliances ON/OFF (i.e. $\chi_{j,i,t}^{Ap}$) or indeed where applicable adjust the value of flexibility (i.e. $L_{j,i,t}^{flex}$) to assist B4G services. To clarify, reducing the value of flexibility to an amount lower than one means the load of an appliance (or collection of appliances) can be adjusted. This means that the market price signal guides the controller to switch on appliances and adjust their consumption to bring about lower cost for ABs.

3.3.8 Pricing Mechanism

Participating in the peer-to-peer energy exchange can bring about several advantages for the prosumers, such as energy bill reduction, and improvement in energy system reliability [92]. It should be noted that the pricing mechanism is based on the local supply-demand imbalance, and does not model bidding strategies. In order to establish a local market and encourage ABs to participate in the B2B and B4G strategies, a suitable pricing mechanism is required. In this study, the mid-market rate method [93], a commonly used pricing mechanism, is adopted for establishing the energy prices within the RMG. The illustrative concept of this method is shown in Fig. 3.3. Based on this mechanism, the RMG local prices are defined as the average of import and export prices with the main grid (i.e. $\hat{\lambda}^{RMG}_{b2b,t} = (\hat{\lambda}^{G_I}_t + \hat{\lambda}^{G_E}_t)/2$). However, due to the fact that the RMG local generation (e.g. G^{RMG}_t) and demand (e.g. D^{RMG}_t) vary at each time-slot, three different scenarios are devised, as outlined below [93]:

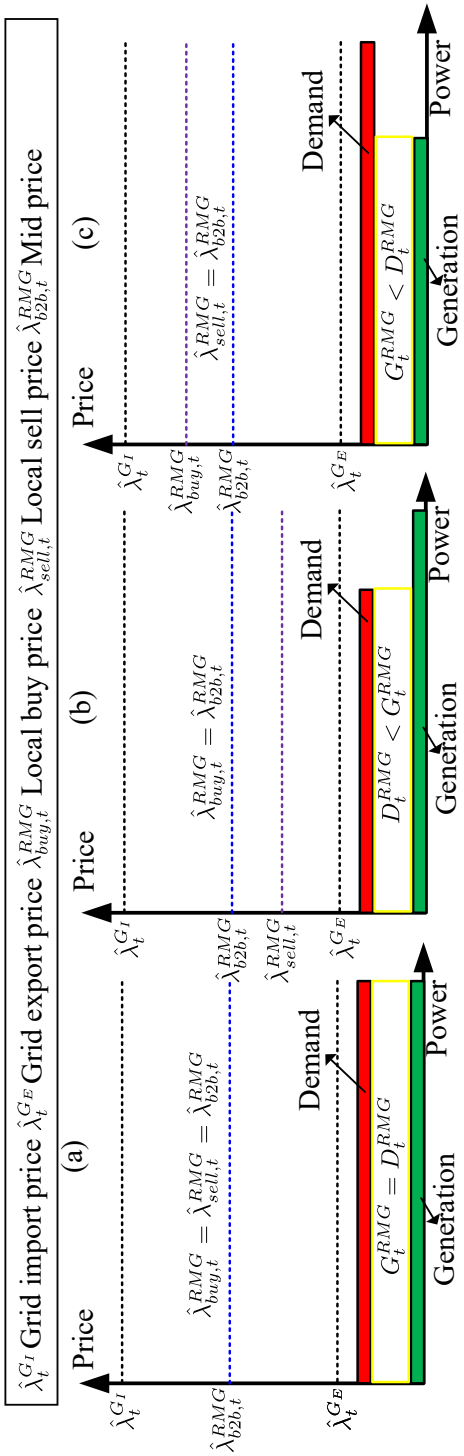

FIGURE 3.3: Value of local market price under different demand-generation scenarios: a) $G_t^{RMG} = D_t^{RMG}$, b) $D_t^{RMG} < G_t^{RMG}$, and c) $G_t^{RMG} < D_t^{RMG}$.

I. RMG generation equals demand ($G_t^{RMG} = D_t^{RMG}$, as in Fig. 3.3-(a)): In this scenario, local buy (i.e. $\hat{\lambda}_{buy,t}^{RMG}$) and sell (i.e. $\hat{\lambda}_{sell,t}^{RMG}$) prices are equal to $\hat{\lambda}_{b2b,t}^{RMG}$. Local energy trading under this scenario happens with the average of grid import and export price. Therefore, buildings participating in the local market under this scenario can benefit from better buy and sell prices compared to those of the main grid.

II. RMG generation is higher than demand ($D_t^{RMG} < G_t^{RMG}$, as in Fig. 3.3-(b)): In this case, the local sell price is lower than average B2B price, while the excess generation can be sold to the main grid with the grid export price (i.e. $\hat{\lambda}_t^{G_E}$). Local buy price is equal to $\hat{\lambda}_{b2b,t}^{RMG}$ while local sell price is obtained by Eq. (3.28). Note that buildings with excess generation can sell their energy to the buyer buildings, whereas the amount of energy that could be sold to the main grid is proportionally allocated between all producers. This enables the fair distribution of price between all buildings in the community.

$$\hat{\lambda}_{sell,t}^{RMG} = \Big(D_t^{RMG}\hat{\lambda}_{b2b,t}^{RMG} + (G_t^{RMG} - D_t^{RMG})\hat{\lambda}_t^{G_I}\Big)\Big/G_t^{RMG} \tag{3.28}$$

III. RMG generation is lower than demand ($G_t^{RMG} < D_t^{RMG}$, as in Fig. 3.3-(c)): The energy deficit is imported from the main grid with the grid price, while local sell price is equal to $\hat{\lambda}_{b2b,t}^{RMG}$ and local buy price is obtained by Eq. (3.29). The energy imported from the main grid is proportionally allocated to all consumers in the community.

$$\hat{\lambda}_{buy,t}^{RMG} = \Big(G_t^{RMG}\hat{\lambda}_{b2b,t}^{RMG} + (D_t^{RMG} - G_t^{RMG})\hat{\lambda}_t^{G_E}\Big)\Big/D_t^{RMG} \tag{3.29}$$

Under this pricing framework, ABs can trade energy locally, while exchanging energy with the main grid based on the grid pricing contracts. As illustrated in Fig. 3.3, the local prices are defined between grid import and export prices. Therefore, participating in the local market brings profit to both buyers and sellers. Those who buy energy can benefit from lower price compared to that of grid import, while sellers can sell their excess generation with a price better than that of grid export price. In addition to the B2B strategy, the B4G

method allows ABs to reduce their prices by utilising their demand flexibility. Accordingly, the energy bill of each AB is written as:

$$\zeta_j = \Delta t \sum_{t \in \psi_t} \left\{ \begin{array}{l} \hat{\lambda}_t^{G_I} P_{j,t}^{G_I} - \hat{\lambda}_t^{G_E} P_{j,t}^{G_E} \\ -\hat{\lambda}_t^{G_E} P_{j,t}^{B4G} \\ \hat{\lambda}_{buy,t}^{RMG} P_{j,t}^{buy} - \hat{\lambda}_{sell,t}^{RMG} P_{j,t}^{sell} \end{array} \right\} \tag{3.30}$$

3.4 Proposed Multi-Level Flexibility Control Scheme

In order to accommodate the proposed mid-market rate pricing mechanism, B2B and B4G service provision models, the RMG controller has to consider three important factors. Firstly, it has to dispatch an ABs participation in B2B and B4G services only if that control action can provide added benefits (i.e. reduced energy bills). Secondly, participation in any local market for a building should honour occupant comfort constraints. Finally, the RMG controller should consider input parameter prediction errors when processing control signals for the community. To address these challenges, this study introduces a multi-level control framework as outlined in the following subsections.

3.4.1 Base-Case Flexibility Control (First Level)

An AB-specified market should present cost saving to the participants. In other words, energy bill of ABs after participating in the B2B and B4G should be lower than that without these strategies. Accordingly, the base-case level of the RMG control strategy minimises the energy bill in Eq. (3.1) without consideration for B2B and B4G constraints, as follows:

$$\min \left(\zeta^{l1} = \zeta\right) \tag{3.31a}$$

$$s.t:$$

$$(3.3) - (3.24) \tag{3.31b}$$

The value obtained for ζ^{l1} is considered as a constraint for other levels of optimisation. Therefore the simulation will be carried out simultaneously for both objective functions. The value obtained for total RMG generation and load is also utilised to define the mid-market rate local prices. This allows the definition of local prices without consideration for an individual AB's benefit, bringing about a fair distribution of benefit among all dwellings.

3.4.2 Multi-Objective Optimisation (Second Level)

This level exploits B2B and B4G strategies to obtain the greatest energy bill saving. The willingness to minimise the cost, however, brings it into a conflict with the occupants comfort. In this regard, it is required to solve this level as a multi-objective optimisation. In this thesis, the $\epsilon - constrained$ method is adopted to solve the optimisation problem. This method does not require manual definition of weights and can deal with convex and non-convex methods as opposed to other approaches such as weighted sum technique [74]. These are important factors that should be considered, especially in automated control methods. In this method, one of the objective functions is transferred into the model constraints, while the other is optimised. The objective function that is considered as a constraint takes its limits from ϵ, which is derived from the maximum and minimum values of the objective function that is being considered as a constraint.

Noting that either objective function could be optimised, the energy bill is minimised in (3.32a) while the comfort level is defined as the model constraint in (3.32b). This process turns the model into a single-objective cost optimisation while the comfort level is constrained by ϵ. The value of ϵ is

defined between maximum and minimum possible comfort level. The interval between the maximum and minimum value is divided into equal steps and the optimisation is solved for each value.

As aforementioned, energy bill with AB flexibility mechanisms should be lower; therefore, constraint (3.32c) is introduced in this level. The other constraints of this optimisation are (3.3)-(3.27). This will enable the generation of all Pareto optimal solutions for a multi-objective problem.

$$OF = \min_{DV} \left(\sum_{j \in \psi_j} \zeta_j \right) \tag{3.32a}$$

$$s.t:$$

$$\Xi \geq \varepsilon \tag{3.32b}$$

$$\zeta_j \leq \zeta_j^{l1} \tag{3.32c}$$

$$(3.3) - (3.27) \tag{3.32d}$$

In (3.32), the energy bill is minimised while the value of ϵ is decreased from the maximum value of occupants comfort (obtained when Ξ is maximised solely) to its minimum value (obtained when ζ is minimised solely). Solving this optimisation problem draws a Pareto optimal set for both objective functions. Considering the fact that all Pareto optimal solution are acceptable, there is a need to select the best compromise solution. To do so, a fuzzy-based min-max method is adopted, in which the minimum value of each membership function is obtained, and the maximum value of the selected membership functions is chosen as the best compromise solution [74]. Note that constraint (3.32c) ensures that participating in the local market does not increase each individual AB's energy bills.

3.4.3 RRH Controller (Third Level)

The schematic illustration in Fig. 3.2 demonstrated that the deviation from predicted data can affect the simulation results. Since the proposed mid-market rate pricing mechanism is developed based on the generation capacity and AB demand, as well as the price signals, it is necessary to consider the effect of uncertainty on the B2B and B4G strategies.

The proposed method is a robust real-time energy management technique which is different from the stochastic optimisation. For more elaboration on this method, consider Fig. 3.4 [94]. As shown in this figure, stochastic methods require precise information on the uncertain input data. This information requires accurate knowledge about the probability density function of each uncertain parameter, which is a strenuous task in cases of input data with unknown behavioural patterns. Furthermore, as illustrated in this figure, stochastic methods produce a large number of scenarios for each uncertain parameter, resulting in a dramatic increase in the computational time. On the other hand, the proposed method which is based on information gap decision theory technique, only requires an uncertainty set which does not need to be known. This method increases the immunity (i.e. robustness) of objective function in face of uncertainty in the input data. This means that

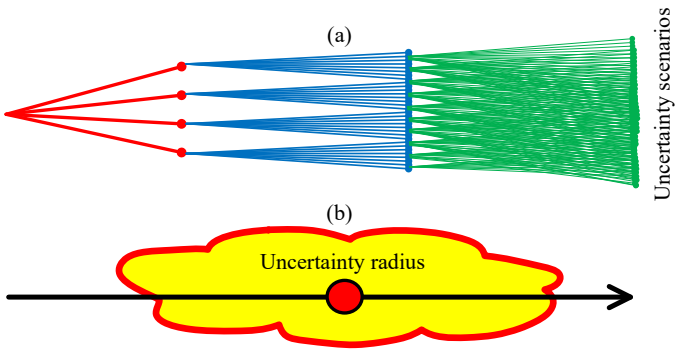

FIGURE 3.4: The conceptual difference of a) stochastic optimisation, and b) information gap decision theory [94].

the optimal value of objective function will remain immune if the input data vary within an unknown threshold.

This thesis utilises the envelope-bounded model of information gap decision theory to improve the robustness of RMG controller in face of uncertainty. This model is mathematically described as follows [95]:

$$U(\alpha, \widehat{\nu}) = \left\{ \nu : \left| \nu(t) - \widehat{\nu}(t) \right| \right\} \leq \alpha \left| \widehat{\nu}(t) \right|, \ \ \alpha \geq 0 \tag{3.33}$$

where $\nu(t)$ is the value of uncertain variable which deviates around the predicted value (i.e. $\widehat{\nu}(t)$). The size of gap between $\nu(t)$ and $\widehat{\nu}(t)$ is defined by α which is called uncertainty variable. Based on this model, the fractional deviation of predicted parameter from the uncertain value is limited by α. The bigger the value of α, the larger the horizon of deviation.

In the proposed model, the predicted values of outside temperature (i.e. $\hat{T}_t^{out}$), natural illuminance level (i.e. $\hat{V}_t^N$), and photovoltaic unit output (i.e. $\hat{P}_t^{PV_F}$) are considered as the weather-related uncertain data. While these parameters are weather-related, the first two data impose demand uncertainty while the third one reflects the generation uncertainty. The import/export electricity prices (i.e. $\hat{\lambda}_t^{I/E}$) are also considered as the market related components of uncertainty. It is worth mentioning that these sources of uncertainty can even affect the local market prices.

Since these parameters are more likely to experience variation over the control horizon, the proposed RRH controller improves the system robustness in face of market price deviation (i.e. α^p) and weather-related forecasted data uncertainty (i.e. α^w) over the control horizon by scheduling AB assets and benefiting from the participation of occupants. Note that these deviations will be obtained based on the control mechanism. To achieve this control philosophy, the RRH controller solves the following optimisation:

$$\max_{DV} \left\{ \alpha^t \left(\begin{array}{c} \min(\zeta) \times (1+\beta) \geq \zeta \\ \max(\Xi) \times (1-\beta) \leq \Xi \end{array} \right) \right\} \tag{3.34}$$

$$s.t:$$

$$\alpha^t = \omega \times \alpha^w + (1-\omega) \times \alpha^p \tag{3.35}$$

$$P_{j,t}^{PV} \leq (1-\alpha^w) \hat{P}_t^{PV_F} \tag{3.36}$$

$$V_t^N \leq (1-\alpha^w)\, \hat{V}_t^N \tag{3.37}$$

$$T_t^{out} \leq (1-\alpha^w) \hat{T}_t^{out} \tag{3.38}$$

$$\lambda_t^{I/E} \leq (1+\alpha^p) \hat{\lambda}_t^{I/E} \tag{3.39}$$

$$\zeta_j \leq \zeta_j^{l1} \tag{3.40}$$

$$(3.3) - (3.27) \tag{3.41}$$

In (3.34), the weighted sum method is utilised to obtain the maximum degree of robustness. The tolerable value of robustness degree which affects both objective functions is specified by parameter β, which is defined in the interval [0,1]. Assuming that the weather-related data affect photovoltaic unit output, natural illuminance level, and outside temperature, the robustness degree is multiplied by these input parameters in (3.36)-(3.38) respectively. Also, the effects of market price robustness degree is obtained in (3.39). Robustness degrees are defined in the interval [0,1].

Knowing that the previous studies which have investigated a robust market price framework [20] introduced a non-linear model such as constraint (3.39) , this equation has been linearised in this study through replacing the term $\lambda_t^I P_{j,t}^{G_I}$ by the variables $P_{j,t}^{G_L^1}$ and $P_{j,t}^{G_L^2}$ as follows:

$$\lambda_t^I P_{j,t}^{G_I} = \left(P_{j,t}^{G_L^1}\right)^2 - \left(P_{j,t}^{G_L^2}\right)^2 \tag{3.42a}$$

$$P_{j,t}^{G_L^1} = \frac{1}{2}\left(\lambda_t^I + P_{j,t}^{G_I}\right) \tag{3.42b}$$

$$P_{j,t}^{G_L^2} = \frac{1}{2}\left(\lambda_t^I - P_{j,t}^{G_I}\right) \tag{3.42c}$$

where the non-linear terms in (3.42a) are linearised using the method described in (3.12). The same approach is adopted to linearising $\lambda_t^E P_{j,t}^{G_E}$ and $\lambda_t^E P_{j,t}^{B4G}$.

3.4.4 Decision Variables

The decision variables of proposed RRH control method consist of temperature and illuminance level in each building, radius of uncertainties, imported/exported power from/to the main grid, output value of distributed energy resources, value of B2B and B4G, and ON/OFF status of appliances. Note that the other variables such as local prices, consumption power for delivering comfort, comfort indices, and demand level of each building are dependent variables which are obtained through solving the proposed problem along with optimising the values of decision variables. The set of decision variables (i.e. DV in equations (3.34) and (3.32)) are defined as below:

$$DV = \left\{ \begin{array}{cc} T^{B}_{j,t} & \forall j \in \psi_j, t \in \psi_t \\ V^{B}_{j,t} & \forall j \in \psi_j, t \in \psi_t \\ \chi^{Ap}_{j,i,t} & \forall j \in \psi_j, t \in \psi_t, i \in \psi_i \\ P^{G_{I/E}}_{j,t} & \forall j \in \psi_j, t \in \psi_t \\ P^{PV/CHP}_{j,t} & \forall j \in \psi_j, t \in \psi_t \\ P^{ESS_{c/d}}_{j,t} & \forall j \in \psi_j, t \in \psi_t \\ P^{B2B}_{j,t} & \forall j \in \psi_j, t \in \psi_t \\ P^{B4G}_{j,t} & \forall j \in \psi_j, t \in \psi_t \\ \alpha^{t} & \end{array} \right\} \tag{3.43}$$

3.5 Framework Description and Simulation Setup

3.5.1 Framework Description

Fig. 6.4 illustrates the framework of the proposed RMG controller. The input data is transferred to the data receiver. Then, for the time period t, the model is solved in three levels, starting from the first level where energy bill is minimised without B2B and B4G strategies. The local prices are determined in this level, while the value of energy bill is considered as a constraint for outer levels. The second level takes into account two conflicting objective functions, while the process ends up with the RRH which improves the robustness of the model in the same time window. The linking variables between second and third levels are energy bill and occupants comfort. At the end of each time period, the controller sends the control signals to the ABs and different assets while re-compiles the process for the next time-slot. This process is continued until the end of operation horizon, when the results for the whole period is analysed.

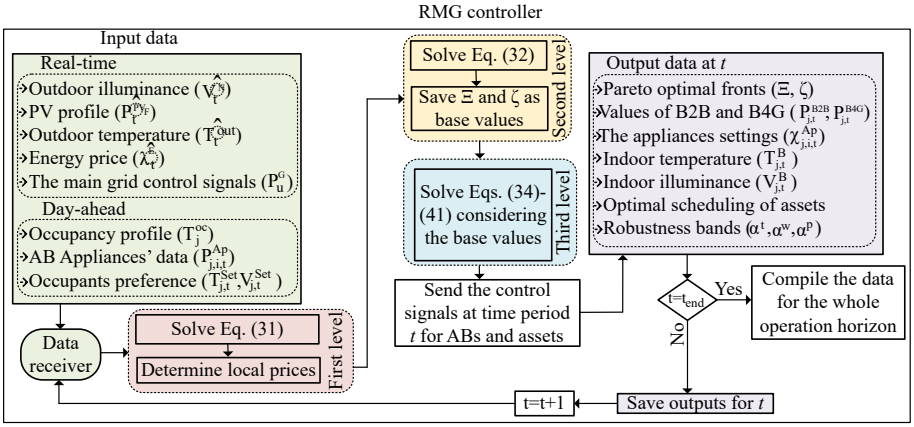

FIGURE 3.5: The process of solving the proposed multi-level optimisation by the RMG controller.

3.5.2 Simulation Setup and Case Studies

The proposed problem is an MILP model which has been simulated in general algebraic modelling system (GAMS) [96] using CPLEX solver. The simulation is performed for 24 hours, using 30-minute time windows, starting from 8:00AM. 10 ABs are considered in the RMG. Buildings are categorised into three types as a function of their occupancy profile. Fig. 3.6 illustrates the occupancy profile and comfort weighting factor index for each AB under normal operating condition and then during a winter day. Buildings are categorised into three types as a function of their occupancy profile. The bold, white and pale colours represents occupied, unoccupied and sleeping periods respectively. The information on buildings and included tasks in each one is given in Table 3.1. The electricity price, consumption pattern of each task, starting and ending time, as well as duration of each task is taken from [57]. The outside temperature, illumination, and PV output is taken from [97]. The characteristics of different technologies and various simulation parameters are given in Table 3.2. The supporting data are available online at [98].

The effectiveness of the proposed model is evaluated by the following case studies:

Case I: The proposed model without B2B and B4G strategies. This case study solves the second and third levels of the optimisation without AB flexibility measures.

Case II: The proposed model with B2B and B4G strategies. This case study is solved for different scenarios.

Case III: The proposed model in an abnormal condition. Case II is solved under different occupancy profile where ABs are always occupied. This case attempts to represent an abnormal scenario such as COVID-19 pandemic lockdown which changed the occupancy profile of residential buildings.

TABLE 3.1: Building and task description.

building No.	Type	Included tasks No.	Task No.	Description
j_1	3	$i_1 - i_{10}$	i_1	Dishwasher
j_2	2	$i_1 - i_6, i_{10}$	i_2	Washing machine
j_3	2	$i_7 - i_{10}$	i_3	Spin dryer
j_4	1	$i_1 - i_4, i_6 - i_7, i_{10}$	i_4	Cooker hob
j_5	1	$i_4 - i_{10}$	i_5	Cooker oven
j_6	3	$i_1 - i_{10}$	i_6	Microwave
j_7	1	$i_1 - i_4, i_8 - i_{10}$	i_7	Laptop
j_8	1	$i_1 - i_4, i_6 - i_{10}$	i_8	Desktop
j_9	3	$i_1 - i_{10}$	i_9	Vacuum cleaner
j_{10}	2	$i_5 - i_7, i_9 - i_{10}$	i_{10}	Fridge

TABLE 3.2: Simulation parameters.

Parameter	Value (unit)	Parameter	Value(unit)	Parameter	Value(unit)
$E_{u/l}^{ESS}$	4/0.4(kWh)	L_l^{flex}	0.7	COP	2.5
$P_u^{ESS_{c/d}}$	1/1(kW)	B	10	N	20
D_j^{th}	0.525 ($^\circ C/kWh$)	R_j^{th}	18 ($^\circ C/kW$)	κ_j	20
η_I^u	0.8	η_I^m	0.8	f_j	5000
$\eta_{ess}^{c/d}$	95/95(%)	A_j	150 (m^2)	β	0.15
$P_{j,u}^{HP}$	3(kW)	$\rho_{j,t}^{PV_{cr}}$	0.4	λ_t^G	2.7(p/kWh)

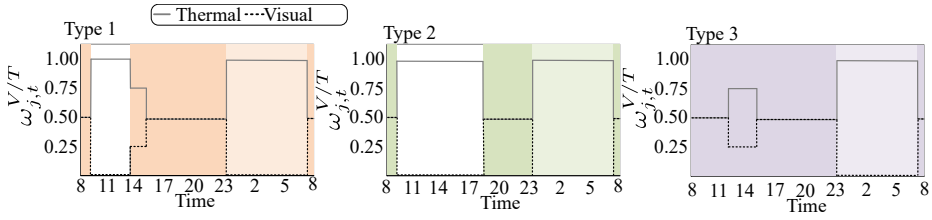

FIGURE 3.6: Occupancy profile and comfort weights of different buildings types.

3.6 Results and Discussion

The results obtained for the proposed model are analysed and discussed in this section through comparison of various case studies. The computation efficiency of the model is also tested.

3.6.1 Pareto Optimal Solutions

In order to investigate the impact of different strategies over the operation horizon, the Pareto optimal fronts for cases I, II, and III reflecting different strategies are depicted in Fig. 6.7. In these solutions, the value of ϵ (i.e. comfort level) is decreased from its maximum value to its minimum value while the energy bill is minimised. For example, in Case I (shown in blue in Fig. 6.7), the value of comfort index is decreased from 0.992 to 0.965 in different levels while the energy bill is minimised for each level. Different solutions and case studies are highlighted and compared in this figure. The main observations are:

1. The Pareto optimal solutions: the cost-optimal solution decreased the comfort index to its minimum allowable level, while comfort-optimal solution seeks temperature and illuminance values that are closest to the set points, resulting in more expenditure for the community. This solution is compatible to the thermostats that are used in the majority of buildings. The compromise solution makes a trade-off between comfort and cost. This solution provides 16.46% lower energy bill

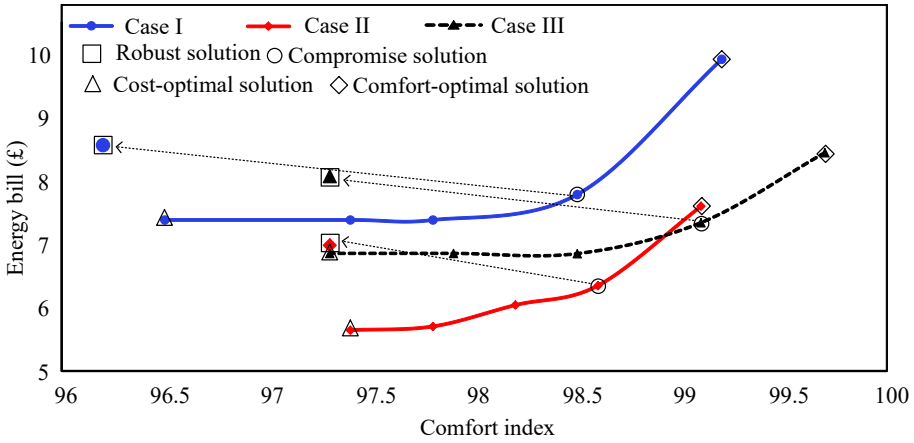

FIGURE 3.7: Pareto optimal front for multiple optimisation solutions.

compared to thermostat-controlled solution while keeping the comfort level close to set points (i.e. only 0.5% decrease compared to comfort-optimal solution). Therefore, this control framework could be a suitable alternative for the current thermostats in each building.

2. Advanced flexibility strategies: it is evident from comparing the solutions for cases I and II that participating in the B2B and B4G strategies brought about better solutions (from both viewpoints of cost and comfort) for ABs. The compromise and robust solutions in Case II are about 18.45% and 18.46% lower than those of Case I. From the comfort index point of view, the robust solution in Case II is 1.1% higher than that of Case I, demonstrating the effect of the proposed AB flexibility strategies in improving occupants comfort with lower cost. This results imply that the flexibility measures can improve the socio-economic aspects of buildings, while demonstrating the importance of local energy markets. It is crucial to consider the fact that the problem is solved from the RMG's perspective, while the advantages for the main grid, no need for expansion planning for instance, are important factors that should be taken into account.

3. Robust solution: the robust solution imposed more cost, while the occupants' expectation is slightly decreased. For instance, in Case II, for a 10% robustness improvement (i.e. $\beta = 0.10$) the energy bill

increases by 63 pence while the occupant comfort decreases 1.3%. This results demonstrates the role of building occupants in boosting the robustness of the proposed control strategy with a negligible cost.

4. Cases II and III: Case III represents constantly occupied ABs and therefore has to deliver greater comfort at a higher cost. Note that increasing comfort levels in Case III also increases the overall energy system loads. Therefore, it is crucial to consider the fact that the pandemics (e.g. COVID-19) can change the consumption pattern of dwellings, which should be taken into account during operation and planning of energy systems.

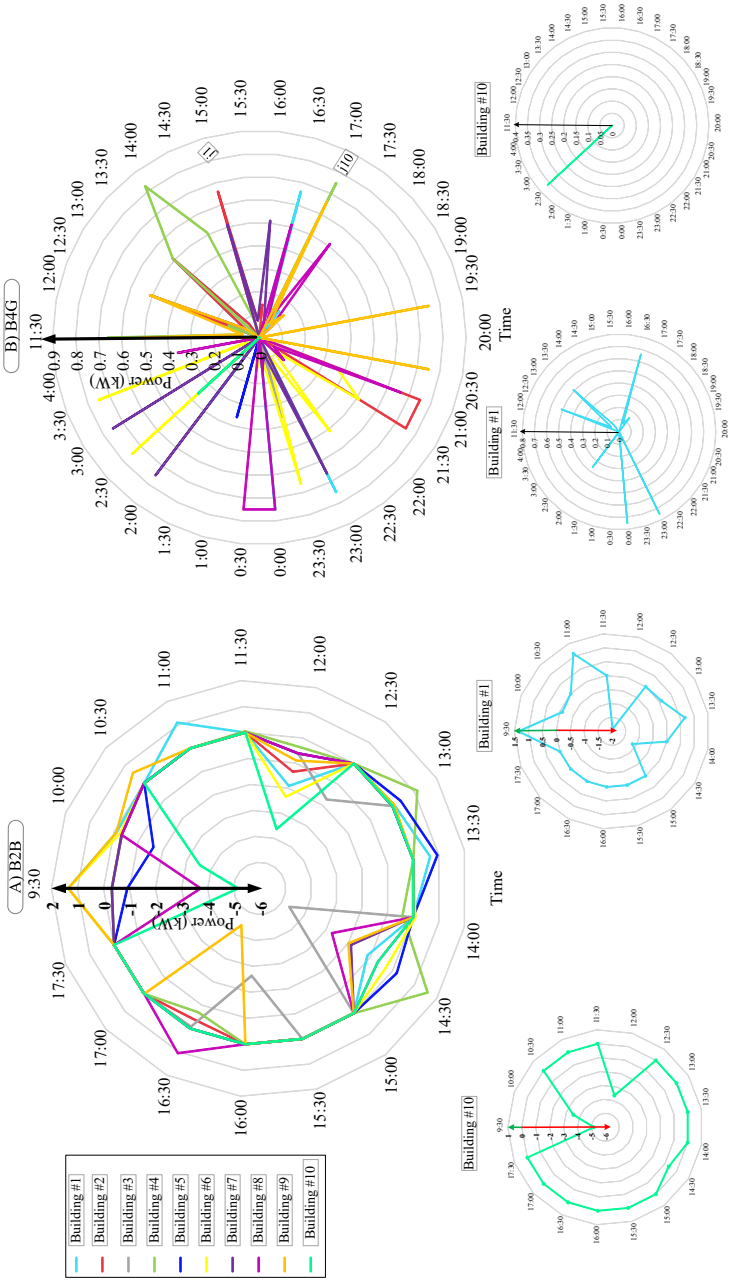

FIGURE 3.8: Power exchange in a) B2B and b) B4G strategies for buildings in the RMG.

3.6.2 Advanced Building Flexibility Values

Figure 4.4 demonstrates Case II scenarios with the left picture outlining the power exchange between ABs in the B2B strategy and the right picture outlining the flexibility service provided by B4G strategy. As an illustration, consumption patterns of buildings j_1 (type three building), and j_{10} (type two building) are separately illustrated on the outer edges of the figure. In the B2B strategy, type three buildings (i.e. occupied the whole day) mostly played the role of the receiver, as opposed to type two buildings (i.e. unoccupied during office hours) which can provide other ABs with their available capacity. Another decisive factor in B2B strategy is the starting time and operation window of buildings appliances, such that the buildings that need to start their tasks at hours with high rates of market price received more energy, compared to other buildings in the same category. For instance, building j_1 received more energy than j_6. In B4G strategy, type three buildings (e.g. j_1) are more active as they are equipped with more adjustable power consuming appliances. On the other hand, type two buildings (e.g. j_{10}) did not participate actively since they do not offer a full range of adjustable appliances. The lower the number of tasks, the less an AB can contribute proactively to the grid in B4G strategy. Therefore, it can be concluded that B2B strategy creates flexibility based on generation capacity and occupancy behaviour, while B4G strategy can be efficient for ABs with a higher operational profile.

3.6.3 Energy Exchange with the Main Grid

The energy exchange between RMG and the main grid in cases I and II is shown in Fig. 6.11. This figure shows that utilising the B2B and B4G strategies affected the power exchange with the main grid. The energy export to the main grid is zero in Case II (both scenarios). This demonstrates that ABs with excess generation have sold their power to other buildings, while those with energy needs purchased energy locally rather than importing from the main grid (see Fig. 4.4). Also, as shown in Fig. 4.4, ABs traded their flexibility in forms of B4G rather than selling it to the retailers with lower price. This strategy

can be an effective alternative for profit-seeking retailers who try to achieve a high retail profit from prosumers by offering high sell prices and low buy prices. In the grid level, it can delay the need for generation investment. On the other hand, comparing robust and compromise solutions of Case II shows how more grid power import occurs in former compared to latter. For example, at 17:00, the imported power from the main grid in robust solution is almost twice as much as that of compromise solution. This means that the decision made by RRH controller is robust against higher price deviation. In other words, in order to improve the robustness against the higher price deviation, the imported power is decreased or at least not changed, especially during high market price periods (i.e. from 19:30 to 23:00).

3.6.4 Role of Occupants

The effect of occupants comfort on the B2B interaction is illustrated in Fig. 3.10, where the power exchange of building j_1 over the control horizon is depicted for different levels of occupants comfort. As can be seen in this figure, building exchanged more power in the local market at lower values of occupants comfort index (i.e. 0.96). However, increasing the value of occupants comfort index resulted in a considerable decrease in participation of building in the local market. Therefore, occupant-related factors (i.e.

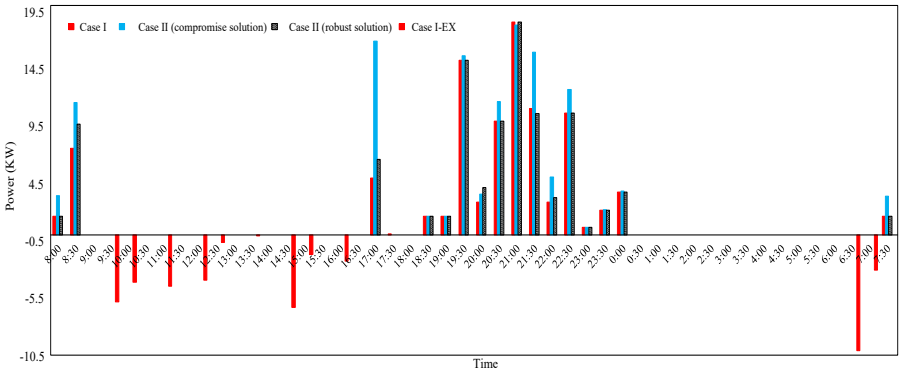

FIGURE 3.9: Energy exchange with the main grid in different cases.

occupant behaviour) can have a considerable influence on the energy interaction in the local markets.

The participation of occupants in improving the system robustness should not be neglected. Fig. 4.3 highlights the contribution of occupants in improving system robustness, by giving an example of the indoor temperature in robust and compromise scenarios of Case II for building j_1. In the compromise solution, the main goal of controller is to keep the temperature around the preferred set point given by the AB while considering the economic factors. Robust solution, however, experiences more fluctuation and lower temperatures, particularly under high market price periods (i.e. from 19:30 to 23:00). This demonstrates that AB occupants can have a considerable role in improving the RMG robustness by alternating their preferred comfort zones. These variations in the temperature of building has affected the comfort index, as shown in Fig. 4.3. It is evident from this figure that the comfort index of the AB fluctuated over the price variations, with slightly lower values in the robust solution. The result obtained for robust solution also shows how ABs can allow the controller to oversee a flexible indoor temperature in response to market price. In doing so, the building thermal inertia is utilised as an energy storage mechanism and indoor temperature is increased to above the set point in morning hours with lower market price and thereafter allowed to fall gradually. The intrinsically slow thermal response of most buildings is a major advantage to exploit as a virtual thermal storage resource. Thermal neutrality (or the ability of an AB to stay within comfort bands) is even more pronounced in well-insulated buildings.

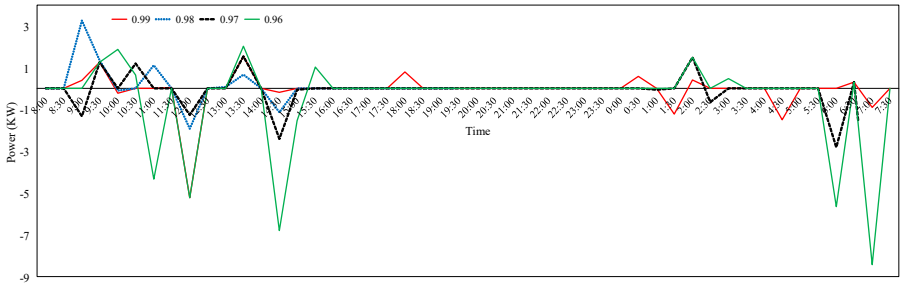

FIGURE 3.10: Variation of B2B value over different levels of occupants comfort.

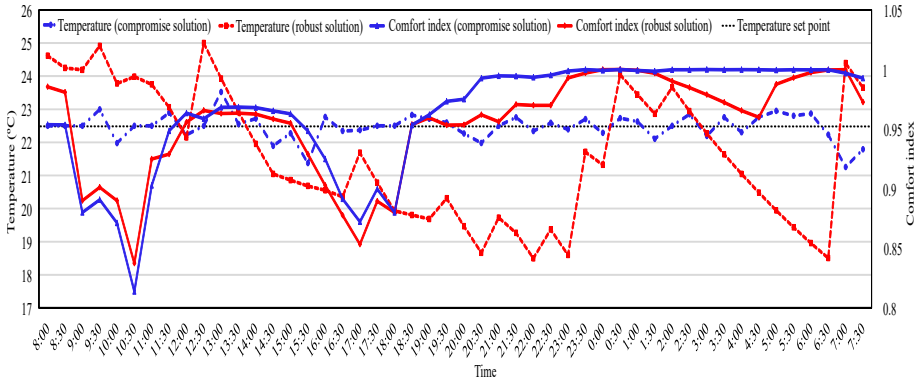

FIGURE 3.11: Variation of temperature and comfort index of building j_1 over the operation horizon for different cases.

3.6.5 Robustness Analysis

In the proposed RRH model, the tolerable value of robustness (i.e. β) and the robustness degrees' weighting factor (i.e. ω) are instrumental in how the robustness degree component performs. This is demonstrated by a sensitivity analysis in Fig. 3.12 that examines variation of α^t over the weighting factor ω for various levels of β. This figure shows that increasing ω raises the value of α^t. This can be interpreted with Equation (3.34) in mind, that increasing ω raises the weight of weather-related robustness, resulting in a dramatic increase in the value of α^t. In another words, it is easier to increase the weather-related robustness as opposed to that of the market price. Besides, increasing the value of β raises the robustness degree.

3.6.6 Computational Efficiency

In order to evaluate the computational and economic merits of the proposed model, it is benchmarked against the conventional rolling horizon method within three different scenarios: [I] S_1 which portrays an optimistic future horizon in which predicted data and the subsequent reality for those forecasts are the same; [II] S_2 with across a 3 hour future horizon assumes the real weather to be 30% different to the initial forecast and the market price to be

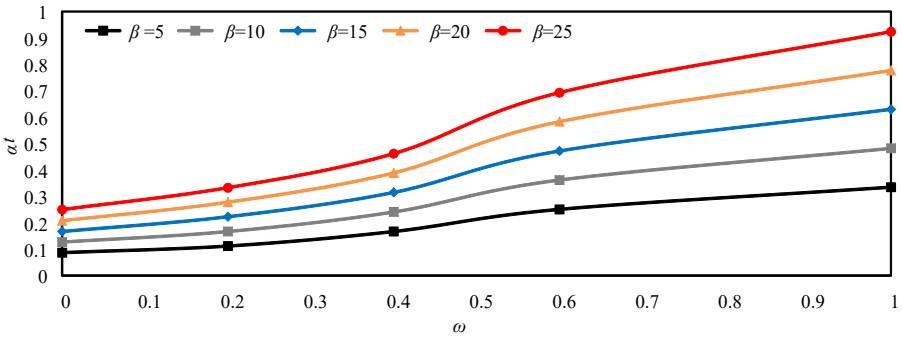

FIGURE 3.12: Variation of robustness over ω for different value of β.

15% different to the initial value and finally [III] S_3 which solves the same optimisation problem as S_1 using 5-min intervals (instead of 30 min). The results for these scenarios are outlined against the proposed RRH in Table 5.3. Scenario S1 solves the model in 34.21s at each time step, while the proposed RRH model takes 42.15s. Comparing scenarios S_1 and S_2 shows that deviations between initial forecast and subsequent reality results in more operational cost. To overcome this problem, S_3 solved the model at finer time intervals that yields 8.6% cost reduction (compared to S_2), but at a penalty of much higher computational time (i.e. 175.25 seconds each iteration). Against these results, the proposed RRH demonstrated superior performance in both computational (e.g. 76% lower compared to S_3) and economic aspects (e.g. 6.3% lower cost as opposed to S_2). The improved accuracy in scenario S_3 imposes considerably higher processing and computational costs which may be viewed as excessive in a residential context. These factors highlights the potential of the proposed RRH as an effective option for controlling RMGs.

TABLE 3.3: Computation efficiency of different techniques.

Scenario (time step)	Computation time (Sec.)		Operational cost (£)	Comfort index
	Per interval	Total		
S_1 (30 min.)	34.21	1,648.08	6.35	0.986
S_2 (30 min.)	34.21	1,648.08	7.13	0.985
S_3 (5 min.)	175.25	50,472.00	6.51	0.976
RRH (30 min.)	41.15	2,023.20	6.68	0.973

Finally, the computational time and accuracy of the proposed RRH controller, derived from the proposed MILP model is compared with those of MINLP model in Table IV, using different solvers. As shown in this table, the relative gap of zero is considered for the model, demonstrating the optimality of the solution obtained from the MILP model. This index shows the difference between the best integer and the best estimate solutions. As described in [99], zero or small relative gap is the indicator of measure of optimality and accuracy of the optimisation model. Furthermore, comparing the MILP and MINLP model demonstrates that the main issue for the later is its computational time. The BARON solver demanded 54.05 minutes for each time interval (i.e. 30 minutes), while DICOPT solved the model in 9.67 minutes. High computational time could be a barrier for MINLP models in a real-time application; since as per our finding, the computational time of BARON solver is twice the duration of the simulation time interval. The MILP solvers achieved a considerably lower computation time while also delivering the same comfort index (Table 3.4). A marginal difference is observed in the operational cost of MINLP and MILP models, which does not question the accuracy of Equation (3.42), and the whole formulation. Considering the residential skill of the proposed framework, it is important to achieve acceptable results without demanding an expensive processor. Besides, such control framework should be fast enough when considering the dynamics of the grid [19]. To summarise, these results show that the solutions of MILP model reflect those of original model, while achieving a significantly lower computational time.

Table 3.4: Comparison of MILP and MINLP models.

Model type	MINLP		MILP	
Solver	BARON	DICOPT	CPLEX	MOSEK
Computation time (min. per interval)	54.05	9.67	0.70	1.92
Operational cost(£)	6.70	6.70	6.68	6.68
Comfort index	0.973	0.973	0.973	0.973
Relative gap (%)	0	0	0	0

3.7 Conclusions

In this chapter, a multi-objective multi-level optimisation model is proposed for control and scheduling of building flexibility in the RMGs, consisting of a community of buildings and several small-scale distributed energy resources. An RRH controller is introduced which boosts the robustness of the system operation in the face of constant and uncertain changes over a short-term horizon. With an MILP model, the proposed controller benefits from considerably lower computation time when benchmarked against conventional methods. The role of ABs in providing flexibility for the energy networks is highlighted by introducing B2B and B4G strategies. The importance of social factors in the energy exchange between buildings is investigated through analysing the effect of occupants comfort on the building flexibility measures. Also, the role of building occupants in improving the system robustness in face of uncertain input data is analysed. The simulation results indicate human comfort and energy cost savings of these strategies and the efficiency of the RRH controller. Notable findings of this study are:

- The B2B and B4G strategies are viable flexibility approaches which exploit differences in timing and extent of occupant thermo-visual comfort to deliver an optimal comfort solution at community level while providing techno-economic advantages for the main grid.
- Utilising the B2B and B4G strategies in a local market level can create potential energy transaction between dwellings, which can bring about cost saving for the community. This can also delay the generation investment in a higher level.
- The RMG controller can be an efficient solution for the conventional thermostats. This controller can achieve desirable comfort zones while decreasing the energy bill.
- If the controller has the autonomy to decrease comfort expectation of AB occupants by 1.3%, the control robustness is improved by 10%. This shows the considerable role of building occupants in improving system robustness in face of uncertainty.

- Building occupants can play a critical role in energy exchange between dwellings. Increasing the occupants expectation in terms of comfort level can have a direct influence on the building participation in the local market.
- The RRH approach reduced the total computation time by approximately 76% when compared with the conventional controllers that for similar comfort and cost optimisation need to shorten simulation intervals from 30min to 5min leading to high computational penalties.

This chapter investigated the flexibility of AB and the advanced methods in unlocking flexibility. The next chapter investigates the role of EVs in boosting the AB flexibility.

4

Role of Electric Vehicles in Enabling Building Flexibility

The following research question has been answered in this chapter:

How can electric vehicles enable more flexibility in the buildings?

Energy systems have been experiencing fundamental changes because of the urgent needs for decarbonisation of these structures. Complying with the requirements of decarbonisation requires a major contribution from the transport sector. Therefore, electrifying the transport sector is considered as a valid plan. Although, linking the transport sector to the electricity network can have a major impact on the demand for electricity, it can present a substantial opportunity for increasing the flexibility. Optimal energy management of Electric vehicles (EVs) can bring about multiple advantages such as delaying transmission and generation investment, and increasing the penetration level of renewable energy sources (RESs) for the whole energy grid. In the building level, EVs can also provide varied advantages through

exploitation of flexibility. Optimal energy management of building assets along with EVs can be considered as a substantial plan in increasing the active building (AB) flexibility while considering the requirements of building users. EVs can even contribute to the advanced AB flexibility methods discussed in Chapter 3 (i.e. building to building (B2B) and building for grid (B4G)). This chapter investigates the role of EVs in enabling higher levels of flexibility in the ABs and the advantages they can bring about for the building owners. A multi-objective mixed integer linear programming (MILP) method is introduced for optimal energy management of EV-integrated buildings with consideration for the driving needs of EV users. The simulation results show that building users can decrease their energy bills through optimal management of EV charge/discharge patterns while utilising them for their transport needs. The results also demonstrate the effect of EVs on boosting the B2B energy exchange, highlighting the role of these technologies in improving the building flexibility.

Sections of this chapter have been published by the candidate as in the following conference paper:

Nikkhah S, Allahham A, Giaouris D, Bialek JW, Walker S. Application of Robust Receding Horizon controller for Real-Time Energy Management of Reconfigurable Islanded Microgrids. In2021 IEEE Madrid PowerTech 2021 Jun 28 (pp. 1-6). IEEE.

Sections of this chapter is under review in the following journal paper:

Nikkhah S, Allahham A, Patsios H, Taylor PC, Walker SL, Giaouris D. Building-to-Building Energy Trading under the Influence of Occupant Comfort. International Journal of Electrical Power & Energy Systems. 2023

Chapter roadmap: Section 4.1 demonstrates the motivation and research gap supported by this Chapter. The mathematical model of EV that has been developed for the control model of Chapter 3 is given in Section 4.2. The simulation setup and results are given in Section 4.3, while Section 4.4 concludes the Chapter.

4.1 Introduction

EVs can be a proactive player in the control and optimisation of building flexibility, as the consumer or even as the service provider for the building or grid. According to the recent global EV outlook, a significant increase in the number of EVs is observed over a year, passing 16 million in 2022, an increase of approximately 50% from the previous year [100]. The worldwide EV stock is shown in Fig. 4.1. Furthermore, EVs can also provide energy for the network, with their discharging properties, enabling them to be a service provider in a small scale, say as a nanogrid, consisting of smart home or a community of buildings. This characteristics of the EVs along with other available smart technologies, existing in smart homes, enable the concept of flexibility for the energy management strategies.

In the energy scheduling of active buildings (ABs), EVs are commonly regarded as a normal load [57]. However, these units are a complicated component of the network which can bring about several challenges for the grid [101]. These units proved to be an efficient storage device for ABs that can decrease the operational cost and co-operate with RESs in response to the price signal changes over the scheduling horizon [102]. This co-operation resulted in 77% decease in the operational cost in [103], which proposed a vehicle-to-building architecture for an residential microgrid (RMG) consisting

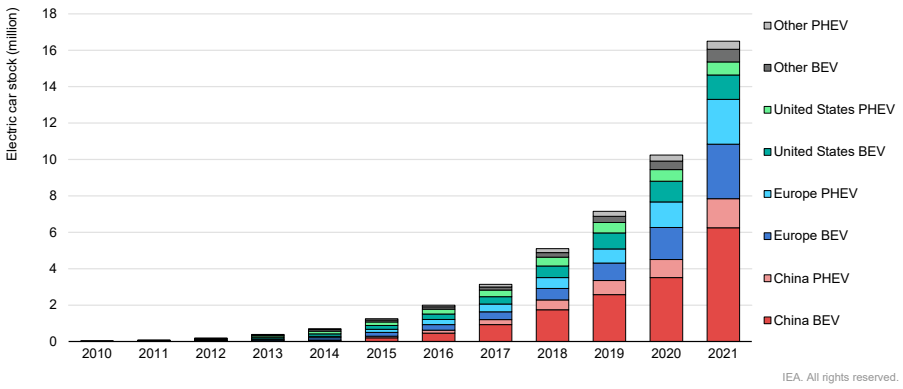

FIGURE 4.1: Worldwide EV stock [100].

of several distributed energy resources. Meanwhile, the driving pattern of EVs is a critical parameter that can effect their role in the energy management strategies [104]. Consequently, a real-time energy management strategy is introduced in [22] considering the driving pattern of EVs as an uncertain parameter, and their effect on the cost of the AB. However, the control strategy has not considered the occupants comfort in the decision making process, where cost related decisions and even EV participation can be affected by the building users preference. The importance of this concept was highlighted in Section 2.3.2.

Although the role of EVs in the smart grids has been widely investigated in the literature, there are some important factors that need more investigation, as outlined below:

(i) Electrification of transport vectors can influence the energy network and consequently building to buildig (B2B) energy trading. Therefore, it is necessary to investigate the effect of multiple-energy vector optimisation on the AB flexibility.

(ii) Although the role of EVs on the economic perspectives has been studied, occupants comfort can have its influence on the decision making process. The EVs' participation in providing flexibility can be affected by the users' preference.

(iii) The papers that have considered EV in energy management strategies have not taken into account EV's driving patterns. This is a simplistic modelling of EV behaviour since the power that is consumed in driving mode of these units is an important factor in definition of their state of charge.

Hence, this chapter attempts to address this gap by adopting a mathematical model for the EVs that is affected by the driving pattern. The effect of electrification of transport on the building flexibility will be studies through adding corresponding EV model to the energy balance model studied in Chapter 3. Furthermore, the effect of EVs on the occupant comfort is studied. Finally, the model investigates the effect of EVs on the B2B.

Therefore, this chapter is the continuation of the previous chapter by adding the EVs as a mobile storage that can be effected by occupants decisions.

4.2 Mathematical Model of EV

The operational model of the EV battery is similar to that of battery energy storage (BES). However, considering the power consumed by transport vector and its effect on the availability of EVs in providing services for the ABs, the operational model of these units should be adopted. Also, participation of an AB in the B2B market is similar to the BES. The mathematical model of EVs is given in the following.

$$E_{j,t}^{EV} = E_{j,t-1}^{EV} + \Delta t P_{j,t}^{C_{ev}} \times \eta_{ev}^{C} - \Delta t P_{j,t}^{D_{ev}} \Big/ \eta_{ev}^{D} - \Delta t P_{j,t}^{T_{ev}} \tag{4.1}$$

$$E_{j}^{EV_{Min}} \leq E_{j,t}^{EV} \leq E_{j}^{EV_{Max}} \tag{4.2}$$

$$0 \leq P_{j,t}^{C_{ev}} \leq B_{j,t}^{C_{ev}} \times P_{j}^{C_{ev}^{\max}} \tag{4.3}$$

$$0 \leq P_{j,t}^{D_{ev}} \leq B_{j,t}^{D_{ev}} \times P_{j}^{D_{ev}^{\max}} \tag{4.4}$$

$$B_{j,t}^{D_{ev}} + B_{j,t}^{C_{ev}} \leq 1 \tag{4.5}$$

$$B_{j,t_{dr}}^{C_{ev}} = B_{j,t_{dr}}^{D_{ev}} = 0 \tag{4.6}$$

where Equation (4.1) denotes the state of charge of EV, which is defined based on the value of energy in the previous time period, charging/discharging power, and the power consumed for the transportation. Note that this model is only applicable for those buildings which have EVs. Constraint (4.2) limits the

state of charge of EV, while constraints (4.3) and (4.4) limit the charging and discharging power of EV. Constraint (4.5) prevents simultaneous charge and discharge while (4.6) indicates that no charging and discharging happens in the time periods that the EV is on the road (i.e. t_{dr}).

Therefore, the energy balance in Equations (3.13) is changed as below:

$$\begin{aligned} &\sum_{i\in\psi_i}\left(\chi^{Ap}_{j,i,t-o}P^{Ap}_{j,i,o}\right)+P^{I}_{j,t}+P^{ESS_c}_{j,t}+P^{G_E}_{j,t}+P^{C_{ev}}_{j,t} \\ &=P^{G_I}_{j,t}+P^{HP}_{j,t}+P^{PV}_{j,t}+P^{ESS_d}_{j,t}+P^{B2B}_{j,t}+P^{D_{ev}}_{j,t} \end{aligned} \tag{4.7}$$

Also, the following equation is added to the energy balance to show the effect of transport on the control model.

$$P^{T_{ev}}_{j,t}=\Delta D^{EV}_{j,t}\times\eta^{t}_{ev} \tag{4.8}$$

4.3 Results

Thanks to the linearisations that have been done in Chapter 3, an MILP model is created which has been processed in GAMS using CPLEX solver. The building data is given in Table 3.1. Assuming the 8:00AM as the starting point of operation, the simulation is performed for 24 hours. The parameters of EVs is given in Table 4.1 [105]. The driving distance of EVs is given in [104].

In order to evaluate the effectiveness of the proposed model, the following case systems are studied.

Table 4.1: Technical parameters of EVs [105].

Parameter	value (unit)	Parameter	value (unit)
$E^{EV_{Max}}_{b}$	15 (kWh)	$E^{EV_{Min}}_{b}$	5 (kWh)
$P^{C^{\max}_{ev}}_{b}$	6 (kW)	$P^{D^{\max}_{ev}}_{b}$	6 (kW)
η^{C}_{ev}	93(%)	η^{D}_{ev}	93(%)
η^{t}_{ev}	(1/6)(kW/km)		

Case I: the best compromise solution of the proposed multi-objective model with EVs.

Case II: the proposed model with EVs from the viewpoint of comfort maximisation. This case study is solved as a single-objective optimisation.

Case III: the proposed model with EVs from the viewpoint of cost minimisation. This case study is solved as a single-objective optimisation.

Case IV: the proposed multi-objective model without EVs.

Figure 4.2 depicts the Pareto optimal front for the proposed multi-objective model, while the solutions obtained in cases I, II, and III are also marked in this picture. As can be seen in this figure, when the operational cost is minimised solely, the comfort index is at its lowest value, meaning that the illuminance level and temperature are set at their lowest points. On the contrary, maximising the comfort index raised its value exponentially, whereas the value of operational cost is increased as well. Meanwhile, the values obtained for the best compromise solution are a trade-off between these objective functions.

In order to evaluate the indoor temperature in the in the aforementioned cases, Fig. 4.3 is depicted, illustrating the temperature inside building j_1 for the operation horizon. It is evident in this figure that Case II fixes the

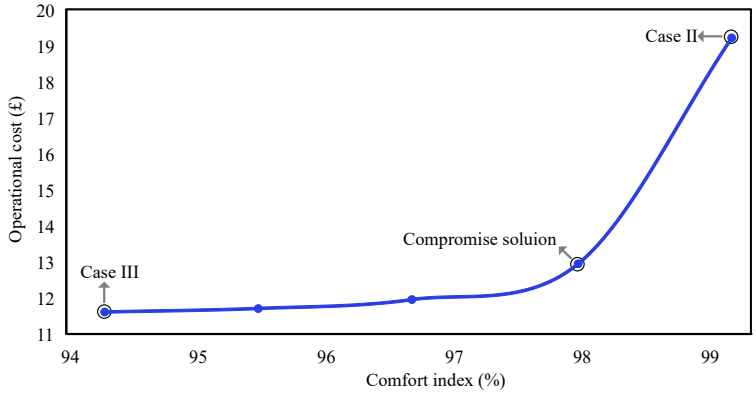

FIGURE 4.2: Pareto optimal front of the proposed multi-objective optimisation.

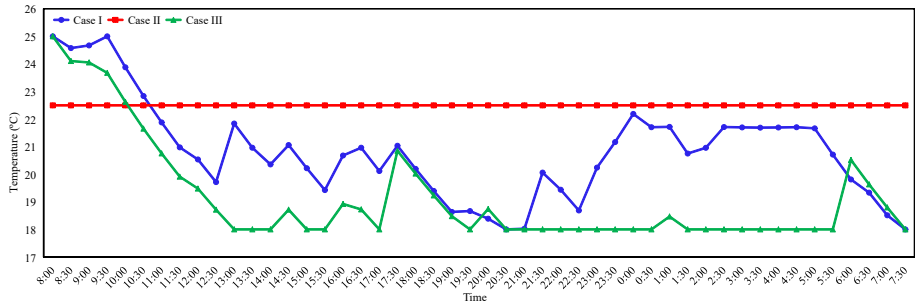

FIGURE 4.3: Variation of the indoor temperature in different cases.

temperature at the set point (i.e. 22.5 °C), while it fluctuates for the other cases, especially Case I which tries to optimise results from both perspectives of cost and comfort. The temperature in Case III is around the minimum point. An important fact that could be observed in this figure is increasing temperature above the set point in cases I and III, and decreasing afterwards. This pattern is similar to the application of energy storage which charge in low electricity price hours and discharge in peak hours. Therefore, the ABs can act like a virtual thermal storage with proper scheduling of their incorporated elements.

The participation of ABs in the B2B program is depicted in Fig. 4.4. This figure is only depicted for the hours that the dwelling units participate in the program, while the right hand side of the picture zooms the figure for the buildings j_1 and j_3, which have been categorised into type three and two houses respectively. This picture demonstrates the active participation of ABs in the B2B program. Comparison of the results for the buildings j_1 and j_3 shows that the former participated mainly as the consumer, since this AB is assumed to be occupied during the whole operation horizon, while the latter's role in the B2B is mainly as the provider, because it is unoccupied from 9:00 to 18:00 and equipped with lower number of tasks.

The Pareto optimal solutions of the proposed multi-objective problem is shown in Fig. 4.5, so as to demonstrate the role of EVs in the RMG. This figure proves the significance of these units in decreasing the energy bill. The value of entire community's energy bill over the scheduling horizon for the compromise solution in this case is £23.19, compared to that of Case I which was £12.95 (i.e.

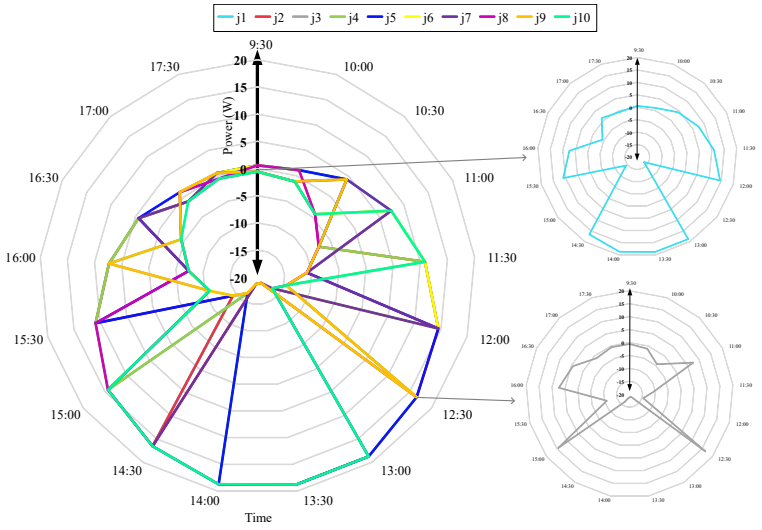

FIGURE 4.4: Power exchange in B2B strategy for building number $J1$ to $J10$.

44% decrease). Therefore, integration of EVs into the AB flexibility can affect the economic goals of the community while keeping the occupants comfort in an acceptable range.

The optimal energy scheduling of the proposed model for Case I and the best compromise solution of Case IV is illustrated in Fig. 6.11. This figure clearly shows the importance of EVs in activating the energy exchange between ABs and the main grid, such that the power exported to the main grid increased

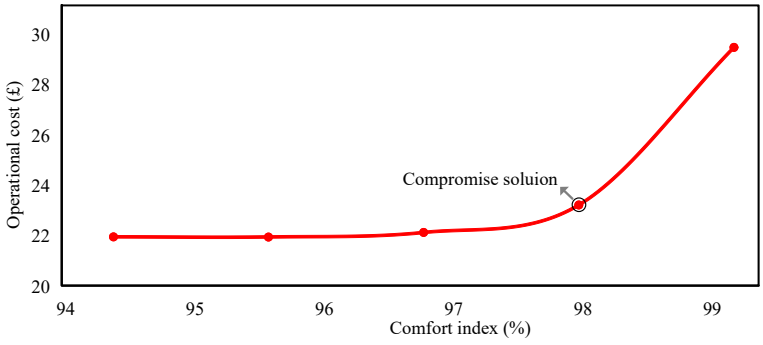

FIGURE 4.5: The Pareto optimal solutions without EVs.

considerably. This means the EVs can increase the value of flexibility for the ABs. On the other hand, in the Case IV, the RMG mainly supplies its load through the energy imported from the main grid.

Finally, the computation efficiency of the proposed MILP model is verified against the MINLP (i.e. Eqs. (3.7) and (3.10) are non-linear) in Table 5.3. The results show that the MINLP model exponentially increased the computation time while it failed to obtain a global optimal solution, as opposed to the MILP model.

4.4 Conclusion

This study proposed a multi-objective energy management system for a community of ABs that form an RMG, consisting of different assets such as

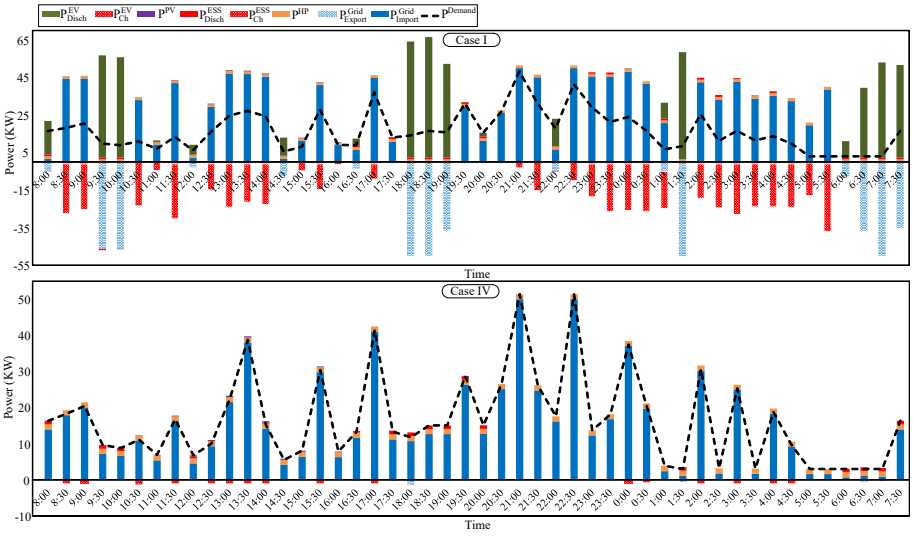

FIGURE 4.6: Optimal energy scheduling in cases I and IV.

TABLE 4.2: Computation efficiency of the different models.

Model	Computation time (Sec.)	Operational cost(£)	Comfort index (%)
MINLP	4049.92	13.46	98.4
MILP	21.96	12.95	98

BES, PV, and heat pump. In addition, a EV is considered for each AB which can contribute to the energy management of the community by charging in off-peak hours and discharging in the peak hours, whereas it should comply with the transport needs of occupants. In addition, a B2B strategy is introduced for each dwelling unit to show the importance of energy exchange between ABs. Generally, the main conclusions of this study are summarised as follows.

- Energy management of ABs requires consideration of multiple goals which often pivots around a compromise arrived at by solving techno-economic constraints assuming that social willingness of occupant is secured..
- The B2B strategy is an efficient approach for activating the energy exchange between ABs.
- EVs can decrease the operational cost of RMGs by 44% while they can increase the energy exchange between ABs' community and and consequently the value of flexibility.
- An AB can be considered as a virtual thermal storage, by optimal energy scheduling of HPs and other similar primary energy conversation assets.

The previous chapters investigated the AB flexibility and the advanced methods in activating higher levels of flexibility in the dwellings. Next chapter will investigate flexibility in a higher level by studying the application of integrated demand, DER, and network flexibility in preserving system stability.

5

Distributed Flexibilities for Preserving System Stability

The following research question has been answered in this chapter:

To what extent can distributed flexibilities be used to preserve system stability?

Coordination between transmission and distribution network is a major challenge for secure and stable operation of the whole power system. The lack of an efficient coordination framework can have major economic and operation loses for the system operators. This challenge is even more crucial in an event of contingency, where a sudden change in the system can bring about significant load curtailment. Due to the importance of flexibility in the in energy network (as discussed in Chapter 1), it can be deployed by system operators to preserve system security and prevent major load curtailment. This chapter investigates the effect of flexibility on the secure coordination of transmission and distribution networks. The aim is to show how flexibility in distributed energy resource (DER), demand, and network topology can be deployed to preserve the whole system voltage stability margin requirements. Therefore, a coordination scheme is proposed for the transmission and

distribution network while focusing on the role of flexibility in preserving voltage stability. A decentralised control framework is proposed for coordination of transmission and distribution networks while maintaining the voltage security of the whole integrated system using different flexibility methods. At the transmission level, the transmission network operator (TSO) solves a centralised optimisation problem to minimise the system load curtailment while maintaining the system security margin from voltage stability point of view. The TSO communicates the required set-points in the interface with distribution grids to the distribution system operators (DSOs.) At the distribution level, the DSOs utilise their available distributed flexibilities, such as conservation voltage reduction (CVR) as the demand flexibility, DER scheduling as the DER flexibility, and feeder reconfiguration as the network flexibility to provide the required set-points and preserve the whole system security margin, with minimum load curtailment. This decentralised optimisation scheme preserves the system security with minimum information exchange between operators, as well as minimum physical load curtailment. The distributed flexibilities of all DSOs are utilised to meet the required security margin of the whole system. The results show that the distributed flexibilities are capable of reducing the system demand to preserve the desired security margin, without any need for imposing direct load curtailment.

Sections of this chapter is published in the following journal paper:

Nikkhah S, Rabiee A, Soroudi A, Allahham A, Taylor PC, Giaouris D. Distributed Flexibility to Maintain Security Margin through Decentralised TSO-DSO Coordination. International Journal of Electrical Power & Energy Systems. Volume 146, March 2023, 108735

Chapter roadmap: Section 5.1 provides an introduction on the coordination of TSO and DSO and provides a brief literature review on the applications of flexibility; the research gap covered by this section is discussed and the methods to fill the gap is explained. Section 5.2 explains the framework of the proposed TSO-DSO coordination. Mathematical formulation is introduced in Section 5.3. Section 5.4 explains the solving

process of the decentralised optimisation approach. The simulation results are given in Section 5.5. Finally Section 5.6 concludes the paper.

5.1 Introduction

Restructuring within the electricity power industry has created opportunities for small businesses, enabling more competition and possibly ending electricity market monopolies. It has also enabled the engagement of DSOs in the energy markets. Despite substantial opportunities created by this new paradigm, the lack of sufficient coordination between TSO and DSOs can create critical challenges, especially during an emergency condition (e.g. sudden changes in the system load or generation failure) in the network. The UK power outage in 2019 can be an example of lack of TSO-DSO coordination, where millions of customers at the distribution level were disconnected from the main grid by under-frequency load shedding [90].

This event highlights the necessity of cooperation between TSO and DSOs. The cooperation between operators can enable a coordinated control architecture in the whole network [106]. Although a coordinated scheme allows the DSOs to have a direct role in the market, in practice, TSOs are still responsible for the secure operation of the whole system [107]. Consequently, under emergency conditions, TSOs can disconnect the distribution feeders and all of their connected loads to preserve system security. This, however, can bring about significant techno-economic losses to the system managers. Therefore, system security is a challenge that questions the effectiveness of available TSO-DSO coordination models [108]. A practical coordinated framework should enable flexibility in the DSOs to preserve system security. This raises an important question (recently considered in the Global Power System Transformation Consortium's Research Agenda Group) [109]: *"How can grid topology be flexibly adapted to various operating conditions?"*

In the literature, network flexibility is mainly achieved through optimal management of different types of DERs at the distribution system level. In [110], a reserve provision capability method is utilised for estimating the reserve requirement of TSOs and the capability of DSOs in complying with the upper-level needs. This proposed model is solved for a planning stage, however, it has not considered the sudden changes in the operation of the coordinated system. The capability of distribution networks in providing

reactive power support for the transmission system is studied in [111], where intermittency of renewable distributed generation units is considered, with the authors proposing a capability chart for investigating the effect of uncertainty on the service provision. In [112], the influence of local markets on the TSO-DSO coordination is investigated with a bi-level optimisation problem considering the conflicting objectives. The results show that both TSOs and DSOs should consider a budget to be robust in face of renewable power generation uncertainty. Reference [113] proposed a real-time energy management strategy for distribution systems, analysing various flexibility services that could be provided for the transmission level in the interface of these networks.

The cooperation between transmission and distribution systems is subjected to several technical and operational challenges, which have been summarised in [107]. These aspects can also affect the policies of cooperation. Each entity has its own objectives. For example, TSOs might aim to minimise their costs. DSOs focus on addressing the reliability of load supply. These different objectives create a substantial challenge in terms of information exchange privacy [114]. A decentralised control approach could address this coordination challenge.A decentralised coordination scheme for distributed generation units is proposed in [12] to meet the reactive power set-points of the TSO-DSO interface, with the aim of minimising the power losses while satisfying the distribution grid constraints. The authors also proposed a control scheme for on-load tap changer so as to unlock higher level of reactive power flexibility. A market clearing framework is proposed in [115] for trading the flexibility provided by the distributed generation in the distribution level. The results show that the flexibility in the distribution level can affect the locational marginal prices in the transmission level. A decentralised control model is introduced in [116], where the DSO and TSO solve their own optimisation and balance the reactive power in their interface. This iterative approach in coordination is also utilised in [117]. Yuan *et al.* [118] proposed a hierarchical coordination approach based on the economic dispatch, where DSOs solve their optimisation at an upper level and report the solution to the TSOs. The final solution is achieved in an iterated manner. Considering the high rate of (R/X) in the distribution systems, however, a simple economic

dispatch or a DC-OPF cannot reflect the operational and dynamic characteristics of the network [119]. In [120], a diagonal quadratic approximation method is utilised for coordinating the OPF problems of the TSOs and DSOs. The security of the coordination with the least information exchange remains a challenge in available methodologies.

Preserving the integrated system security is a challenging issue of the coordination [121]. An important indicator for evaluating system security is the voltage stability margin [122, 123]. Therefore, voltage stability assessment has been followed by researchers to evaluate the security of TSO-DSO coordination. A joint static voltage stability analysis is introduced in [124] for evaluating the security of integrated distribution and transmission systems. In [125], voltage stability requirement is translated into the need for reactive power and a methodology is proposed to defer investment in reactive power compensation equipment while satisfying the required margin through optimal control of synchronous and non-synchronous generation units. The impact of DER technologies installed in the distribution level is shown by the authors. Tang *et al.* [126] compared the accuracy of data-driven methods with the OPF-based models in the coordination of TSO and DSOs. The positive role of flexibility services, provided by the distribution networks, on the heavily loaded buses of the transmission network is shown in [127]. The dynamics of the distribution system are neglected and the evaluation of transmission contingency analysis is performed based on the forecasted load and generation. In [5], the role of distribution network in providing the voltage support for the transmission level is studied in a real-time centralised optimisation method. A model-free framework is introduced in [128] for exploiting the flexibility provided by the low-voltage level DERs in order to provided voltage support both in normal and emergence condition for the transmission network. Reference [129] proposed a security constrained unit commitment for TSO-DSO coordination with the aim of reducing the computational time. In an emergency condition, however, the objective functions of system operators would focus on secure operation of the system rather than a cost-optimal unit commitment. The main challenge that remains, however, is how to introduce security measures as critical components of TSO-DSO coordination.

TABLE 5.1: Taxonomy of control models in TSO-DSO coordination literature.

	Flexibility measure				Control method		Power flow constraints		
Ref. No	DER	Reconfiguration	CVR	load	Centralised	Decentralised	Transmission network	Distribution network	Voltage stability
[110, 111, 113, 125]	✓	x	x	x	✓	x	x	✓	x
[112, 116, 118, 120]	✓	x	x	x	x	✓	✓	✓	x
[12, 117]	✓	x	x	x	x	✓	x	✓	x
[115]	✓	x	x	✓	x	✓	✓	✓	x
[124]	✓	x	x	x	x	✓	✓	✓	x
[126]	✓	x	x	x	✓	x	✓	✓	x
[5, 127]	✓	x	x	✓	✓	x	x	✓	x
This chapter	✓	✓	✓	x	x	✓	✓	✓	✓

The taxonomy of TSO-DSO coordination mathematical models is shown in Table 5.1. Although the coordination between TSOs and DSOs has been studied before, the amount of data exchange, distribution system flexibility, and system security are three important considerations that need more investigation.

1. With increasing numbers of distribution systems connected to a transmission network, it is important to reduce the volume of data exchange. This can help in optimising TSO problems with short computational time. Therefore, an efficient method that solves the optimisation on both sides with the least information exchange and while preserving the system security needs to be developed.

2. The study of distribution system flexibility focuses mainly on the potential of distributed generation to provide services for the upper network in a normal situation. Nevertheless, there are other practical methods that should be studied for evaluating the distribution level flexibility under different circumstances including an emergency condition (e.g. conservation voltage reduction and network reconfiguration).

3. Although voltage stability analysis has been studied to evaluate the security of TSO-DSO coordination, it is not considered a critical constraint in designing decentralised optimisation models. This security measure should be added to the OPF model of decentralised optimisations of TSO and DSO. Such a scheme should highlight the importance of DSOs in preserving the security of TSO-DSO coordination.

This chapter aims at addressing these challenges by introducing a decentralised security-constrained TSO-DSO coordination framework. The proposed method investigates the practical flexibility options at the distribution level for preventing load curtailment in an emergency condition. A decentralised control architecture is proposed for optimising the critical components of the power flow model (i.e. active/reactive power, and voltage magnitude) in the interface between transmission and distribution networks. Rather than considering models of coordination, this method is designed to achieve optimal values in the boundary points connecting the transmission and distribution networks. To ensure secure coordination, the proposed model considers the loading margin as the security measure. This measure should be satisfied under different circumstances. The TSO optimises the system operation while preserving the system security. The desired values of power exchange and voltage level in the interface are sent to the DSOs. To respond to the required set-point given by the TSO, the distributed DSO optimisers try to benefit from available network flexibility options while respecting the integrity of their internal constraints. The first promising flexibility option is the use of voltage regulators in the distribution level, as the demands are voltage-dependent. This scheme is widely known as conservation voltage reduction (CVR) [13]. The next network flexibility option is the reconfiguration of the distribution network, which has been used to improve different techno-economic characteristics of distribution grid separately [14]. The solutions of DSO optimisers are sent to the interface and compared with the requirement of TSO. This process is repeated by optimisers until a degree of convergence is achieved. If the DSOs fail in satisfying the required boundary points, they would apply the load curtailment to preserve the security of the whole system. This paradigm highlights the role of DSOs in providing flexibility measures for preserving the TSO-DSO coordination. This framework can converge with a small number of iterations and with a short computational time (only seconds), which enables it as a suitable practical TSO-DSO coordination scheme for research and industry. The main contributions of this chapter are:

- A decentralised control framework is introduced for TSO-DSO coordination with the least information exchange between them. In this

method, DSOs use their available flexibility measures or/and load curtailment to comply with the requirements of the TSO. This proposed method benefits from short computational time spans and achieves the required convergence degree with a small number of iterations.

- Distributed optimal DER scheduling, conservation voltage reduction and network reconfiguration are adopted as the flexibility measures preserving the security of TSO-DSO coordination with minimum physical load curtailment. In the upper level, the TSO ensures the minimum loading margin for the transmission network considering the critical components of the power flow model. In the lower-level distributed optimisation models, DSOs aim at minimising the actual load curtailment, using the available flexibility options. Each DSO provides a different level of flexibility in the proposed distributed framework. However, the total flexibility provided comply with the requirements of the TSO.

- The transmission network's loadability constraint is considered as the main security margin influencing the TSO-DSO coordination. This index can be utilised as a measure for evaluating the degree of security of TSO-DSO coordination.

5.2 Framework Description

A visualisation of the proposed TSO-DSO coordination framework is presented in Fig. 5.1. This framework is suggested for a known number of parallel distribution feeders that are connected to a transmission network in the interface of these networks. Based on this architecture, an optimisation problem is first solved by the TSO. Since voltage stability is an important security criterion in the cooperation between TSO and DSO [124], it can be considered as the main influence on the coordination between networks. Accordingly, the optimisation in the transmission level always considers a degree of loading margin (i.e. security margin) as an important constraint of the model. This is shown in the upper left-hand side of Fig. 5.1. In this

regard, a sudden change in the system load (e.g. increasing above the generation capacity) can create security issues for the TSO if the aim is to keep the loading margin in the preferred range.

In a conventional TSO-DSO coordination scheme, the TSO optimiser is more likely to apply load curtailment to some heavily loaded buses which are connected to the lower-level distribution grids. However, TSOs can benefit from the flexibility measures in the distribution networks. The methodology designed in this chapter highlight the role of the flexibility measures in the distribution networks for preserving the system security. Therefore, the outcomes of the TSO optimiser in the point of connection with the distribution grids are sent to the distributed DSO optimisers. These values are shown with $U_{1...n}^{TSO}$ in Fig. 5.1. Each DSO compiles its distributed optimisation based on the received data. To prevent load curtailment, DSOs try to utilise the available flexibility options in the distribution level to comply with the requirements of the TSO. To do so, they utilise the CVR to

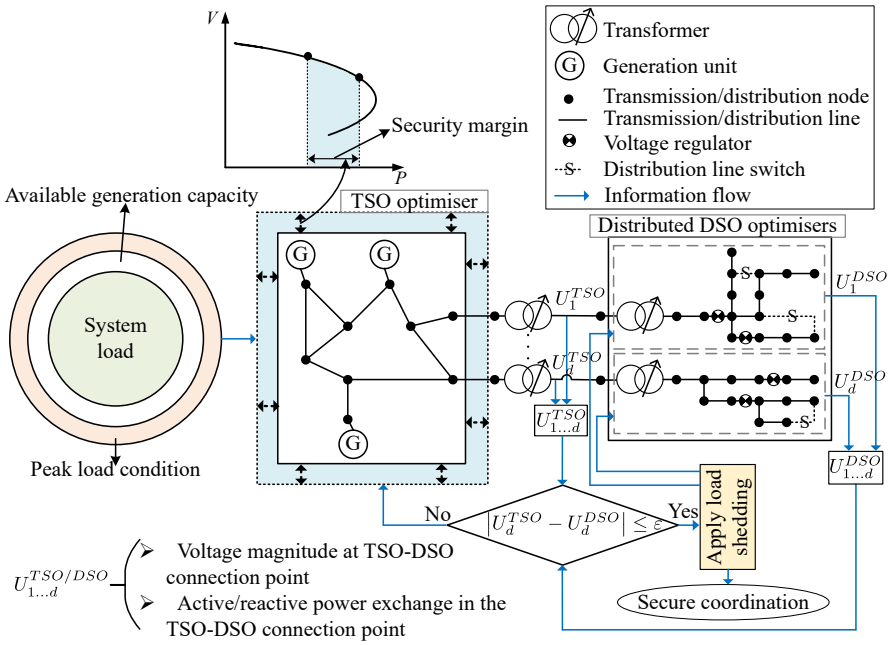

FIGURE 5.1: Conceptual illustration of the proposed architecture.

adjust voltage within the permissible range which can result in load reduction. Simultaneously with this strategy, the DSOs adopt the network reconfiguration to decrease the power loss and improve the voltage profile. After applying these strategies to the distribution network via an optimisation model, the DSOs compare the preferred values (i.e. $U_{1...n}^{DSO}$) with those received from the TSO. If the values are lower than that of the TSO, they are sent to the TSO optimiser for another round of optimisation. This process is repeated until the DSO values are equal or bigger than those of the TSO. The DSOs would apply load curtailment if they cannot decrease their load level to preserve the security of coordination. The proposed method converges in a small number of iterations and respects data privacy by considering only critical components of the power flow model in the interface of the networks.

It is worth mentioning that this framework investigates the role of distributed flexibilities in TSO-DSO coordination while complying with the security margin. Therefore, it does not address the sizing of distribution networks. The number of distribution networks is assumed as a known parameter. In the meantime, sensitivity analysis has been performed to show the variation of the results over the changes in the number of distribution networks.

5.3 Formulation of the Proposed TSO-DSO Coordination Framework

The proposed formulation for the decentralised control method is illustrated in Fig. 5.1. At the transmission level, the optimisation is solved with the aim of minimising the load curtailment under a peak loading condition while satisfying the required loading margin (i.e. security margin). The desired solutions of the optimisation in the connection point with the distribution networks are reported to the DSOs. The distributed DSO optimisers then utilise their available flexibility options to minimise the value of load curtailment and the difference between their required decision variables in the point of connection with the upper network. The following subsections express the mathematical model of the optimisation at each level.

5.3.1 TSO Centralised Optimiser

At the transmission network level, the TSO optimiser aims at minimising load curtailment and the difference between set-points in the interface with the distribution networks under a peak loading condition (i.e. emergency condition) while satisfying the operational and security constraints.

5.3.1.1 Objective function

The objective function of the TSO is given below:

$$OF^{TSO} = \min\left\{w_1 \times of_{lc}^{tso} + (1 - w_1) \times of_{dif}^{tso}\right\} \tag{5.1}$$

$$of_{lc}^{tso} = \sum_{b \in \Omega_b} P_b^{LC} \tag{5.2}$$

$$of_{dif}^{tso} = \sum_{b \in \Omega_b} \begin{pmatrix} \left|(P_b^D - P_b^{LC}) - p_b^{I_{dso}}\right| \\ + \left|(Q_b^D - Q_b^{LC}) - q_b^{I_{dso}}\right| + \left|V_b - v_b^{I_{dso}}\right| \end{pmatrix} \tag{5.3}$$

Equation (5.2) represents the load curtailment in the transmission system, while Eq. (5.3) is the difference between the set-points in the interface with the distribution networks.

5.3.1.2 Power flow and network constraints

Concerning the security of the system, it is necessary to consider the current operation power flow constraints in the transmission level simultaneously with those of the security limit point (SLP). This level also contains physical and operational constraints of the transmission grid (e.g., voltage magnitude/angle). The power flow and network constraints at the current operation point (COP) of the network are presented as below ($\forall b, j \in \Omega_b$):

$$P_b^G + P_b^{LC} - P_b^D = V_b \sum_{j \in \Omega_b} V_j Y_{bm} \cos(\theta_b - \theta_m - \phi_{bm}) \tag{5.4}$$

$$Q_b^G + Q_b^{LC} - Q_b^D = V_b \sum_{j \in \Omega_b} V_j Y_{bm} \sin(\theta_b - \theta_m - \phi_{bm}) \tag{5.5}$$

$$P_b^{G_{min}} \leq P_b^G \leq P_b^{G_{max}} \tag{5.6}$$

$$Q_b^{G_{min}} \leq Q_b^G \leq Q_b^{G_{max}} \tag{5.7}$$

$$0 \leq P_b^{LC} \leq P_b^{LC,max} \tag{5.8}$$

$$0 \leq Q_b^{LC} \leq Q_b^{LC,max} \tag{5.9}$$

$$V_b^{\min} \leq V_b \leq V_b^{\max} \tag{5.10}$$

$$-S_{bm}^{\max} \leq S_{bm} \leq +S_{bm}^{\max} \tag{5.11}$$

Constraints (6.8) and (6.9) are active and reactive power flow at the COP respectively; constraints (6.10) and (6.11) limit the upper and lower capacity of generation units respectively; constraints (6.34)-(6.17) show the limits on the load curtailments. Constraint (5.10) represents the limits on the voltage magnitude of system buses; constraint (6.35) shows the the transmission line capacity.

5.3.1.3 Security constraints

Due to the importance of security measures in the TSO-DSO coordination, they are considered as the critical component of the optimal power flow (OPF) model in the TSO optimisation. To do so, as shown in the top left corner of Fig. 6.4, the loading margin is considered as the security measure of TSO-DSO coordination. This security margin is defined by generation capacity requirements to supply rises in the system demand prior to the violation of SLP [130]. In the P-V curve shown in Fig. 6.4, the distance from point A (i.e. COP) to point B (i.e. SLP) is the loading margin (i.e. security margin). This margin is defined by the system load. For example, increasing the system demand from P_{D_0} (i.e. point A) to P (i.e. point B) leads to a violation of the operational constraints of the network. Consequently, the system loading

margin should be more than/equl to the preset level to keep the entire network in a secure operational state. In order to address this concept, the power flow equations in COP (i.e. (6.8)-(6.17)) should be simultaneously considered along with those of SLP, which are represented as below ($\forall b, m \in \Omega_b$):

$$\hat{P}_b^G - \hat{P}_b^D = \hat{V}_b \sum_{m \in \Omega_b} \hat{V}_m Y_{bm} \cos(\hat{\theta}_b - \hat{\theta}_m - \phi_{bm}) \tag{5.12}$$

$$\hat{Q}_b^G - \hat{Q}_b^D = \hat{V}_b \sum_{m \in \Omega_b} \hat{V}_m Y_{bm} \sin(\hat{\theta}_b - \hat{\theta}_m - \phi_{bm}) \tag{5.13}$$

$$P_b^{G_{\min}} \leq \hat{P}_b^G \leq P_b^{G_{\max}} \tag{5.14}$$

$$Q_b^{G_{\min}} \leq \hat{Q}_b^G \leq Q_b^{G_{\max}} \tag{5.15}$$

$$V_b^{\min} \leq \hat{V}_b \leq V_b^{\max} \tag{5.16}$$

$$-S_{bm}^{\max} \leq \hat{S_{bm}} \leq +S_{bm}^{\max} \tag{5.17}$$

$$\hat{P}_b^D = (1 + \Lambda_b^D \times \lambda) \left(P_b^D - P_b^{LC}\right) \tag{5.18}$$

$$\hat{Q}_b^D = (1 + \Lambda_b^D \times \lambda) \left(Q_b^D - Q_b^{LC}\right) \tag{5.19}$$

$$\hat{P}_b^G = \min\left(P_b^{G_{\max}}, (1 + \Lambda_g^G \times \lambda) P_g^G\right) \tag{5.20}$$

$$\hat{V}_b = V_b + v_b^l - v_b^u \tag{5.21}$$

$$(Q_b^{G_{\max}} - \hat{Q}_b^G) \times v_b^u \leq 0 \tag{5.22}$$

$$(\hat{Q}_b^G - Q_b^{G_{\max}}) \times v_b^l \leq 0 \tag{5.23}$$

$$v_b^l, v_b^u \geq 0 \tag{5.24}$$

$$\lambda \geq \lambda_{des} > 0 \tag{5.25}$$

where constraints (5.12) and (5.13) represent the active and reactive power flow at SLP respectively; limit on active and reactive power, voltage magnitude, and transmission line capacity at SLP are shown by constraints (5.14)-(5.17) respectively. The amount of increase in the active and reactive system demand from COP to the SLP is shown by (5.18) and (5.19) respectively. This increase in the system demand should be supplied by generation units, as represented by Equation (5.20). Constraints (5.21)-(5.24) describe the dynamics of load increase from COP to the SLP and the way it would affect the voltage at the

system buses. Finally, the desired loading margin of the system can be defined by Constraint (5.25).

By solving the above optimisation model for the TSO, the required load curtailment and voltage level at the interface of TSO-DSO are obtained. The following parameters will be determined:

$$\begin{bmatrix} P_b^{I_{tso}} \\ Q_b^{I_{tso}} \\ V_b^{I_{tso}} \end{bmatrix} = \begin{bmatrix} P_b^D - P_b^{LC} \\ Q_b^D - Q_b^{LC} \\ V_b \end{bmatrix} \tag{5.26}$$

The active and reactive power shares (i.e., $\pi_{b,d}^p$ and $\pi_{b,d}^q$) of d-th downstream feeder in the DSO's overall demand at the boundary point with the TSO (i.e. at bus b) is a known parameter for the DSO, which can be expressed as follows:

$$p_{b,d}^{I_{dso}} = \pi_{b,d}^p \times P_b^{I_{tso}} \tag{5.27}$$

$$\sum_d^{N_b} \pi_{b,d}^p = 1 \tag{5.28}$$

$$q_{b,d}^{I_{dso}} = \pi_{b,d}^q \times Q_b^{I_{tso}} \tag{5.29}$$

$$\sum_d^{N_b} \pi_{b,d}^q = 1 \tag{5.30}$$

5.3.2 Distributed DSO optimisers

After receiving the set-points required by the TSO at the TSO-DSO interface, a set of distributed optimisation models are solved in the distribution level to comply with the TSO's set-points, with minimum actual load curtailment, as the demands are mainly connected to the distribution level. In the

distribution level optimisation model, the DSOs aim at minimising the physical load curtailment required by the TSO, via optimal coordination of distribution-level flexibilities. In this chapter, network reconfiguration and CVR are considered as the DSO flexibility options. By optimising the distribution network topology via feeder reconfiguration, power losses and voltage profile of the network can be modified to achieve the DSO goals. Moreover, since the demand connected to the distribution feeder is mainly voltage-dependent, CVR can be considered as an effective flexibility option for DSOs. To implement CVR, coordinated operation of voltage regulators (i.e. boosting transformers) along the feeders can be utilised. The system demand can be modified through the coordinated operation of voltage regulator transformers. In the following, the distributed optimisation model for DSOs is presented, taking into account the network reconfiguration and voltage regulators' flexibilities.

5.3.2.1 Objective function

In the distribution level, each grid's optimiser tries to minimise the load curtailment and the difference between its set-points in the TSO-DSO connection point with those obtained by the TSO's centralised optimiser, as below:

$$OF^{DSO} = \min\left\{w_2 \times of_{lc}^{dso} + (1 - w_2) \times of_{dif}^{dso}\right\} \tag{5.31}$$

$$of_{lc}^{dso} = \sum_{b \in B_b} p_{b,d}^{lc} \tag{5.32}$$

$$of_{dif}^{dso} = \sum_{b \in \mathcal{B}_s} \left(\left|p_{b,d}^{S} - p_{b,d}^{I_{dso}}\right| + \left|q_{b,d}^{S} - q_{b,d}^{I_{dso}}\right| + \left|v_{b,d} - V_b^{I_{tso}}\right|\right) \tag{5.33}$$

where w_2 is a weight coefficient defining the importance of each objective in the distribution level optimisers.

5.3.2.2 Power Flow and Network Constraints

In this chapter, the power flow constraints in the distribution level are adopted by adding two important flexibility measures: network reconfiguration and CVR. The former adds a binary variable to the branch flow model and the voltage-dependent loads are considered for the latter. The power flow constraints in the distribution level are represented as below ($\forall b, m \in \mathcal{B}_b$):

$$p^S_{b,d} + p^{LC}_{b,d} - p^D_{b,d} = \sum_{m \in \mathcal{B}_b} \chi^l_{bm,d} \times p_{bm,d} \tag{5.34}$$

$$q^S_{b,d} + q^{LC}_{b,d} - q^D_{b,d} = \sum_{m \in \mathcal{B}_b} \chi^l_{bm,d} \times q_{bm,d} \tag{5.35}$$

$$\begin{aligned} p_{bm,d} = &+g_{bm,d}\tau^2_{bm,d}v^2_{b,d} \\ &-\tau_{bm,d}v_{b,d}v_{m,d}\left(g_{bm,d}cos(\theta_{bm,d}) + b_{bm,d}sin(\theta_{bm,d})\right) \end{aligned} \tag{5.36}$$

$$\begin{aligned} q_{bm,d} = &-b_{bm,d}\tau^2_{bm,d}v^2_{b,d} \\ &-\tau_{bm,d}v_{b,d}v_{m,d}(g_{bm,d}sin(\theta_{bm,d}) - b_{bm,d}cos(\theta_{bm,d})) \end{aligned} \tag{5.37}$$

$$p^D_{b,d} = \hat{p}^D_{b,d} \sum_{\psi} kp^{\psi}_{b,d} \left(\frac{v_{b,d}}{\hat{v}_{b,d}}\right)^{\alpha^{\psi}_{b,d}} \tag{5.38}$$

$$q^D_{b,d} = \hat{q}^D_{b,d} \sum_{\psi} kq^{\psi}_{b,d} \left(\frac{v_{b,d}}{\hat{v}_{b,d}}\right)^{\beta^{\psi}_{b,d}} \tag{5.39}$$

$$p^{S_{\min}}_{b,d} \leq p^S_{b,d} \leq p^{S_{\max}}_{b,d}, \quad \forall b \in \mathcal{B}_S \tag{5.40}$$

$$q^{S_{\min}}_{b,d} \leq q^S_{b,d} \leq q^{S_{\max}}_{b,d}, \quad \forall b \in \mathcal{B}_S \tag{5.41}$$

$$0 \leq p^{LC}_{b,d} \leq p^{LC,max}_{b,d} \tag{5.42}$$

$$0 \leq q^{LC}_{b,d} \leq q^{LC,max}_{b,d} \tag{5.43}$$

$$v^{\min}_{b,d} \leq v_{b,d} \leq v^{\max}_{b,d} \tag{5.44}$$

$$(v_{b,d} \times i_{bm,d})^2 = p^2_{bm,d} + q^2_{bm,d} \tag{5.45}$$

$$0 \leq i_{bm,d} \leq \chi^l_{bm,d} \times i^{\max}_{bm,d} \tag{5.46}$$

where constraints (5.34) and (5.35) represent the active and reactive power balance in the distribution network respectively. Constraints (5.36) and (5.37) show the active and reactive power flow in the distribution network respectively, where $\tau_{bm,d}$ indicates the tap level of the voltage regulator on the line between buses b and m in the d-th parallel distribution feeder. Binary variable $\chi^{l}_{bm,d}$ indicates the status of line connecting the distribution buses b and m. Due to the fact that the majority of loads in the distribution level are voltage-dependent, the exponential load model for active and reactive loads are considered in equations (5.38) and (5.39) respectively. In these equations, it is assumed that the load in each distribution bus b, comprises of residential, commercial and industrial components. Constraints (5.40) and (5.41) respectively limit the active and reactive power imported from the transmission network to the distribution network from the substation bus. Constraints (5.42) and (5.43) limit the active and reactive load curtailment in the distribution network respectively. The voltage magnitude of system buses is limited by Constraint (5.44). Finally, the power flow through the distribution system lines is represented by (5.45) and limited by constraint (5.47).

5.3.2.3 DER flexibility

Distribution-level DERs can play a vital role in providing flexibility for the transmission network [12]. In order to unlock higher levels of flexibility, the network reconfiguration and CVR can be used along with DER. To do so, active and reactive power output of DERs are added to the power balance equations in constraints (5.34) and (5.35), as below:

$$p^{S}_{b,d} + p^{dg}_{b,d} + p^{LC}_{b,d} - p^{D}_{b,d} = \sum_{j \in \mathcal{B}_b} \chi^{l}_{bj,d} \times p_{bj,d} \tag{5.47}$$

$$q^{S}_{b,d} + q^{dg}_{b,d} + q^{LC}_{b,d} - q^{D}_{b,d} = \sum_{j \in \mathcal{B}_b} \chi^{l}_{bj,d} \times q_{bj,d} \tag{5.48}$$

$$0 \leq p_{b,d}^{dg} \leq \pi_{b,d}^{dg} \tag{5.49}$$

$$-tg(\varphi_{lead}) \times P_{b,d}^{dg} \leq Q_{b,d}^{dg} \leq tg(\varphi_{lag}) \times P_{b,d}^{dg} \tag{5.50}$$

where constraints (5.47) and (5.48) represent the active and reactive power balance equations with consideration for active and reactive power output of DG units respectively. Constraint (5.49) represents the active power output of DG units based on their available capacity. Finally, Constraint (5.50) limits the reactive power output of DGs.

5.3.2.4 Distribution network's flexibility

Network reconfiguration is considered as one of the more efficient methods in improving system characteristics [131]. This method has been utilised to improve different aspects of the network including voltage profile. Therefore, it can be adopted to improve the distribution system voltage profile when the substation voltage level is reduced to save energy. In this chapter, the network reconfiguration is modelled based on the graph theory. Accordingly, to have a radial configuration, the number of distribution lines should be equal to the number of nodes minus one. This concept can be mathematically modelled as below [132] ($\forall b, m \in \mathcal{B}_b$):

$$s_{b,d} - d_{b,d} = \sum_{(bm)\in\Omega_l} f_{bm,d} - \sum_{(jb)\in\Omega_l} f_{mb,d} \tag{5.51}$$

$$f_{bm,d} + f_{mb,d} = 0 \tag{5.52}$$

$$|f_{bm,d}| \leq \chi_{bm,d}^{l} f_{bm,d}^{max} \tag{5.53}$$

$$0 \leq s_{b,d} \leq s_{b,d}^{max}, \quad \forall b \in \mathcal{B}_S \tag{5.54}$$

$$\sum_{(bm)\in\mathcal{B}_b} \chi_{bm,d}^{l} = 2 \times (card(\mathcal{B}_b) - 1) \tag{5.55}$$

$$\chi_{bm,d}^{l} = \chi_{mb,d}^{l} \tag{5.56}$$

where $\chi^{l}_{bm,d}$ is a binary variable indicating the status of lines. It is equal to one if the circuit is closed and 0, otherwise. Combining (5.51) and (5.55) ensures that there is a path to every node and the graph connectivity is ensured. Therefore, in the proposed model for the distribution system, in addition to constraints (5.55) and (5.56), there is a need to have a path from the substation to all system loads, which has been reflected in equations (5.34) and (5.35).

By solving this, the model will determine the distributed DSO optimisers, the realised load absorbed by the downstream distribution networks, as well as the optimal voltage at the interface point of TSO-DSO. Usually, several distribution feeders are supplied on the downstream side of a given interface point of the TSO-DSO. Therefore, the DSO aggregates the obtained load of all parallel feeders as follows:

$$\begin{bmatrix} p_b^{I_{dso}} \\ q_b^{I_{dso}} \\ v_b^{I_{dso}} \end{bmatrix} = \begin{bmatrix} \sum_{d=1}^{N_b} p_{b,d}^{S} \\ \sum_{d=1}^{N_b} q_{b,d}^{S} \\ \frac{1}{N_b} \sum_{d=1}^{N_b} v_{b,d} \end{bmatrix} \tag{5.57}$$

5.4 TSO-DSO Coordination Procedure

At the connection bus between transmission and the downstream distribution networks, the boundary variables including voltage magnitude, active and reactive power are obtained via the above optimisation models. The vector of these boundary variables should converge to the same values for both the TSO and DSO optimisations. Hence, the convergence condition is as follows:

$$\begin{bmatrix} \epsilon_p \\ \epsilon_q \\ \epsilon_v \end{bmatrix} = \begin{bmatrix} |P_b^{I_{tso}} - p_b^{I_{dso}}| \\ |Q_b^{I_{tso}} - q_b^{I_{dso}}| \\ |V_b^{I_{tso}} - v_b^{I_{dso}}| \end{bmatrix} \leq \begin{bmatrix} \epsilon_p^{des} \\ \epsilon_q^{des} \\ \epsilon_v^{des} \end{bmatrix} \tag{5.58}$$

The process of solving the proposed coordination scheme is shown in Fig. 5.2. Based on this flowchart, the process starts with initialising the model

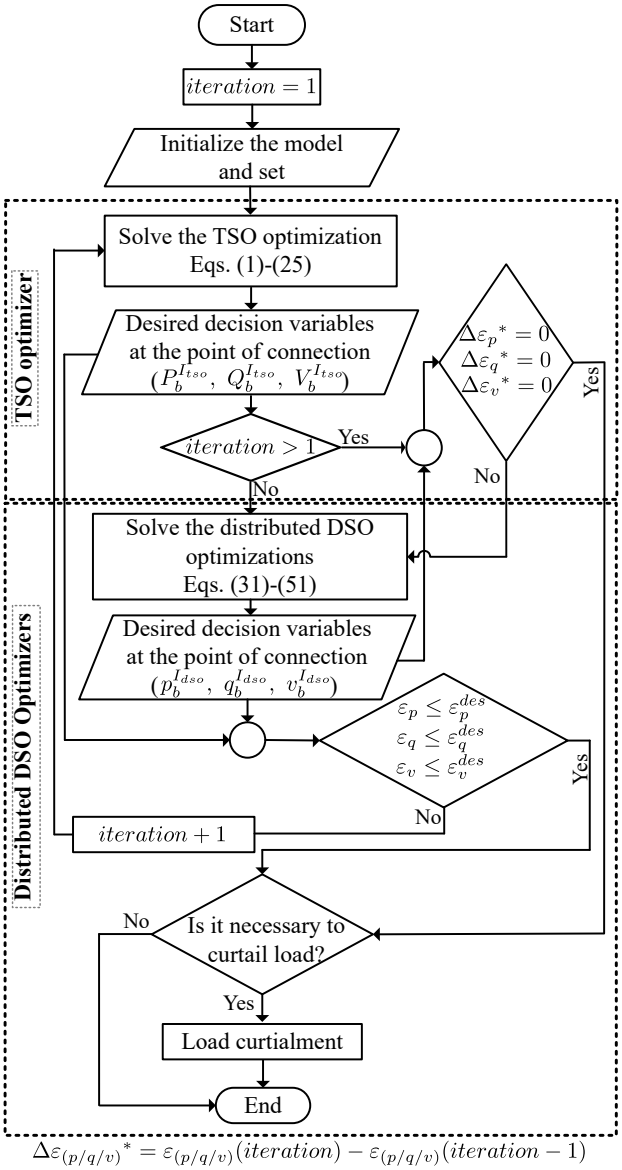

FIGURE 5.2: Flowchart of the proposed framework for TSO-DSO coordination.

parameters and defining the preferable degree of security (i.e. λ_{des}). Then, the TSO performs the following optimisation:

$$\min \left\{ OF^{TSO}(X_{tso}^{DV}) \right\} \tag{5.59}$$

$$Subject\ to:$$

$$H^{tso}(X_{tso}^{DV}) \leq 0 \tag{5.60}$$

$$G^{tso}(X_{tso}^{DV}) = 0 \tag{5.61}$$

where (5.59) is the TSO optimiser's objective function (i.e. (5.1)), and the constraints (5.60) and (5.61) represent all equality and inequality constraints of the transmission network (i.e. the constraints (5.4)-(5.25)). X_{tso}^{DV} represents the decision variables of the transmission network optimiser including those of the boundary points. The optimal solution of the boundary variables is reported to the DSO's distributed optimisers via (5.27)-(5.30). For any given transmission bus, the corresponding downstream distribution feeders are optimised based on (5.62)-(5.64) in a distributed manner.

$$\min \left\{ OF^{DSO}(X_{dso}^{DV}) \right\} \tag{5.62}$$

$$Subject\ to:$$

$$H^{dso}(X_{dso}^{DV}) \leq 0 \tag{5.63}$$

$$G^{dso}(X_{dso}^{DV}) = 0 \tag{5.64}$$

where (5.62) is the objective function of the distribution network d and equations (5.63) and (5.64) are the equality and inequality constraints of each distribution network (i.e. constraints (5.34)-(5.56)). X_{dso}^{DV} is the set of decision variables for each distribution network. At the distribution level, each DSO applies its available flexibility measures in all feeders in a distributed manner to comply with the requirements of the TSO. While each DSO can provide a different degree of flexibility based on their capabilities,

secure coordination is achieved if the convergence condition (i.e. (5.58)) is met.

If the convergence criterion is not met in the current iteration, the boundary set-points obtained by the DSO's distributed optimisers, are aggregated via (5.26) and sent back to the centralised TSO optimiser to set up the next iteration. The TSO then solves the optimisation in equations (5.59)-(5.61). From the second iteration, the TSO has the autonomy to check the desired values of set points in the point of connection. If the values of the boundary set-points obtained from the TSO are equal to those received from the previous iteration of the DSOs, it is not possible to apply further changes using the flexibility measures at the distribution level. At this point, the TSO sends the order to the DSOs to check for the load curtailment. The necessary load curtailment is then applied by the DSOs. In the first iteration and for the TSO's centralised optimiser, it is worth noting that , the DSOs' distributed optimisation models have not been solved yet, Eq. (5.3).

Conversely, if there is a difference between the set-points, the TSO allows the DSOs to perform their own distributed optimisations and utilise their flexibility measures to decrease load curtailment. This process is repeated by the TSO and distributed DSO optimisers until the convergence criterion is met or it is not possible to apply more adjustment to the set-points indicated by TSO.

5.5 Case study

The optimisation models in the TSO and DSO levels are non-linear programming and mixed-integer non-linear programming, respectively. Both models are implemented in general GAMS software [96]. The IEEE 118-bus system, here, is considered the test transmission network. The data of this system is available in [133]. The 83-bus practical distribution network of Taiwan Power Company [134] and the IEEE 33-bus distribution feeder [135] are considered as the sample downstream distribution networks.

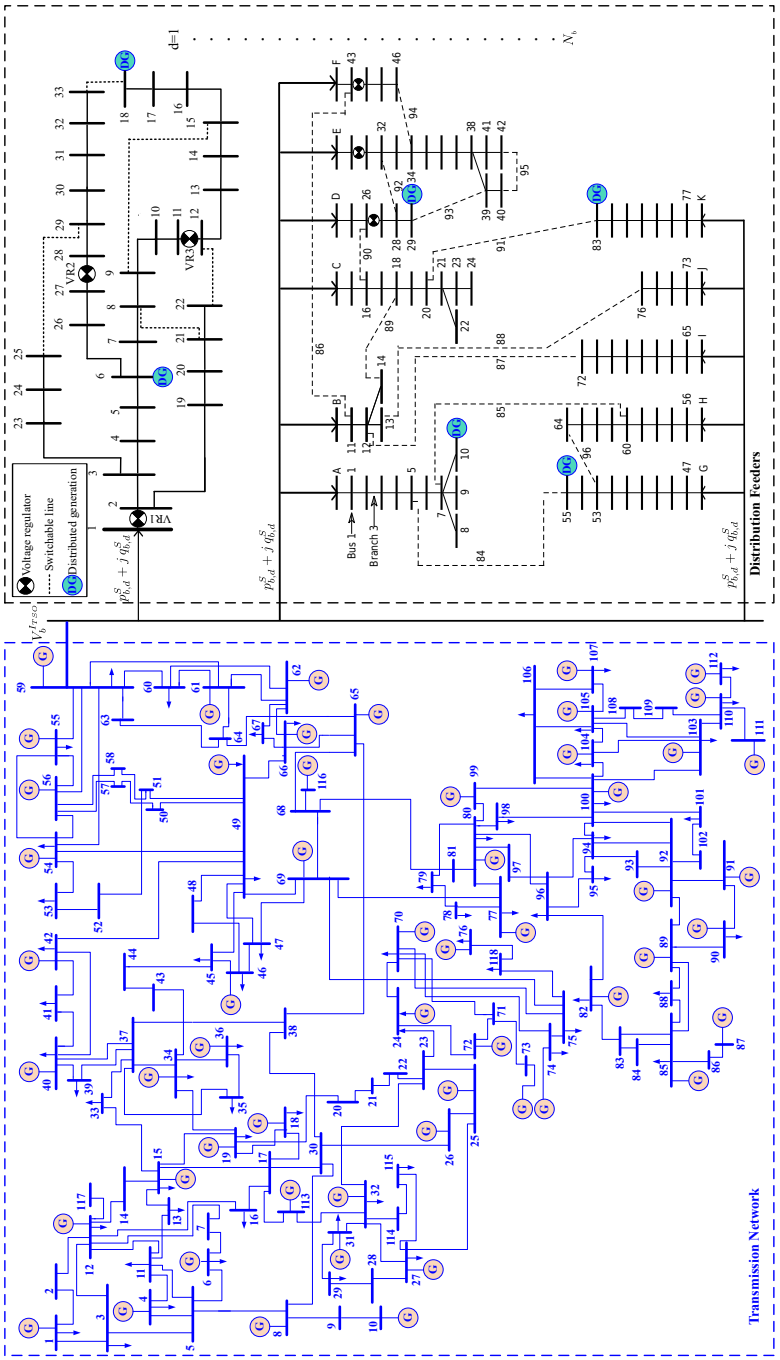

FIGURE 5.3: One-line diagram of the studied transmission and distribution networks.

It is assumed that 8 parallel IEEE 33-bus distribution feeders and 5 parallel 83-bus Taiwan Power Company distribution networks are connected to Bus 59 of the IEEE 118-bus transmission system. This bus has the largest amount of load in the transmission network and is more likely to experience load shedding in case of an emergency condition (e.g. sudden load increase). The rest of the load in this bus, and other buses of the transmission network, are assumed as aggregated load in transmission level. The one-line diagram of IEEE 118-bus transmission network and connected distribution networks including the location of voltage regulators and potentially switchable lines in each feeder is shown in Fig. 5.3. The location of distributed generation (DG) units in distribution level is shown in this figure. The data of DGs is taken from [115].

The active and reactive power share of each distribution network (i.e., $\pi^{p}_{b,d}$ and $\pi^{q}_{b,d}$ in (5.27) and (5.29)) is defined based on their total load. Therefore, the values of $\pi^{p}_{b,d}$ and $\pi^{q}_{b,d}$ are 0.178 and 0.156 for IEEE 33-bus distribution feeders respectively, and they are respectively 0.822 and 0.844 for 83-bus Taiwan Power Company distribution networks. Moreover, $\epsilon_{(}p/q/v)^{des}$ are assumed to be 0.004 $p.u$ in (5.58). Furthermore, w_1 and w_2 are both assumed to be 0.5 in (5.1) and (5.31), respectively. The share of various demand models, including the residential (R), commercial (C) and industrial (I) loads in exponential (EXP) load model is summarised in Table 5.2.

To analyse the effectiveness of the proposed TSO-DSO coordination scheme under an emergency condition, it is assumed that the transmission system's load is increased by 10% (evenly in all buses). The desired security margin of the TSO-DSO coordination (i.e. λ_{des}) is taken to be 10%.

TABLE 5.2: Various demands share in EXP load model.

Load model	ψ	$\alpha^{\psi}_{b,d}$	$\beta^{\psi}_{b,d}$	$kp_{\psi,b}$	$kq_{\psi,b}$
EXP	R	1.20	2.90	0.33	0.33
	C	0.99	3.50	0.33	0.33
	I	0.18	6.00	0.34	0.34

R: Residential, C: Commercial, I: Industrial and EXP: Exponential load model

TABLE 5.3: Computational size of the proposed TSO-DSO coordination model.

Parameter	TSO	DSO (33-bus)	DSO (83-bus)
# of model variables	8,398	808	2,022
# of model constraints	6,256	708	2,048
Total execution time [s]	36.19	1.28	2.25

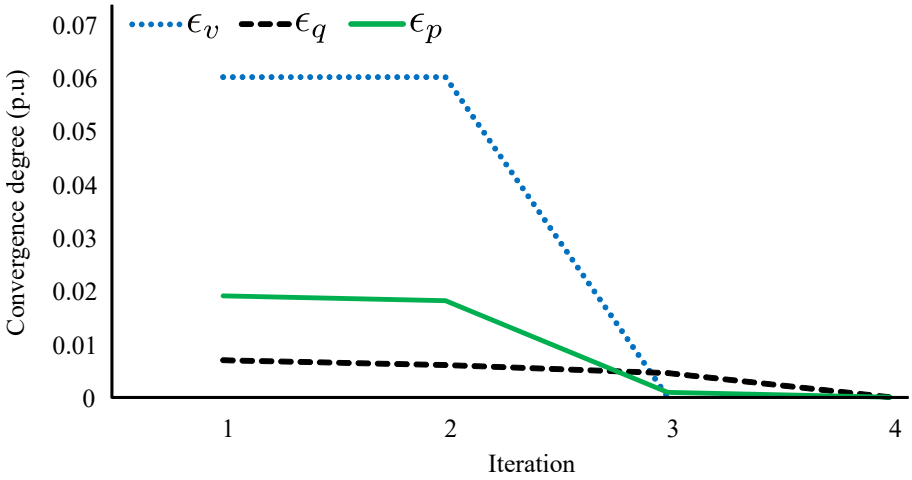

FIGURE 5.4: The convergence characteristics of the TSO-DSO coordination model for $N_b = 13$ and $\lambda_{des} = 10\%$.

5.5.1 Flexibility with Network reconfiguration and CVR

The computational data of the proposed model is summarised in Table 5.3. The simulations are performed on an Intel(R) Core(TM) i5-6600 CPU 3.30GHz with 16 GB of RAM. Table 5.3 demonstrates that the proposed method achieved a particularly short computational time, in order of seconds. The distributed DSO optimisation models can be solved in a distributed manner via parallel computing. The convergence characteristics of the proposed TSO-DSO coordination model are shown in Fig. 5.4 for 8 parallel IEEE 33-bus distribution feeders and 5 parallel 83-bus Taiwan Power Company distribution networks connected to Bus 59 and the security margin of 10%. It can be seen that the proposed decentralised TSO-DSO coordination model converges in a few iteration (e.g. four iterations for

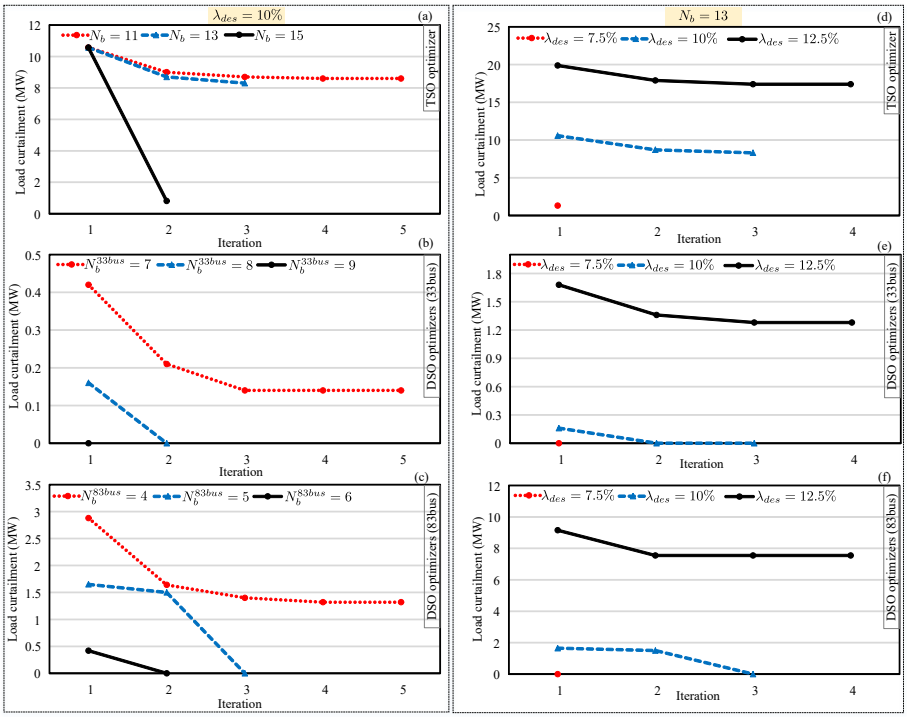

FIGURE 5.5: Load curtailment for different values of N_b and λ_{des}: (a)-(c) TSO and DSO optimisers' results for $\lambda_{des} = 10\%$ and different values of N_b, (d)-(f) TSO and DSO optimisers' results for $N_b = 13$ and different security margins.

$\lambda_{des} = 10\%$). Moreover, voltage at the interface point is converged even faster, such that $\epsilon_v \leq \epsilon_v^{des}$ after three iterations. Having the voltage regulators in distribution feeders enables more flexibility in both active and reactive power demands to enhance the convergence degree of the proposed framework.

It is worth mentioning that this study performed the simulation for the similar distribution networks (i.e. the simulation has been solved for two different distribution networks and has been scaled to 8 parallel IEEE 33-bus distribution feeders and 5 parallel 83-bus Taiwan Power Company distribution networks). However, increasing the number of distribution network can add higher level of complexity and increase the simulation time. Also, since this study investigated network reconfiguration as a network

flexibility option, radiality has been considered as a constraint. However solving the model for meshed distribution networks (i.e. without consideration for network flexibility) can decrease the degree of complexity since the binary variable showing the status of lines (i.e. $\chi^{l}_{bm,d}$ in Eq. (5.53)) is not considered by optimisation model. This can decrease the degree of flexibility while reducing the computational complexity.

Figure 5.5 shows the changes in the optimal value of load curtailment for different number of distribution networks connected to the Bus 59, and different levels of the security margin. The main observations based on this figure are:

1. Number of parallel distribution networks (i.e. N_b): it can be seen from Figs. 5.5-(a)-(c) that increasing the number of connected distribution networks can reduce the number of iterations. Increasing the number of distribution networks raises the degree of flexibility and contribution in the load reduction. The optimisation achieved the desired convergence degree in two iteration for $N_b = 13$. Also, this factor can influence the load curtailment. For example, in Fig. 5.5-(b), the total amount of load curtailment for the distributed DSO optimisers is zero for $N_b^{33bus} = 15$ and $N_b^{33bus} = 13$, while it is 0.14 MW for $N_b^{33bus} = 7$. The value of actual load curtailment is 1.32 MW in 83-bus distribution network for $N_b^{83bus} = 4$. This means that the actual value of load curtailment increases for the larger distribution networks.

2. The role of distributed flexibility measures: these techniques play a crucial role in decreasing the load curtailment in the distribution networks. For instance, for $N_b = 11$ in Fig 5.5-(a), although the TSO requested 8.6 MW load curtailment in the TSO-DSO interface, the distribution network optimisers only curtailed 0.14 MW and 1.32 MW in Figs. 5.5-(b) and 5.5-(c) respectively. This means that $8.6 - (1.32 + 0.14) = 7.0$ MW (i.e. 81%) of the requested load curtailment by the TSO is handled via the available flexibility measures, namely feeder reconfiguration and conservation voltage reduction. It is worth mentioning that no physical load curtailment is realized by the DSO optimisers for $N_b = 13$ and $N_b = 15$.

3. Security margin (i.e. λ_{des}): this transmission-level parameter has a significant impact on the load curtailment. Increasing the security margin from 10% to 12.5% in Fig. 5.5-(d) doubles the amount of required load curtailment by the TSO optimiser in the boundary point (i.e. Bus 59). Additionally, one can observe from Figs. 5.5-(e) and 5.5-(f) the higher the λ_{des} the more the actual load curtailment by DSO. Moreover, this measure also influences the number of iterations for achieving desired convergence degree.

4. Secure coordination: in Figs. 5.5-(e) and 5.5-(f), since the TSO optimiser has not observed any changes in the interface set-points from iteration 3 to 4 for $\lambda_{des} = 12.5\%$, the DSO optimisers observed load curtailment in iteration 3 for maintaining the desired security margin over the whole system.

Active and reactive power of an IEEE 33-bus distribution network connected to Bus 59 before and after applying the flexibility measures is shown in Fig.

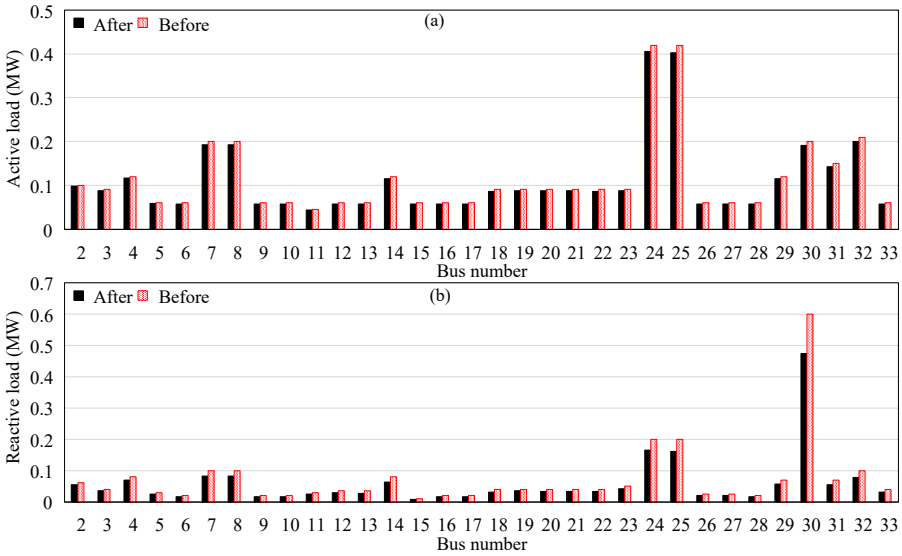

FIGURE 5.6: Nodal demand values in IEEE 33-bus distribution feeder before and after applying the flexibility measures (for $N_b = 13$ and $\lambda_{des} = 10\%$): (a) active power, (b) reactive power.

5.6. It is observed that the flexibility measures reduce the active and reactive loads, especially for high demanded buses. The total active and reactive power of each distribution feeder before applying the flexibility measures are 3.72 MW and 2.30 $MVAr$ respectively, while after applying the CVR and feeder reconfiguration the net active and reactive demands of each feeder decrease to 3.57 MW and 1.86 $MVAr$, respectively. This means that each distribution network is capable of reducing its active and reactive demands by 0.14 MW (i.e. 3.8% of total active power demand) and 0.43 $MVAr$ (i.e. 19% of total reactive power demand), respectively, without any need for actual load curtailment (as also shown in Fig. 5.5-(b) for $N_b^{33bus} = 8$ and $\lambda_{des} = 10\%$). For the 83-bus Taiwan Power Company distribution network, 2.6% and 14.2% of active and reactive power is compensated by the distribution flexibilities without the need for physical load curtailment (as also shown in Fig. 5.5-(c) for $N_b^{83bus} = 5$ and $\lambda_{des} = 10\%$).

Figure 5.7 investigates the voltage profile obtained by the distributed DSO optimisers for a specific feeder connected to bus 59 in the following three cases:

- ***Case I:*** With CVR and without feeder reconfiguration;
- ***Case II:*** Without CVR and with feeder reconfiguration;
- ***Case III:*** With both CVR and feeder reconfiguration.

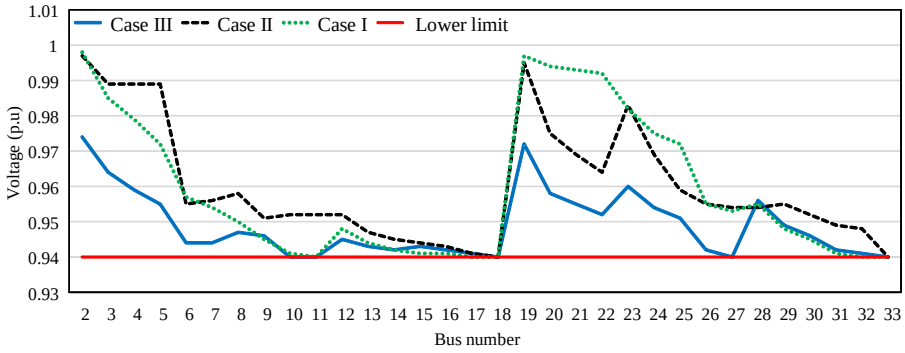

FIGURE 5.7: Optimal value of voltage magnitude in the IEEE 33-bus distribution network for different case studies (for $N_b = 13$ and $\lambda_{des} = 10\%$).

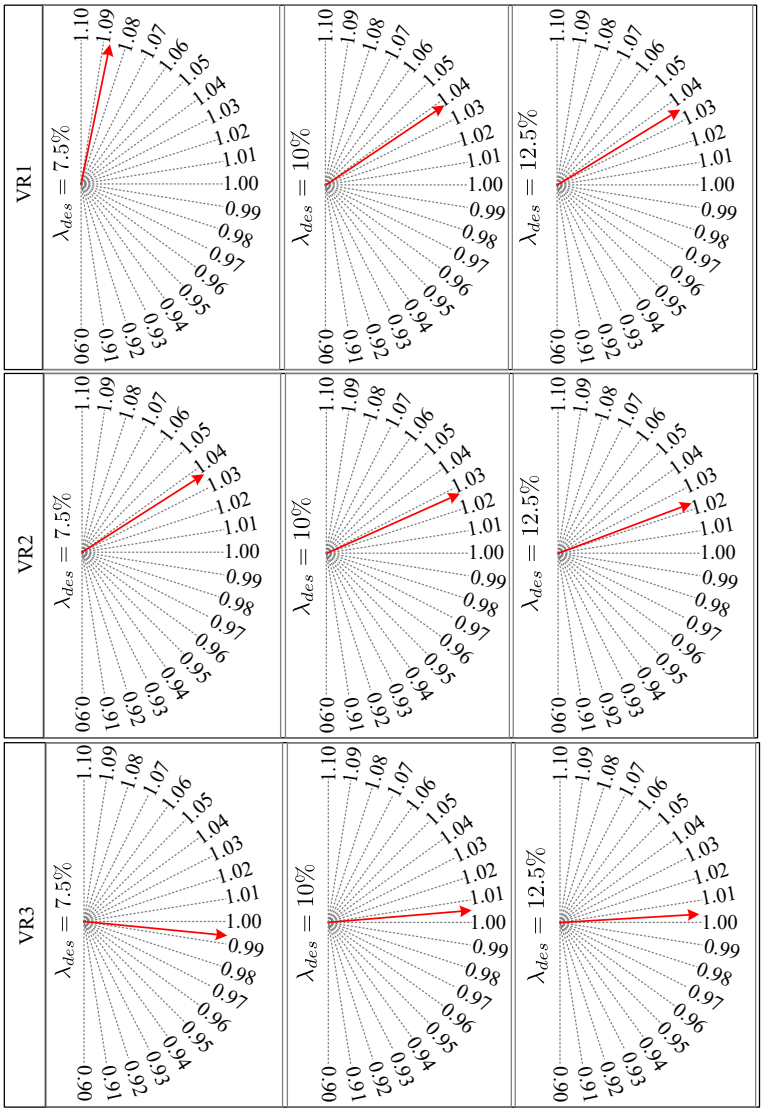

FIGURE 5.8: The optimal setting of voltage regulators installed in the IEEE 33-bus distribution network for different values of security margin and $N_b = 13$.

This figure shows that solely using CVR (i.e. *Case I*) decreases the voltage level in the end buses to the corresponding lower limit. In *Case II*, however, just feeder reconfiguration has resulted in better values of voltage level across the

feeder.In *Case III*, where both CVR and feeder reconfiguration are considered as the flexibility measures, the voltage level is reduced in a coordinated manner to satisfy the demand reduction forced by the TSO. The active and reactive demands, in this case, have already been shown in Fig. 5.6.

Moreover, for $N_b = 13$ and $\lambda_{des} = 10\%$, the overall active power curtailment in all distribution networks in cases *I*, *II* and *II* is 3.6 MW, 2.4 MW, and 0.0 MW, respectively. Although each of the CVR and feeder reconfiguration flexibilities can individually decrease the actual load curtailment, their coordinated utilisation is a better practice for reducing the load curtailment in the TSO-DSO coordination process.

Finally, the effect of security margin on the voltage regulators' settings as well as the optimal configuration of each sample distribution feeder are shown in Figs. 5.8 and 5.9, respectively. Figure 5.8 demonstrates how the tap setting is changed for voltage regulators to cope with the TSO's requirements in terms of the desired security margin. For example, the voltage regulator installed on the line between buses 1 and 2 (i.e., VR1) changes its tap by 5% in order to cope with a 2.5% rise in the security margin. These results can also be seen in Fig. 5.9, where the distribution feeder's configuration is changed for different values of λ_{des}. Note that the radial configuration is preserved for all security margins.

5.5.2 Value of DER flexibility

This section evaluates the effectiveness of DERs in providing flexibility services for the TSO-DSO coordination. As shown in Fig. 5.3, a number of DGs are installed in the distribution network and their effect on decreasing the needs for load curtailment in the emergency condition is analysed.

The simulation result shows that the coordination with the IEEE 33-bus distribution network converges in one iteration and the value of load shedding is zero with the DGs in the system; the 83-bus Taiwan Power Company distribution networks converges after two iteration, also with zero load shedding. These results show the importance of DERs in decreasing the needs

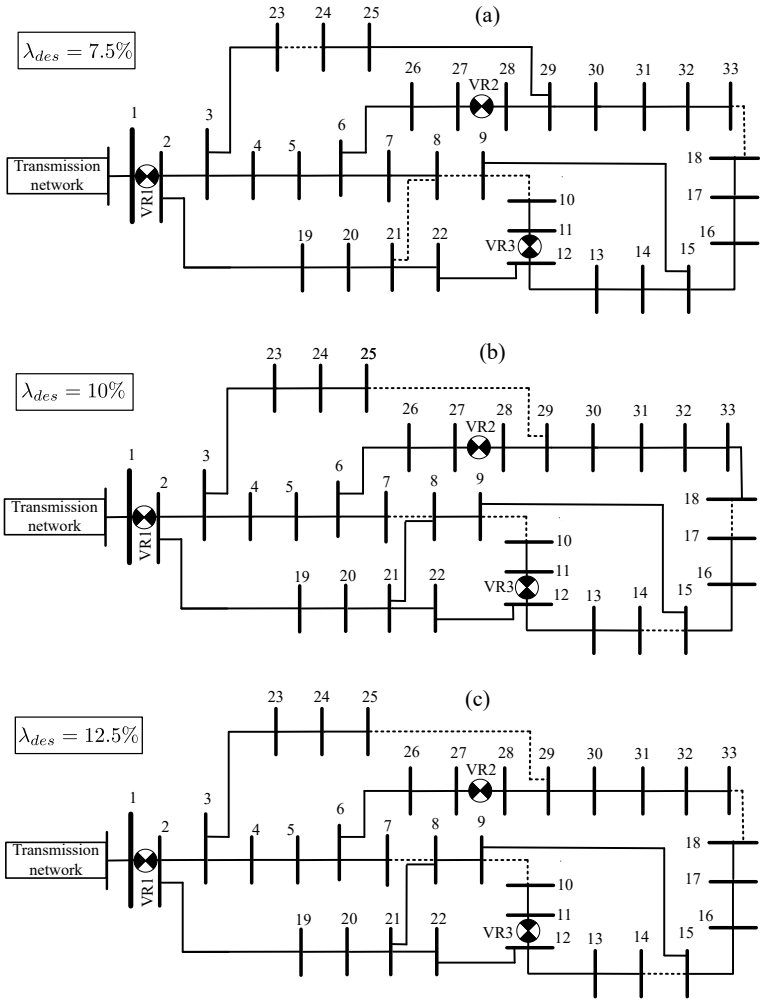

FIGURE 5.9: Variation of the IEEE 33-bus distribution network configuration for different values of security margin and $N_b = 13$.

for extra communication between DSO and TSO, while achieving zero load shedding. Therefore, optimal coordination of DERs is an efficient method in achieving the secure TSO-DSO coordination.

In order to evaluate the effect of DERs on voltage profile, the case studies described in Fig. 5.7 are compared against a case study with DERs, network reconfiguration and CVR (called Case IV). The result of this comparison is

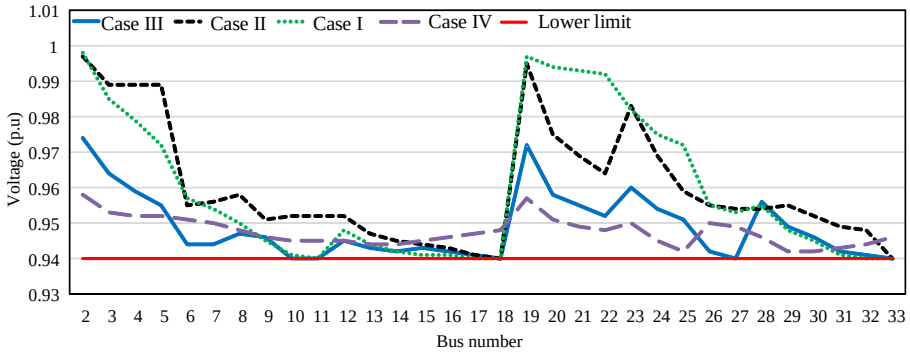

FIGURE 5.10: Optimal value of voltage magnitude in the IEEE 33-bus distribution network for different case studies with consideration for the DER effect (for $N_b = 13$ and $\lambda_{des} = 10\%$).

given in Fig. 5.10. It can be seen from this figure that the combination of distributed flexibility methods with DERs provides better threshold for the voltage profile, without the need for load curtailment.

Also, the optimal setting of voltage regulators in Case III and Case IV are compared in Fig. 5.11. This figure shows that adding the DERs decreased the need for higher level of tap changing in the voltage regulators. This means the local generation decreases the need for higher contribution from the loads in complying with the security measures of the TSO-DSO coordination.

5.6 Conclusion

The transformation of power systems towards integrated networks of different entities in which distribution and transmission system operators cooperate together towards a coordinated TSO-DSO scheme is a promising development. This scheme enables traditionally passive distribution networks to be active entities of such coordination. However, the challenge of voltage security and distributed flexibilities provided by DSOs for keeping the whole system in the desired loading margin needs further investigations. This chapter highlights the distributed flexibility measures for preserving the voltage security margin of the TSO-DSO coordination approach via a

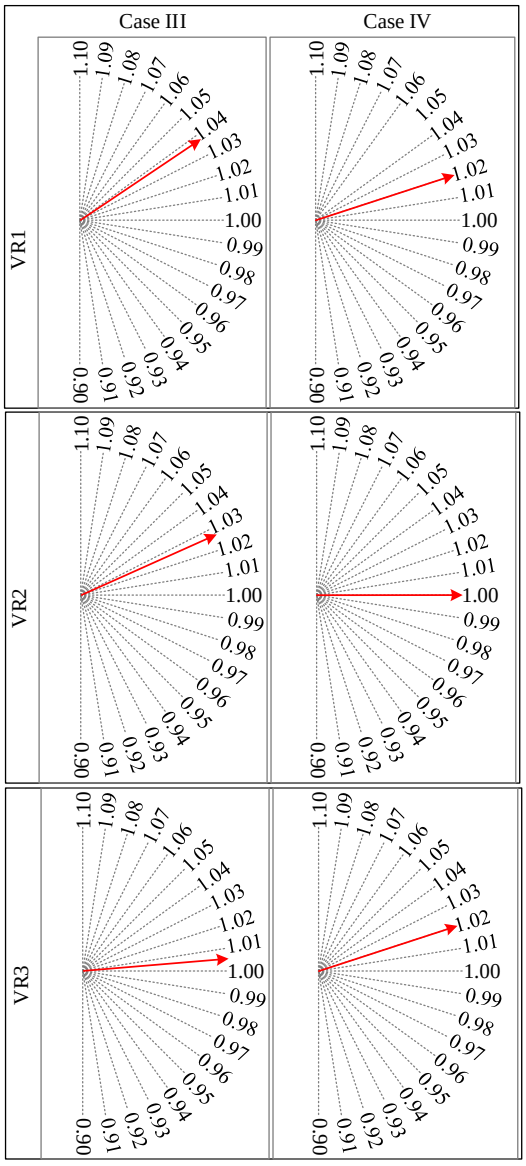

FIGURE 5.11: The optimal setting of voltage regulators installed in the IEEE 33-bus distribution network for cases III and IV (for $N_b = 13$ and $\lambda_{des} = 10\%$).

decentralised optimisation framework. At the transmission level, the centralised TSO optimiser aims at minimising the load curtailment in the

heavily loaded transmission network buses to preserve the required security margin under a contingency condition (i.e. sudden increase in the system load). The optimal set-points of transmission buses in terms of active/reactive power and voltage level, are determined by this optimisation model and sent to the downstream distribution networks at the point of connection between these grids. At the distribution level, the distributed optimisers of DSOs aim at minimising the difference between their set-points and the corresponding values sent by the TSO in the TSO-DSO boundary points as well as physical load curtailment, simultaneously. To achieve these goals with minimum unavoidable load curtailment, DSOs utilise their distributed flexibilities such as DER, CVR, and feeder reconfiguration. The efficiency of these flexibility methods is evident in the results. These distributed flexibility measures compensated 81% of load curtailment requested by the TSO. This result shows the importance of benefiting from flexibility measures in the distribution networks, highlighting their role as an active player in the TSO-DSO coordination. The results show that the number of distribution feeders available in the DSO distributed optimisers can reduce both the actual load curtailment and the number of iterations for the TSO-DSO coordination. This means that the proposed framework can achieve short computational time, in order of seconds, when the number of distribution networks is increased. According to the results, it can be concluded that:

- The coordinated utilisation of CVR and feeder reconfiguration is a promising option for the reduction of physical load curtailment in the TSO-DSO coordination process. Joint utilisation of CVR and feeder reconfiguration reduced the need for curtailing the active and reactive load in each individual distribution network by 3.8% and 19% respectively. These methods can be utilised along with DER flexibility options in the future studies to guarantee system security.

- Increasing the security margin raises the required load curtailment by the TSO and consequently the actual load curtailment by DSOs. Increasing the security margin by 2.5% resulted in a twofold increase in the required load curtailment by the TSO. This criteria is important in the coordination schemes that require a higher level of security. Under

such paradigm, the system operators need to curtail load to preserve higher security margins.

- A 2.5% increase in the security margin requires 5% change in the tap settings of voltage regulators installed in the distribution networks. This shows the effect of security margin in the transmission level on the flexibility measures taken by DSOs. It also highlights the active role of distributed flexibilities in preserving the whole system security.

This chapter investigated the application of different flexibility methods in preserving the system stability and avoiding load curtailment or disconnection of distribution networks from the main grid. The next chapter investigates a case where the distribution network is separated from the main grid and it should utilise its flexibility methods to preserve its security.

6

Application of Flexibility in Providing System Security

The following research question has been answered in this chapter:

To what extent can flexibility methods preserve security of an islanded microgrid?

The developments that have taken place in microgrid design accelerated the possibility of working in both islanded and grid-connected modes. High penetration of intermittent renewable energy sources (RESs) and unexpected disruptions (e.g., natural disasters) are fundamental challenges which can threaten the secure operation of microgrids, especially during the islanded condition, with no support from the upstream grid. Under such circumstances, efficient utilisation of different flexibility methods (e.g. demand, distributed energy resources (DER), and network flexibility) can be a valid solution to deal with islanded microgrid's operational challenges. The optimal management of demand and DER flexibility could be a valid solution to deal with uncertainty of RESs, while network reconfiguration could be a post-contingency flexibility method in dealing with security challenges causing the load curtailment. This chapter introduces a hierarchical tri-layer

min-max-min joint risk- and security-constrained model predictive control (RSC-MPC) framework for real-time energy scheduling of flexible islanded microgrids (FIMGs) under the influence of uncertainty and real-time time-varying contingency conditions. The proposed method benefits from demand, DER, and network flexibilities to supply FIMG demand under different conditions. Different forms of preventive and corrective flexibilities are used in this model. Different layers of such an optimisation problem are defined for different proposes. While the first layer process a pre-scheduling day-ahead optimisation, the second layer detects the worst-case contingency conditions by maximising the load curtailment and the mismatch between pre-scheduling (i.e., first layer) and real-time operation. The third layer implements the corrective flexibility measures to minimise the negative effect of contingency conditions while accounting to the cost associated with the risk of uncertainty in the forecasted inputs. The third layer also explores the economic effects of the RES' uncertainty on the proposed RSC-MPC, considering the risk and energy procurement cost as conflicting objectives. The computational efficiency of the proposed hierarchical control system in terms of accuracy and processing time is guaranteed through a mixed integer conic programming model. The proposed RSC-MPC is tested in different case studies and its efficiency is validated by numerical results. The results show the efficiency of the proposed preventive and corrective flexibility methods in preserving system security while dealing with risk of uncertainty.

Sections of this chapter is published in the following journal paper:

Nikkhah S, Sarantakos I, Zografou-Barredo NM, Rabiee A, Allahham A, Giaouris D. A Joint Risk and Security Constrained Control Framework for Real-Time Energy Scheduling of Islanded Microgrids. IEEE Transactions on Smart Grid. 2022 May 2.

Chapter roadmap: Section 6.1 provides and introduction on the microgrid energy scheduling and defines the research gap based on the literature. Overview of the proposed RSC-MPC is given in Section 6.2. The description of different layers and the problem formulation is presented in Section 6.3. Section 6.4 introduces the framework description and case study. Simulation

results are given in Section 6.5, while conclusions are summarised in Section 6.6.

6.1 Introduction

Security issues have been increasing in power systems in recent years due to the extreme weather events leading to breakdown of infrastructure networks as a result of climate change. On the one hand, more frequent natural disasters have highlighted the necessity of accounting for security measures. On the other hand, increased penetration of volatile renewable generation (to decrease environmental pollution) has created more opportunities, but also challenges for system operators. Therefore, greater share of RES as well as increased frequency of natural disasters in systems without suitable decentralised control frameworks have provoked substantial challenges to the electricity networks. For instance, the UK power grid outage on August 2019 was the result of high penetration of RES and the lack of suitable control strategies in the local networks which were disconnected from the main grid by the under-frequency load shedding [90]. Such an event triggered the necessity of designing the flexible microgrids that are capable of operating in islanded mode, while accounting for security issues caused by low-probability high-impact contingencies utilising their available flxibilities. This operation strategy can prevent, or at least decrease the load shedding of local networks that are disconnected from the main grid.

The islanded operation requires an efficient control mechanism that ensures different operational and physical constraints. Efficient controlling of FIMGs can enhance the grid reliability and resilience, while improving the RES penetration [136]. Optimal control and energy scheduling of FIMGs, however, can be challenged by a wide variety of technical/operational problems. Firstly, due to the inclusion of different inverter-based technologies in the network, the FIMG controller should be able to deal with the time-scale discrepancy between the responses of different technologies on a real-time basis. On the other hand, due to the high probability of RES uncertainty, even in a minute-to-minute real-time tracking [137], the risk associated with uncertainty should not be neglected. Therefore, the FIMG controller needs to take into account forecasted parameter uncertainty (e.g., in renewable generation) and the potential response delays of different assets in real-time

control. Secondly, such a real-time FIMG controller should be able to tolerate possible contingency conditions (e.g., a sudden disruption caused by a natural disaster) that can affect grid elements such as distribution system's lines. This problem raises the necessity of accounting for security measures in the FIMG's real-time controls. Finally, such control framework should be computationally efficient, while considering important physical and operational constraints of the network.

Several approaches have been proposed in the literature to deal with the aforementioned challenges.

6.1.1 Real-time control

model predictive control (MPC) has been regarded as an efficient approach that is capable of considering system constraints at each time step, enabling real-time control of complex systems. The utilisation of MPC approach in [87] has brought higher RES penetration as well as improvement in the microgrid efficiency. In [138] the MPC is adopted to predict future voltage deviations in the microgrid and adjust the reactive power generation to prevent voltage instability. Regardless of the efficiency of MPC-based methods, the main issue in the application of these approaches is the possibility of changes in the predicted data of future time slots. As it has been shown in [22], there is a considerable difference between the actual and predicted photovoltaic generation output, which is caused by the inherent uncertainty of solar irradiance. The effect of RES uncertainty on the voltage stability of microgrid and optimal capacity of electric vehicle parking lots is analysed in [122]. This factor also has been considered as an important challenge which can affect the system operation [139], load curtailment [140], and system reliability [141]. However, the conventional MPC approaches fail to capture the critical uncertainties (e.g., those associated with RES) and consequently to handle their associated technical and economic risks. Although it has been considered as the future research work in [87], there is not any research which has investigated the performance of the MPC-based control approaches under an uncertain environment. It should be noted that the effect of uncertainty on the energy management of microgrids has been

analysed in recent literature [142, 143], where robust optimisation has been utilised to improve the system robustness in face of uncertainty in the renewable generation. Furthermore, the risk associated with uncertainty of predicted data in the MPC requires more investigation.

6.1.2 System security

The occurrence of several natural disasters in recent years [144] obliged system operators to contemplate the contingency conditions as a challenging issue which can affect the power grid [145]. The importance of such constraints in energy management of microgrids has been clearly shown in the previous researches [146–150], and different preventive and corrective measures have been taken into account to improve the system security. Reference [146] introduced a conservative energy scheduling framework which minimised the dependency on susceptible lines, while concerning the voltage and reactive power constraints as important criteria of secure grid operation. Sun *et al.* [147] proposed a self-healing strategy for microgrids to prevent security problems when the grid is facing a contingency condition. The steady state voltage stability of islanded AC-DC microgrids with limited reactive power support in the off-grid mode and under the influence of contingencies is studied by [148]. In [149], the security constraints have been integrated into the optimal power flow model in energy management of multi-microgrids in a stochastic environment. Contingency conditions have been considered as the main means of defining different security measures [145]. In [150] the role of reserve constraints in providing security margin for isolated microgrids against forecast errors and intra-dispatch fluctuations is analysed by introducing a capacity allocation method. The reserve requirements can be provided by dispatchable units, or optimal management of controllable loads. In [151] optimal management of thermostatically controllable loads is considered as flexibility option for primary frequency regulation. In reality, however, the contingency situations are mainly uncertain phenomena (e.g., natural disasters) that change over a geographical area in a specific period of time. These two factors (i.e., uncertainty in the occurrence of disruptions,

and changeability over the system structure) have not been considered in the definition of security.

Network reconfiguration has been regarded as a viable solution to enhance the system security, while keeping a radial structure for the system to facilitate the protection measures. The results obtained in [152] show that the network reconfiguration can change the maximum active droop coefficient through tolerating the impedance. A worst line contingency detection method for the microgrids is proposed in [153], while the mobile RES and network reconfiguration are considered as preventive actions to minimise the load curtailment. Application of this method in improving system security is even evident when it has been subjected to different limitations, such as loss-of-load and line capacity constraints [154], or dynamic line rating limitations [155]. A new network reconfiguration in the presence of RES has been introduced in [156] for post failure system restoration. This method helped in decreasing the costs of restoration program. In [157], the joint optimisation of network reconfiguration and distributed generation is considered as a solution for decreasing the time and cost of system restoration after major faults in the distribution network. The network reconfiguration, however, has been mainly studied as a preventive rather than a corrective measure. Also, the majority of post/pre-reconfiguration problems has been designed based on the known location of faults. However, considering the highly uncertain nature of contingency conditions, changing the system configuration prior to the occurrence of any contingency condition may not influence the elements that will be affected by the event of disruptions.

6.1.3 Computational efficiency

Including the security measures in a real-time control mechanism, requires a computationally efficient mathematical model. The existing literature on the real-time energy scheduling of microgrid have mainly adapted MINLP [158] or MILP [159] models. Also, those studies which have considered network reconfiguration as a flexibility option for improving the system security have mainly utilised MINLP [153] or MILP [147] models. The main classification criterion for these mathematical methods is the power flow algorithm.

Considering a full AC power flow model results in an MINLP problem, and is often solved employing heuristic optimisation methods [160]. However, the MINLP models fail to ensure global optimality (or quantify the optimality gap), while imposing a significant computational burden. The MILP models use some simplifications and approximations in order to linearise the non-convex constraints, which introduce a layer of inaccuracy to model outputs.

The taxonomy of relevant literature on the energy scheduling of microgrid is given in Table 6.1. The studied literature clearly highlighted the importance of including security measures in microgrid operation, as well as the need for using different flexibility methods in the control mechanism. However, there are several important points in the literature that have not been considered, including: a) importance of security in real-time energy scheduling, b) influence of uncertainty on the real-time flexibility of system, c) economic factors associated with risk of uncertainty in the real-time energy scheduling, d) real-time flexibility measures created by the energy grid, and e) computational efficiency of a framework that concerns points in (a)-(d). These factors have been highlighted as important research program questions in the Global Power System Transformation (G-PST) Consortium's Research Agenda Group [109]. The relevant questions mentioned in this agenda are [109]:

1. How can operators identify critical stability situations in real-time and optimise system security?
2. How can system operators get relevant real-time visibility and situational awareness of the state of the power system with increasing penetrations of RES and DER?
3. How do control rooms address uncertainties in weather conditions that impact loads and renewable energy output and rate of change (ramps)? How can probabilistic forecasting techniques be better incorporated into real-time operations?
4. How can grid topology be flexibly adapted at various operating conditions?

TABLE 6.1: Taxonomy of microgrid energy scheduling literature.

		Constraints			Real-time approach		Reconfiguration		Security measures		
Ref. No	Uncertainty	Risk	Security	Reserve	Conventional	Risk-constrained	Normal	Stochastic	Corrective	Preventive	Model type
[87]	x	x	x	✓	✓	x	x	x	x	x	MILP[I]
[138]	x	x	✓	x	✓	x	x	x	x	VVC[II]	MILP
[140]	✓	x	✓	✓	x	x	x	x	x	x	MILP
[145]	x	x	✓	x	x	x	x	x	x	NR[III]	MINLP[IV]
[146]	x	x	✓	x	✓	x	✓	x	DR[V]	NR	MILP
[148]	x	x	✓	✓	x	x	x	x	x	VVC	MINLP
[149]	✓	x	✓	x	x	x	✓	x	x	NR	MINLP
[150]	✓	x	✓	✓	✓	x	x	x	DR	x	MILP
[153]	✓	x	✓	x	x	x	✓	x	x	NR	MINLP
[154]	✓	✓	x	x	x	x	✓	x	x	x	MICP[VI]
[157]	x	x	x	x	x	x	✓	x	NR	x	MILP
This chapter	✓	✓	✓	✓	x	✓	x	✓	NR	DR	MICP

I: Mixed integer linear programming, II: volt-var control, III: Network reconfiguration, IV: mixed-integer nonlinear programming,
V: demand response, VI: mixed-integer conic programming.

In view of the above requirements, this chapter proposes a tri-layer min-max-min joint RSC-MPC framework for real-time energy scheduling of FIMGs under the influence of uncertainty and real-time time-varying contingency conditions. The control philosophy starts from first layer cost optimisation, which applies the preventive measures based on the predicted data. The preventive flexibility measures in this layer are adopted through optimal pre-scheduling of DERs, and applying the demand flexibility program. The second layer aims at identifying the worst-case contingency conditions by maximising the load curtailment and the mismatch between the pre-scheduling energy procurement cost (i.e. first layer) and that of real-time (i.e. second layer). Convex time-varying security constraints are developed for the RSC-MPC controller in the second layer, which consider changeability in the location of disruptions over different zones of the FIMG. Finally, in the third layer, the controller develops a convex real-time network reconfiguration as a corrective flexibility measure against the contingency conditions, while re-scheduling the FIMG with a trade-off decision making (i.e. making compromise between energy procurement cost and risk of uncertainty in the predicted data). Note that solving the model without the first two layers results in an optimistic decision making which neglects contingency condition or risk of uncertainty. The proposed model benefits from a MICP which is computationally efficient in terms of accuracy and processing time. These developments allow the inclusion of risk and security measures in the real-time energy management of flexible microgrids that have to operate in islanded mode. To summarise, the main contributions of this chapter are:

- Proposing a multi-layer MICP model for multi-objective energy scheduling of FIMGs. The introduced model is computationally efficient and can provide an accurate representation of the flexibility in the power flow model for inclusion in the RSC-MPC.
- Developing a min-max-min RSC-MPC framework which considers the uncertainty of predicted data and the risk associated with them. The introduced control model allows the inclusion of uncertainties in real-time energy scheduling of FIMGs while accounting for structural changes in the network topology.

- Building time-varying security constraints based on a MICP power flow model. The proposed framework takes into account the real-time disruptions which change over the grid zones. This framework allows the inclusion of more realistic contingency conditions.
- Developing a corrective real-time network reconfiguration model which improves system security, while guaranteeing the network radiality over uncertainty scenarios (i.e. stochastic network reconfiguration). This framework enables the system controller to change the system configuration so as to prevent load curtailment caused by real-time contingency, while considering the uncertainty.

6.2 Risk- and Security-Constrained MPC

Using an optimisation-based approach and incorporating the system constraints while also accounting for future timeslots in predicting the state variables are unique advantages of MPC approach, enabling it as a widely-used control mechanism for real-time energy scheduling of microgrids. This controller compiles the optimal control decisions through optimising an objective function for a finite time horizon while only considering the results for the current time interval. For the next timeslot, the controller re-dispatches the system while considering the grid dynamics, past and present control signals. Although such a control framework is efficient in optimising the state variables according to the objective function, it cannot fully address the real-time structural changes in the system topology and the uncertainty of RES. These challenges reinforce the needs for boosting the efficiency of this control scheme.

The conceptual illustration of the conventional and the proposed MPCs is shown in Fig. 6.1. In the conventional MPC, the controller dispatches the system for each time interval while considering the whole control horizon. This controller, however, does not account for the uncertainty of RES, and the risk associated with stochastic generation of these energy sources. For example, when compiling the model at time period $t_{(1)}$, the predicted RES

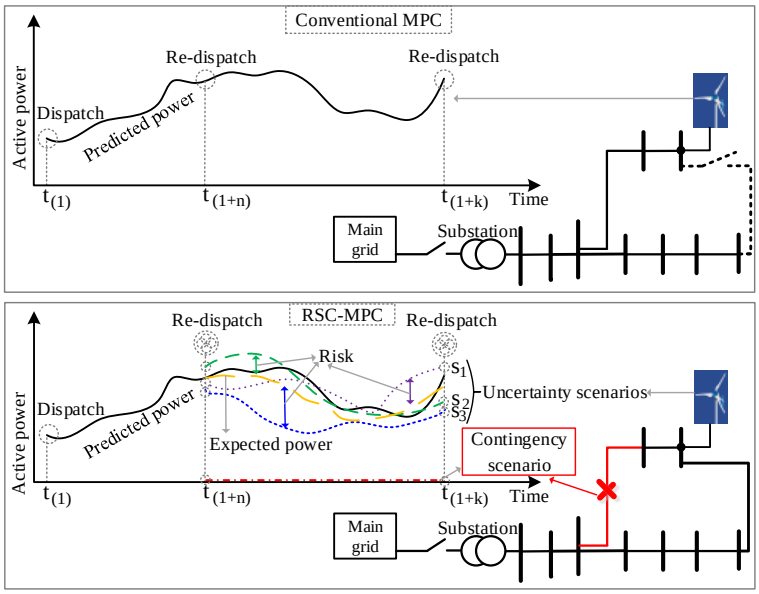

FIGURE 6.1: Comparison of conventional and the proposed MPCs.

output between time periods $t_{(1+n)}$ and $t_{(1+k)}$ are uncertain and more likely to have different generation scenario from the predicted values. Besides, the occurrence of contingency in the future time intervals cannot be predicted by the conventional control systems. For instance, any disruption between the line connecting the RES to other parts of the network results in a contingency situation that requires a real-time security measure. Concerning these challenges, this chapter introduces a RSC-MPC, which is conceptually illustrated in Fig. 6.1. This controller accounts for the uncertainty of prediction data, while considering the risk associated with each scenario. Such a risk is defined based on the difference between the expected amount of objective function and its value in different uncertainty scenarios. The proposed RSC-MPC also accounts for real-time contingency condition, and re-dispatches the available sources and upgrades the FIMG structure to guarantee the system security.

Note that the proposed method investigates the energy management of a FIMG. Therefore, there is no need to optimise the power exchange with the main grid,

which requires a tertiary control level [161]. This chapter performs a MPC-based energy management strategy which is part of secondary control level. It considers the economic aspects of the FIMG operation and manages the optimal power flow.

6.3 Problem formulation

Figure 6.2 illustrates the proposed RSC-MPC framework for FIMG energy scheduling, comprising dispatchable units (DUs), and wind turbines (WTs) as the available generation capacity, as well as battery energy storage (BES) and demand flexibility as the FIMG flexibility sources. The proposed architecture is a hierarchical tri-layer min-max-min optimisation. The problem is solved hierarchically with consideration for here-and-now and wait-to-see decision variables. The first layer of the model is a day-ahead scheduling which does not consider MPC and uncertainty scenarios. The second and third layers are MPC-based stochastic optimisation, taking into account contingencies and uncertainty scenarios. The second and third layers are performed on a real-time basis over the control horizon.

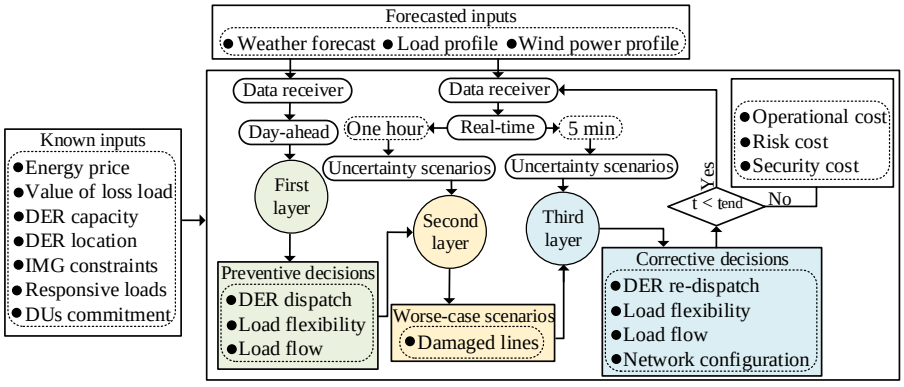

FIGURE 6.2: The process of solving the proposed hierarchical RSC-MPC architecture.

The timeline of the each layer is shown in Fig. 6.3. Considering the availability of weather forecast data on an hourly basis, the second level is solved for one-hour time intervals over the control horizon. Meanwhile, in order to increase

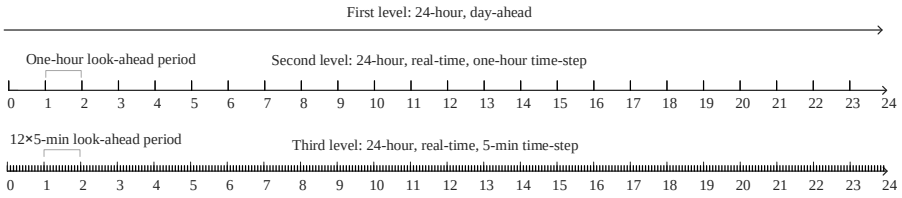

FIGURE 6.3: The proposed RSC-MPC time steps.

the performance and adaptability of the proposed control method to real-time condition [162], the third layer is solved for 5-min time periods.

In the first layer, a pre-scheduling day-ahead cost optimisation is solved so as to determine the preventive measures, consisting of the DER flexibility and the load flow variables (i.e. voltage magnitude/angle of system buses and active/reactive power flow through system branches). These decision variables are obtained for the normal operation of the system and are considered as a reference point for the constraints in second and third layers. They are used for evaluating the risk of uncertainty and the contingency condition in the real-time operation of the network. The outputs of the first layer are scenario independent (i.e. $X^{l1}_{i,t,s} = X^{l1}_{i,t}$), and considered as here-and-now control actions.

The second layer tries to identify the worst real-time contingency scenarios that can affect the pre-scheduling preventive measures (i.e. the system state in the first layer) under the influence of wind power output uncertainty. The contingency conditions determine the worst line outage scenarios that can affect the normal operation of the system. The optimisation in this layer maximises the mismatch between preventive and real-time actions along with the system load shedding as the objective function, while the location of line-outage scenarios is defined at each time interval on a real-time basis. The decision variables of the second layer (i.e. $X^{l2}_{i,t,s}$) identify the worst contingency scenarios at time period t and the uncertainty scenario s. This information is transferred to the third layer which tries to re-schedule the IMG based on the wort-case scenarios.

The third layer receives the real-time data from the forecast platform and that of previous layers, and re-solves the model to proceed the corrective

flexibility actions. The corrective decision variables (i.e. $X^{l3}_{i,t,s}$) are preformed by re-dispatching DERs while using the network reconfiguration as a flexibility measure. DER re-dispatching and topology reconfiguration flexibility strategies are taken by the third layer at time interval t in face of real-time contingency conditions and the risk associated with uncertainty of wind power prediction at the same time interval. Since the control signals in this layer are proceeded according to the current state of the system in different scenarios, they are identified as the wait-to-see variables (i.e. scenario dependent). At the end of operation horizon, the controller analyses the costs associated with the risk of uncertainty and the security measures. In this section, the mathematical formulation of the proposed MICP stochastic optimisation is presented.

6.3.1 Objective function

The mathematical model of the proposed RSC-MPC is built upon an objective function comprised of expected energy procurement cost of FIMG, and expected cost of load curtailment, represented by Equation (6.1). Considering the energy price inside the FIMG as a known input [158], the former includes cost of purchasing power from DUs and WTs, the cost of energy arbitrage with the BES, and the cost of incentivising the responsive loads for participating in the flexibility program, while the latter represents the load shedding cost based on the value of lost load, as follows:

$$of = \sum_{s \in \Omega_s} \pi^W_s \times \left(C^{EP}_s + C^C_s \right) \tag{6.1}$$

$$C^{EP}_s = \sum_{t \in \Omega_t} \Delta t \times \gamma^m_t \left\{ \begin{array}{l} \sum\limits_{b \in \Omega_g} P^G_{b,t,s} + \sum\limits_{b \in \Omega_w} P^{WT}_{b,t,s} \\ + \sum\limits_{b \in \Omega_e} \left(P^{DCh}_{b,t,s} - P^{Ch}_{b,t,s} \right) \\ + \sum\limits_{b \in \Omega^f_b} \left(P^D_{b,t,s} - P^{D_0}_{b,t,s} \right) \end{array} \right\} \tag{6.2}$$

$$C_s^C = \sum_{t\in\Omega_t}\sum_{b\in\Omega_b^c} \Delta t \times \left(L_b^C P_{b,t,s}^C\right) \tag{6.3}$$

where (6.2) is the energy procurement cost of the FIMG in each scenario, in which the first and second terms are respectively costs of purchasing power from DUs and WTs; the third and fourth terms represent the cost/income of discharging and charging power from/to the BES respectively; the last term is cost of flexibility in the responsive loads. Note that the energy price is determined by the upstream network and the microgrid operator tries to minimise the energy procurement cost based on available resources. Equation (6.3) represents the load curtailment cost at each scenario.

6.3.2 Including Risk Constraints in the Objective Function

The first layer of the proposed optimisation is a cost minimisation for here-and-now decision variables. Therefore, the objective function given in (6.1) is minimised (i.e. min $\{\Theta^{l1} = of\}$) in this layer. The second layer, however, tries to identify the worst contingency scenarios by maximising the expected load curtailment cost, while maximising the mismatch between the real-time and preventive energy scheduling. This allows the third layer flexibility measures to deal with real-time contingency conditions, and re-dispatch the FIMG at each time interval to prevent the security problems that could be the result of energy scheduling mismatch and/or unexpected disruptions. The objective function of the second layer is written as:

$$\max\left\{\Theta^{l2} = \sum_{s\in\Omega_s} \pi_s^W \times \left((C_s^{EP_{l2}} - C_s^{EP_{l1}}) + C_s^C\right)\right\} \tag{6.4}$$

The solution obtained in (6.1), however, is subject to the risk of uncertainty, meaning that it is more likely to observe a considerable difference between expected value of objective function and its individual value in some scenarios. To deal with this risk, several methods have been introduced such

as variance, shortfall probability, expected shortfall, value at risk, and conditional value at risk (CVaR). In this chapter, CVaR is adopted for handling the risk measures due to its advantages, numerical efficiency and stability of calculation for instance, over other techniques [163]. Based on the objective function, the process of including risk measure in the objective function of the proposed RSC-MPC is expressed as:

$$\Re = \sigma - \frac{1}{1-\rho} \sum_{s \in \Omega_s} \varphi_s \pi_s^W \tag{6.5}$$

$$\left(C_s^{EP} + C_s^C\right) - \sigma \leq \varphi_s \,, \forall s \in \Omega_s \tag{6.6}$$

where, (6.5) gives the optimal value of the CVaR (i.e. $\Re$), with $(1-\rho)100\%$ of total cost in each scenario worse than value of VaR (i.e. σ). The difference between expected value and total cost in each scenario is shown by (6.6), where $\varphi_s \geq 0$.

To consider the risk constraints in the third layer, the expected cost should be increased, based on the value of ρ. In other words, minimising the degree of risk increases the value of energy procurement cost. Under such circumstances, a proper solution can make a trade-off between expense of risk measures and energy procurement cost. To do so, the third layer of the optimisation is solved as multi-objective problem using weighted sum method. Note that the general model is convex and could be solved by different multi-objective handling techniques. Based on this explanation, the general min-max-min objective function of the proposed RSC-MPC is defined as follows:

$$\min \left\{ \begin{array}{l} \beta \times of \left[\max \left(\Theta^{l2} \min \Theta^{l1}\right)\right] \\ +(1-\beta) \times \Re \left[\max \left(\Theta^{l2} \min \Theta^{l1}\right)\right] \end{array} \right\} \tag{6.7}$$

6.3.3 Power Balance Constraints

The proposed power balance in this chapter takes into consideration the power output of DUs, WTs, as well as the charge and discharge power of BES, the participation of responsive loads, and the branch power flow, as follows ($\forall b, m \in \Omega_b, \forall t \in \Omega_t,\ \forall s \in \Omega_s$):

$$\begin{aligned} &P^{UN}_{b,t,s} + P^{G}_{b,t,s} + P^{WT}_{b,t,s} + P^{DCh}_{b,t,s} + P^{C}_{b,t,s} \\ &-P^{D}_{b,t,s} - P^{Ch}_{b,t,s} = \sum_{m} P^{\ell}_{bm,t,s} \end{aligned} \tag{6.8}$$

$$\begin{aligned} &Q^{UN}_{b,t,s} + Q^{G}_{b,t,s} + Q^{WT}_{b,t,s} \\ &+ \tan\left(\frac{Q^{D}_{b,d,t}}{P^{D}_{b,d,t}}\right) \times P^{C}_{b,t,s} - Q^{D}_{b,t,s} = \sum_{m} Q^{\ell}_{bm,t,s} \end{aligned} \tag{6.9}$$

$$P^{\ell}_{bm,t,s} = G^{\ell}_{bm} V^{2}_{b,t,s} - V_{b,t,s} V_{m,t,s} (G^{\ell}_{bm} \cos\theta_{bm,t,s} + B^{\ell}_{bm} \sin\theta_{bm,t,s}) \tag{6.10}$$

$$\begin{aligned} Q^{\ell}_{bm,t,s} = &-\left(B^{\ell}_{bm} + \frac{B^{Sh}_{bm}}{2}\right) V^{2}_{b,t,s} - V_{b,t,s} V_{m,t,s} (G^{\ell}_{bm} \sin\theta_{bm,t,s} \\ &-B^{\ell}_{bm} \cos\theta_{bm,t,s}) \end{aligned} \tag{6.11}$$

where, constraints (6.8) and (6.9) represent the real and reactive power injections at each bus, respectively. Constraints (6.10) and (6.11) are the real and reactive power flow from bus b to bus m at time step t and scenario s. These constraints, however, are non-convex nonlinear and are more likely to result in a local optimal solution, with a dramatic computation time. On the other hand, linearising the non-linear equations decreases the accuracy of the model. Generally speaking, as mentioned in [164], *"the large boundary is not between linearity and non-linearity, but between convexity and non-convexity"*.

Convex relaxation of the original problem can be a valid solution to deal with this challenge. To do so, the continuous variables of the original problem are reformulated as a convex second-order cone program. Therefore, the continuous

variables are redefined as follows [165] ($\forall b, m \in \Omega_b, \forall t \in \Omega_t,\ \forall s \in \Omega_s$):

$$U_{b,t,s} = \frac{V_{b,t,s}^{\ 2}}{\sqrt{2}} \tag{6.12a}$$

$$R^{\ell}_{bm,t,s} = V_{b,t,s} V_{m,t,s} \cos\theta_{bm,t,s} \tag{6.12b}$$

$$T^{\ell}_{bm,t,s} = V_{b,t,s} V_{m,t,s} \sin\theta_{bm,t,s} \tag{6.12c}$$

Therefore, the power flow equations in (6.10) and (6.11) are reformulated as follows:

$$P^{\ell}_{bm,t,s} = \sqrt{2}\, G^{\ell}_{bm} U_{b,t,s} - G^{\ell}_{bm} R^{\ell}_{bm,t,s} - B^{\ell}_{bm} T^{\ell}_{bm,t,s} \tag{6.13}$$

$$Q^{\ell}_{bm,t,s} = -\sqrt{2}\left(B^{\ell}_{bm} + \frac{B^{Sh}_{bm}}{2}\right) U_{b,t,s} + B^{\ell}_{bm} R^{\ell}_{bm,t,s} - G^{\ell}_{bm} T^{\ell}_{bm,t,s} \tag{6.14}$$

Based on (6.12) sum of the square of $R^{\ell}_{bm,t,s}$, $T^{\ell}_{bm,t,s}$, can provide a constraint for the system lines, as mathematically described below:

$$\begin{aligned} &\left(V_{b,t,s} V_{m,t,s} \cos\theta_{bm,t,s}\right)^2 + \left(V_{b,t,s} V_{m,t,s} \sin\theta_{bm,t,s}\right)^2 \\ &= \left(V_{b,t,s}\right)^2 \left(V_{m,t,s}\right)^2 \left(\cos\theta_{bm,t,s}^{\ 2} + \sin\theta_{bm,t,s}^{\ 2}\right) \\ &= \left(V_{b,t,s}\right)^2 \left(V_{m,t,s}\right)^2 = 2\mathrm{U_{b,t,s}U_{m,t,s}} \end{aligned} \tag{6.15}$$

Therefore, variables $R^{\ell}_{bm,t,s}$ and $T^{\ell}_{bm,t,s}$ are new variables that are defined for each line and can be constrained as follows:

$$2U_{b,t,s} U_{m,t,s} = \left(R^{\ell}_{bm,t,s}\right)^2 + \left(T^{\ell}_{bm,t,s}\right)^2 \tag{6.16}$$

This non-convex equation can be relaxed by inclusion rotated quadratic cones, as below:

$$2\,U_{b,t,s}\,U_{m,t,s} \geq \left(R^{\ell}_{bm,t,s}\right)^2 + \left(T^{\ell}_{bm,t,s}\right)^2 \tag{6.17}$$

Constraint (6.17) represents the relaxed conic quadratic constraint for branch bm, with free variable $T^{\ell}_{bm,t,s}$ and positive variable $R^{\ell}_{bm,t,s}$. When the optimisation problem is solved, the values of $R^{\ell}_{bm,t,s}$ is increased until the inequality constraint in (6.17) is activated, which causes the relaxed inequality constraint in (6.17) to be binding at optimality [165]. This is achieved by minimising the energy procurement cost in (6.1), leading to the minimisation of net active power injections, which results in an increase of $R^{\ell}_{bm,t,s}$ (since $G^{\ell}_{bm} \geq 0$ in (6.13)). It is worth mentioning that due to the fact that the solution of the load flow for a radial distribution network is unique [166], the solution of the optimisation problem converges to a true solution.

In this Chapter, the proposed conic programming optimisation is solved using MOSEK which benefits from well-approved theoretical algorithms [167]. Such commercial solver benefits from high-powered software tools and can provide accurate results, even for ill-conditioned radial networks [168]. This solver scales the problem efficiently resulting in the definition of a suitable search direction. Another advantage of this method is that it gives reliable certificate of infeasibility if the load flow problem does not has a solution, compared to the load flow algorithms proposed in [169] and [170] which diverge and terminate if the number of iterations exceed the maximum allowed number. Finally, the computational efficiency of the proposed MICP model is compared against other approaches in Reference [165], which has been the main reference in developing the proposed method in this chapter. As shown in [165], the proposed MICP model enjoys accurate solution with a rapid processing time when the relative optimiality gap is 5%, compared to MILP models. However, the computational time is increased when the relative gap is reduced to 0.01%. It is worth mentioning that the explanation of relative gap is provided in [74].

6.3.4 Distributed Energy Resources

The following constraints represent the capacity and technical limits of different DERs within the FIMG, including BES, WTs, and DUs ($\forall t \in \Omega_t,\ \forall s \in \Omega_s$):

$$SOC_{b,t,s}^{BES} = SOC_{b,t-1,s}^{BES} + \Delta t \left(P_{b,t,s}^{Ch}\, \eta_b^{Ch} - p_{b,t,s}^{DCh} / \eta_b^{DCh} \right) \ , \forall b \in \Omega_e \tag{6.18}$$

$$SOC_{\min}^{BES} \leq SOC_{b,t,s}^{BES} \leq SOC_{\max}^{BES} \ \ , \forall b \in \Omega_e \tag{6.19}$$

$$0 \leq P_{b,t,s}^{Ch} \leq \lambda_{b,t,s}^{Ch} P_{\max}^{Ch} \ \ , \forall b \in \Omega_e \tag{6.20}$$

$$0 \leq P_{b,t,s}^{DCh} \leq \lambda_{b,t,s}^{DCh} P_{\max}^{DCh} \ \ , \forall b \in \Omega_e \tag{6.21}$$

$$\lambda_{b,t,s}^{Ch} + \lambda_{b,t,s}^{DCh} \leq 1 \ \ , \forall b \in \Omega_e \tag{6.22}$$

$$0 \leq P_{b,t,s}^{WT} \leq \psi_{b,s}^{WT} P_R^{WT} \ \ , \forall b \in \Omega_w \tag{6.23}$$

$$-\tan(\varphi_{lead}) P_{b,t,s}^{WT} \leq Q_{b,t,s}^{WT} \leq \tan(\varphi_{lag}) P_{b,t,s}^{WT} \, \forall b \in \Omega_w \tag{6.24}$$

$$P_{b,\min}^{G} \chi_{b,t}^{G} \leq P_{b,t,s}^{G} \leq P_{b,\max}^{G} \chi_{b,t}^{G} \, , \forall b \in \Omega_g \tag{6.25}$$

$$Q_{b,\min}^{G} \chi_{b,t}^{G} \leq Q_{b,t,s}^{G} \leq Q_{b,\max}^{G} \chi_{b,t}^{G} , \forall b \in \Omega_g \tag{6.26}$$

$$P_{b,t,s}^{G} - P_{b,t-1,s}^{G} \leq \ R_b^U \ \ , \forall b \in \Omega_g \tag{6.27}$$

$$P_{b,t-1,s}^{G} - P_{b,t,s}^{G} \leq \ R_b^D \ \ , \forall b \in \Omega_g \tag{6.28}$$

$$\sum_{\forall b \in \Omega_g} \left(\chi^G_{b,t} P^G_{\max} - P^G_{b,t,s}\right) \geq Res_t \tag{6.29}$$

$$0 \leq P^C_{b,t,s} \leq P^D_{b,t,s} \ , \forall b \in \Omega^c_b \tag{6.30}$$

Constraints (6.18)-(6.22) represent the BES model: (6.18) shows the state of charge of BES which is defined based on its value of energy in the previous time period and current state of charge and discharge; (6.19) limits the upper and lower limit of storage energy; (6.20) and (6.21) respectively limit the charge and discharge power; (6.22) is a logic preventing the simultaneous charge and discharge.Note that BES can also provide reactive power in Eq. (6.9). However, it is assumed that the BESs are operating in unit power factor and only exchange active power with the network, while the reactive power of WTs and DUs is enough to support system demand. The WT active and reactive power is limited by (6.23) and (6.24) respectively. Note that the parameter $\psi^{WT}_{b,s}$ represents the available power of WT in Scenario s. Finally, constraints (6.25)-(6.28) define the DUs capacity limit, where constraints (6.25) and (6.26) show the upper and lower limit of active and reactive power respectively; the ramp up and ramp down limits are applied through (6.27) and (6.28) respectively. Constraint (6.29) shows the reserve requirements at each time interval which is provided by DUs. Consideration of this constraint along with (6.25) guarantees the provision of reserve requirements. The parameter Res_t is defined by the decision maker which is assumed to be 10% in this chapter [171]. Finally, Constraint (6.30) limits the maximum amount of active load that could be curtailed.

6.3.5 Demand Flexibility

A certain degree of flexibility is considered for some responsive loads in the system to adjust their consumption based on the electricity price. The load curtailment is also included in the model so as to prevent unrecoverable damages to the FIMG in the emergency condition, which helps to keep

important security factors (e.g. voltage and frequency) within acceptable range. The demand flexibility programs are introduced as ($\forall t \in \Omega_t,\ \forall s \in \Omega_s$):

$$(1-\beta^{res}_{b,t,s})P^{D_0}_{b,t,s} \leq P^{D}_{b,t,s} \leq (1+\beta^{res}_{b,t,s})P^{D_0}_{b,t,s}\,, \forall b \in \Omega^f_b \tag{6.31}$$

$$\sum_{t\in\Omega_t} P^{D}_{b,t,s} = \sum_{t\in\Omega_t} P^{D_0}_{b,t,s} \quad , \forall b \in \Omega^f_b \tag{6.32}$$

$$Q^{D}_{b,t,s} = \tan\left(\frac{Q^{D_0}_{b,t,s}}{P^{D_0}_{b,t,s}}\right) \times P^{D}_{b,t,s} \quad , \forall i \in \Omega^f_b \tag{6.33}$$

where, (6.31) denotes the maximum and minimum amount of flexibility in the active power demand of responsive loads, while (6.32) ensures that the total changes in the responsive loads would be equal to the base load by the end of operation period. Constraints (6.33) represents the changes in the reactive power of responsive loads.

6.3.6 Microgrid Constraints

The branch current, and voltage limits are critical grid constraints which should be satisfied in all layers as follows ($\forall b, m \in \Omega_b, \forall t \in \Omega_t,\ \forall s \in \Omega_s$):

$$\begin{aligned}&\left(I^{\ell}_{bm,t,s}\right)^2 = \sqrt{2}\left(\left(G^{\ell}_{bm}\right)^2 + \left(B^{\ell}_{bm}\right)^2\right)\\ &\times\left(U_{b,t,s} + U_{b,t,s} - \sqrt{2}R^{\ell}_{bm,t,s}\right) \leq \left(I^{\ell}_{\max}\right)^2\end{aligned} \tag{6.34}$$

$$\frac{\left(V^{\min}_{b}\right)^2}{\sqrt{2}} \leq U_{b,t,s} \leq \frac{\left(V^{\max}_{b}\right)^2}{\sqrt{2}} \tag{6.35}$$

where constraint (6.34) shows the squared current of branch ij as a linear equation. Also, voltage magnitude is limited by (6.35).

6.3.7 Time-varying Security Constraints

Unexpected disruptions can change the structure of the microgrids dramatically, and cause serious security issues, especially during the islanded operation. According to [172], most of the failures in the electrical network are related to weather events, while the majority of these events affect the distribution networks. Given a wide variety of weather events, this chapter concerns high winds and their impact on the security of microgrids. The contingency scenario is referred to as a high intensity wind which can cause damage to the overhead lines, such as storm Malik and storm Corrie in the UK [173]. The overhead lines are considered to be the most susceptible elements of the network. Considering the fact that these storms affected parts of Europe and UK from hours to days, the control horizon of 24 hours is assumed as the duration of the weather event. Considering a synoptic wind which is a large moving pressure with a horizontal effect over hundreds of kilometres [174], a set of time-varying security constraints are introduced in the proposed RSC-MPC model, which change over the FIMG zones and are influenced by the uncertainty of wind power generation. The term 'time-varying' refers to the real-time changeability of disruption over the operation horizon at each time interval. As opposed to the previous studies which have considered known locations for the damaged elements of the system, the proposed method defines the location of fault at each time interval on a real-time basis.

While a non-linear model multiplies a binary variable into the active and reactive power flow constraints [153], this chapter introduces variables $U^{\ell}_{bm,t,s}$ and $U^{\ell}_{mb,t,s}$ for identifying the status of branches, as follows $(\forall b, m \in \Omega_b, \forall t \in \Omega_t,\ \forall s \in \Omega_s)$:

$$0 \leq U^{\ell}_{bm,t,s} \leq \frac{\left(V_b^{\max}\right)^2}{\sqrt{2}} \vartheta^{\ell^-}_{bm,t,s} \tag{6.36}$$

$$0 \leq U^{\ell}_{mb,t,s} \leq \frac{(V^{\max}_{m})^2}{\sqrt{2}} \vartheta^{\ell-}_{bm,t,s} \tag{6.37}$$

$$0 \leq U_{b,t,s} - U^{\ell}_{ij,t,s} \leq \frac{(V^{\max}_{b})^2}{\sqrt{2}} (1 - \vartheta^{\ell-}_{bm,t,s}) \tag{6.38}$$

$$0 \leq U_{m,t,s} - U^{\ell}_{mb,t,s} \leq \frac{(V^{\max}_{m})^2}{\sqrt{2}} (1 - \vartheta^{\ell-}_{bm,t,s}) \tag{6.39}$$

$$\vartheta^{\ell-}_{bm,t,s} = \vartheta^{\ell-}_{mb,t,s} \tag{6.40}$$

$$\sum_{bm \in \Omega^{z}_{b}} \frac{\left(1 - \vartheta^{\ell-}_{bm,t,s}\right)}{2} = \Im_{z} \ , \forall t \in \Omega^{z}_{t} \tag{6.41}$$

$$\frac{\sum\limits_{t}^{t^r} \left(\Delta t \times \vartheta^{\ell-}_{bm,t,s}\right)}{RT} \leq 1 \tag{6.42}$$

where constraints (6.36)-(6.39) represent the branch connection status, based on variables $U^{\ell}_{bm,t,s}$ and $U^{\ell}_{mb,t,s}$. These variables take the values of $U_{i,t,s}$ or $U_{j,t,s}$, if the branch is closed (i.e. $\vartheta^{\ell-}_{mb,t,s} = 1$), and are set to zero, if the branch is open (i.e. $\vartheta^{\ell-}_{mb,t,s} = 0$). Therefore, $\vartheta^{\ell-}_{mb,t,s}$ is suggested in this chapter for identifying the location of disruption in the FIMG. Constraint (6.41) indicates the occurrence of a specific number of disruptions in each zone (i.e. $\Im_z$) over the period of time at which the zone is experiencing contingency condition (i.e. Ω^{z}_{t}), based on the set of buses located in each zone (i.e. Ω^{z}_{b}). Finally, constraint (6.42) ensures that the damaged line is out-of-service for time periods $\mathrm{t} \in [\mathrm{t}, \mathrm{t}+\mathrm{t}^r]$, where $\mathrm{t}^r = \left(\frac{1}{\Delta t}\right) \times RT$. The proposed constraints in (6.36)-(6.42) are adaptable with the proposed MICP power flow model, and are a novel characteristic of the introduced convex security-constrained optimisation model. By introducing variables $U^{\ell}_{bm,t,s}$ and $U^{\ell}_{mb,t,s}$ there is a need to modify equations (6.13), (6.14), and (6.17), as below:

$$P^{\ell}_{bm,t,s} = \sqrt{2}\, U^{\ell}_{bm,t,s} G^{\ell}_{bm} - G^{\ell}_{bm} R^{\ell}_{bm,t,s} - B^{\ell}_{bm} T^{\ell}_{bm,t,s} \tag{6.43a}$$

$$Q^{\ell}_{bm,t,s} = -\sqrt{2}\left(B^{\ell}_{bm} + \frac{B^{Sh}_{bm}}{2}\right) U^{\ell}_{bm,t,s} + B^{\ell}_{bm} R^{\ell}_{bm,t,s} - G^{\ell}_{bm} T^{\ell}_{bm,t,s} \tag{6.43b}$$

$$U^{\ell}_{bm,t,s}\, U^{\ell}_{mb,t,s} \geq \left(R^{\ell}_{bm,t,s}\right)^2 + \left(T^{\ell}_{bm,t,s}\right)^2 \tag{6.43c}$$

$$\begin{aligned} &\left(I^{\ell}_{bm,t,s}\right)^2 = \sqrt{2}\left(\left(G^{\ell}_{bm}\right)^2 + \left(B^{\ell}_{bm}\right)^2\right) \\ &\times \left(U^{\ell}_{bm,t,s} + U^{\ell}_{mb,t,s} - \sqrt{2} R^{\ell}_{bm,t,s}\right) \leq \left(I^{\ell}_{\max}\right)^2 \end{aligned} \tag{6.43d}$$

The variables $U^{\ell}_{bm,t,s}$ and $U^{\ell}_{mb,t,s}$ which identify the status of branch bm, equal to $U_{b,t,s}$ and $U_{m,t,s}$, respectively, in normal situation (before occurrence of any disruption). These constraints are defined based on the status of lines connecting buses. Therefore, they are solved for each time step over the operation horizon on a real-time basis.

6.3.8 Corrective flexibility Measures

Several methods have been introduced in the literature to respond to the contingency conditions. Among those methods, network reconfiguration has been regarded as an effective solution in improving the system security [152]. This method can prevent load curtailment in a contingency condition while ensuring the radiality of the network. In the previous literature [146, 155], however, the network radiality constraints are adopted based on the graph theory (i.e. number of lines=number of buses-1). Although this constraint is a necessary condition for the reconfiguration, it cannot guarantee radiality. Besides, this method has been considered as a preventive measure, rather than a real-time action that can deal with unexpected real-time contingency conditions, while taking the uncertainty into account. To deal with these issues, a new convex model is introduced in this chapter to guarantee secure

load supply within the FIMG after occurrence of disruptions (i.e. equations (6.36)-(6.41)), while keeping the radial configuration of the system in an uncertain environment. A binary variable (i.e. $\vartheta^{\ell^+}_{bm,t,s}$) is introduced to correct the possible damage caused by the contingency binary variable (i.e. $\vartheta^{\ell^-}_{bm,t,s}$). Also, network radiality for an FIMG is achieved by ensuring that the characteristic of spanning trees holds true, meaning that every node has exactly one parent. Therefore, the proposed method in this chapter is a stochastic network reconfiguration which operates as a corrective real-time measure in the FIMG. Note that the high-frequency reconfiguration is considered as a practical measure since only some specific switches actively participate in the process [175]. Based on this explanation, the branch connection constraints are reformulated as follows $(\forall b, m \in \Omega_b, \forall t \in \Omega_t,\ \forall s \in \Omega_s)$):

$$0 \leq U^{\ell}_{bm,t,s} \leq \frac{\left(V^{\max}_{b}\right)^2}{\sqrt{2}}(\vartheta^{\ell^+}_{bm,t,s} + \vartheta^{\ell^-}_{bm,t,s}) \tag{6.44}$$

$$0 \leq U^{\ell}_{mb,t,s} \leq \frac{\left(V^{\max}_{m}\right)^2}{\sqrt{2}}(\vartheta^{\ell^+}_{bm,t,s} + \vartheta^{\ell^-}_{bm,t,s}) \tag{6.45}$$

$$0 \leq U_{b,t,s} - U^{\ell}_{bm,t,s} \leq \frac{\left(V^{\max}_{b}\right)^2}{\sqrt{2}}\left(1-(\vartheta^{\ell^+}_{bm,t,s} + \vartheta^{\ell^-}_{bm,t,s})\right) \tag{6.46}$$

$$0 \leq U_{m,t,s} - U^{\ell}_{mb,t,s} \leq \frac{\left(V^{\max}_{m}\right)^2}{\sqrt{2}}\left(1-(\vartheta^{\ell^+}_{bm,t,s} + \vartheta^{\ell^-}_{bm,t,s})\right) \tag{6.47}$$

$$\vartheta^{\ell^+}_{bm,t,s} + \vartheta^{\ell^-}_{bm,t,s} \leq 1 \tag{6.48}$$

$$\vartheta^{\ell^+}_{bm,t,s} = \vartheta^{\ell^+}_{mb,t,s} \tag{6.49}$$

$$\alpha^{\ell}_{bm,t,s} + \alpha^{\ell}_{mb,t,s} = (\vartheta^{\ell^+}_{bm,t,s} + \vartheta^{\ell^-}_{bm,t,s}) \tag{6.50}$$

$$\sum_{m \in \Omega^m_b} \alpha^{\ell}_{bm,t,s} = 1 \tag{6.51}$$

$$\alpha^{\ell}_{bm,t,s} + \alpha^{\ell}_{mb,t,s} = 0 \qquad , \forall b \in \Omega^s_b \tag{6.52}$$

Constraints (6.44)-(6.47) represent the branch connection status based on the binary variable indicating the disruption (i.e. $\vartheta^{\ell^-}_{bm,t,s}$) and the binary variable that corrects the system configuration (i.e. $\vartheta^{\ell^+}_{bm,t,s}$). Since it is not practically possible to repair the damaged line at time period t in a real-time paradigm, constraint (6.48) is introduced to arrange the new system configuration at time period t with consideration for the disruption on a real-time basis. In addition, constraints (6.50)-(6.52) ensure the network radiality after applying the corrective actions. Constraint (6.50) shows that the branch bm is in the spanning tree, if one node is the parent of the other. Constraint (6.51) indicates that each bus must have exactly one parent. For an FIMG, the status of the line connecting the grid to the upstream network is open. Therefore, the slack bus is not parent node to any buses and vice versa. This has been modelled by Constraints (6.52).

Note that this chapter investigates a case of contingency in a grid-connected MG. Therefore, the right-hand side of constraint (6.52) is equal to zero, indicating the islanded operation of MG. The storage units and load shedding capability can be utilised in an FIMG for preventing the voltage and frequency excursion. This formulation is different for an isolated microgrid. In this type of grid, there is no point of common coupling between MG and the upstream grid, and it operates permanently in stand alone mode [161]. Therefore, the variables indicating the power exchange with the main grid in constraints (6.8) and (6.9) (i.e. $P^{UN}_{b,t,s}$ and $Q^{UN}_{b,t,s}$)are neglected. Also, there is no need to define constraint (6.52) in an isolated microgrid. The voltage and frequency control in an isolated microgrid is a more strenuous task.

6.4 Framework Description and Case Studies

This section summarises the solution framework for the proposed RSC-MPC, and provides information on the test system and data utilised for validating the model.

6.4.1 Framework Description

The framework of implementing the mathematical model (given in Section 5.3) on the proposed RSC-MPC architecture is sketched in Fig. 6.4. At the core of this framework (blue box), the predicted data is received. Then, the first layer optimisation is processed, where the energy procurement cost is minimised to produce here-and-now decision variables. The microgrid is in its normal condition and there is no change in the configuration of the system, i.e., without consideration for constraints (6.36)-(6.52). Note that it is assumed the microgrid is self-sustainable, with adequate DER capacity to supply the demand in the normal condition; therefore, load curtailment is not expected in the first layer.

The information obtained from this layer is utilised to evaluate the security measures and the consequences of mismatch between the predicted and real-time data along with the risk associated with uncertainty of renewable power generation. Therefore, as a multi-layer optimisation, other layers are optimised with regard to the information processed in the first layer, including the energy procurement cost. Although different sources of uncertainty (e.g. energy price, system load) and various assets (e.g. photovoltaic, micro-hydro) can be considered in the definition of the problem, the main focus of this chapter is on the effect of uncertainty on the MPC-based real-time energy management methods. Therefore, no uncertainty has been considered in the forecast of other input data and wind power generation is taken into account as the only uncertain input. The second layer (green box in 6.4) tries to detect the worst real-time line contingency scenarios in the system, and maximise the mismatch between real-time FIMG dispatch and that of pre-scheduling. The output of this layer

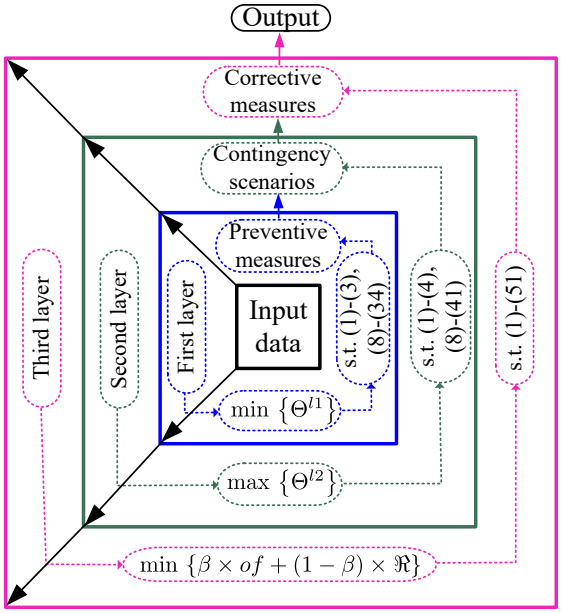

FIGURE 6.4: The framework of solving the proposed model from the inner layer (shown with blue box) to the third layer (shown with pink box).

is considered as a security constraint for the inner layer, to be corrected at each time interval of operation horizon. Therefore, the third layer's optimisation (pink box in 6.4) is processed subject to the unavailability of critical lines and the mismatch between real-time and pre-scheduled data. Also, constraint (6.52) is considered in this layer, meaning that the microgrid experience an islanded mode after a contingency condition. Since the third layer tries to minimise the cost associated with risk of uncertainty, the energy procurement cost is more likely to rise. Therefore, the third layer optimisation tries to make a trade-off between energy procurement cost and the expense of dealing with the risk of exceeding the expected cost. Without the first two layers, the model would be solved in an optimistic manner and can not tolerate any contingency condition or risk of uncertainty. It is assumed that cloud computing enables the real-time communication, while observing privacy and reliability of communication.

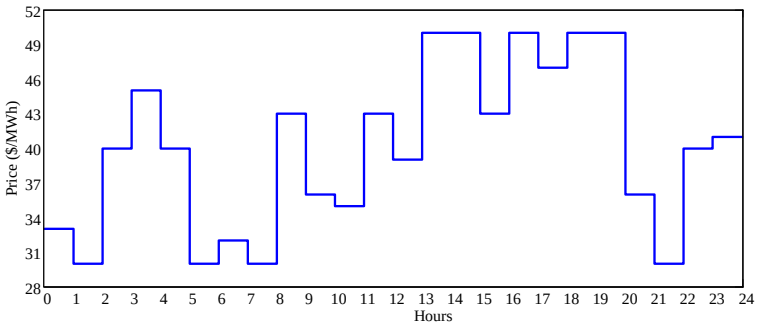

FIGURE 6.5: Day-ahead energy price signals.

6.4.2 Case Studies

The proposed MICP model is executed in GAMS using MOSEK solver. The IEEE 33-bus test system is adapted as the test microgrid, with 5 tie switches that are considered at the third layer as the means of corrective measures. The data of the system under study is taken from [176]. The day-ahead energy price profile is given in Fig. 6.5. Therefore, the proposed multi-period optimal power flow model in this chapter is solved following a unit commitment which defined the ON/OFF status of DUs. Since the chapter investigates the real-time security issues in an emergency condition, it has only focused on the the proposed three-layer framework through the proposed AC optimal power flow model. Therefore, the commitment status of DUs is considered as an input parameter in Fig. 6.2. The islanded operation of the system is guaranteed based on (6.46). The one-line diagram of the test system, with the location of DERs, curtailable and responsive load buses, along with the operation horizon of the control system are illustrated in Fig. 6.6. It is assumed that distribution lines are located in three different zones, shown with different colours in Fig. 6.6. The lines located in each zone are assumed to be in a close geographical location in the FIMG. An operation horizon of 24 hours with respectively one-hour and 5-min time steps for the second and third layers is considered for the controller. Note that the majority of weather forecast or natural disaster tracking platforms are working on an hourly basis. Since the second layer of the simulation captures the effects of contingency (caused by natural disaster) on the operation of the microgrid, one-hour time intervals are considered for this

layer. Meanwhile, to increase the performance and adaptability of the system to real-time conditions the third layer is solved for 5-min time steps.

Considering a 9.85 MVA conductor with R = 0.259 Ω/km, it can be derived that the total length of the IEEE 33-bus network is approximately 80 km. Considering a synoptic wind which passes with a horizontal effect over hundreds of kilometers, it is assumed the weather event moves translational speed over a 24 hours period. Therefore, the duration of the high wind at each zone of the system is assumed to be 8 hours. It is assumed that the overhead lines

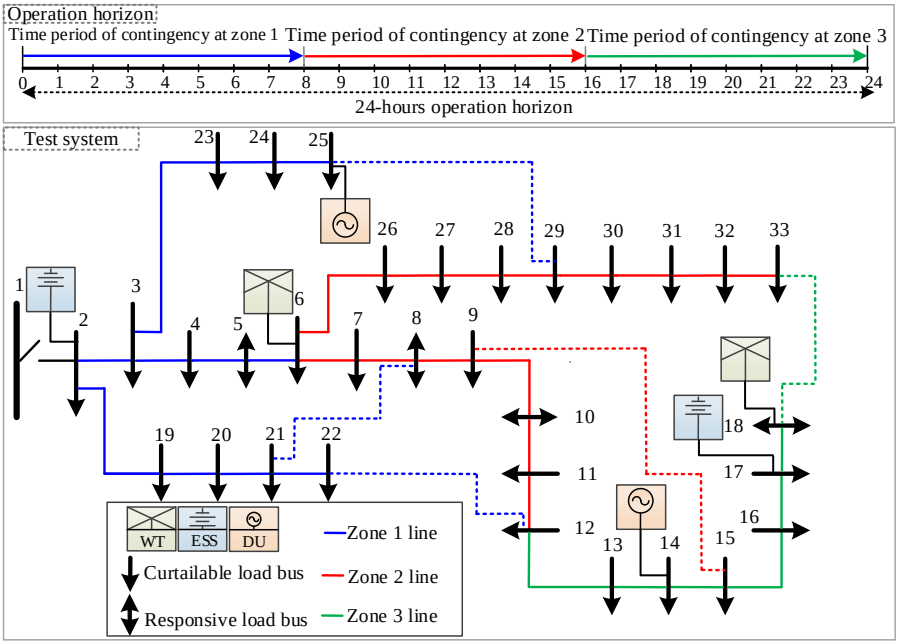

FIGURE 6.6: Schematic diagram of the test FIMG, and the operation horizon.

TABLE 6.2: Wind power output uncertainty scenarios.

Scenario number	$\psi_{i,s}^{WT}$ [%]	π_s^W
s_1	0.0	0.069
s_2	12.9	0.204
s_3	49.4	0.404
s_4	86.8	0.199
s_5	100	0.123

are the most susceptible elements of the FIMG. Two hours of repair time is considered for each branch [177], while assuming that additional manpower and resources are prepared for the event of storm. Also, the network reconfiguration is considered on hourly basis.

The rated capacity of WTs is considered to be 1000 kW, while the minimum and maximum output of DUs is assumed to be 500 kW and 1500 kW respectively. The storage capacity, and charge/discharge power is 1000 kWh, and 200 kW respectively, with the battery efficiency of 90%. The maximum flexibility of responsive loads is assumed to be 15%, and the value of loss load is assumed to be 10 $\$/kWh$. The power output of the WTs is considered as the source of uncertainty in the system. Five uncertainty scenarios are generated for the wind power uncertainty, using historical data and scenario-based method. Uncertainty scenarios are generated according to [122]. The wind power output scenarios are summarised in Table 6.2.

Various aspects of the model are examined through the following case studies:

Case I: The model is solved without consideration for risk of uncertainty, and security constraints (i.e. neglecting constraints (6.36)-(6.52)). This case is equivalent to conventional MPC models.

Case II: The model is solved with consideration for security measures, while neglecting the risk of uncertainty (i.e. $\beta = 1$ in (6.7)). The case is also called risk neutral (RN).

Case III: Risk and security are the main concern of the controller in this case and the decisions are made without considering the economic consequences (i.e. $\beta = 0$ in (6.7)). The solution of this case is called risk averse (RA).

Case IV: The controller makes a trade-off between cost associated with risk of uncertainty, security measures and the energy procurement cost.

6.5 Simulation results

In the following, the important aspects of the model are evaluated based on different case studies, while the performance of the model is further demonstrated by sensitivity analyses and computational statistics.

When the system is operating in a normal condition, any intentional or unintentional disruptions can affect its performance, requiring the FIMG operator to take corrective measures. Rescheduling the system under such circumstances, however, is more likely to impose additional costs to the FIMG operator. Figure 6.7 illustrates the Pareto optimal front of the CVaR and the energy procurement cost in different case studies. This figure provides the economic figures for different case studies of the proposed RSC-MPC. The solutions of the Pareto set vary from a RN (i.e. *Case II*) to a RA (i.e. *Case III*). The difference between the cost of these cases is considered as the expense of accounting for the risk associated with uncertainty. Also, the difference between cases I and II is the security cost. Accordingly, with a cumulative cost of \$62.12, the microgrid operator paid \$32.50, and \$29.62 for dealing with risk and security respectively. These costs should be considered in the energy management of the microgrids that are more prone to contingency and are under the penetration of RES. To make a

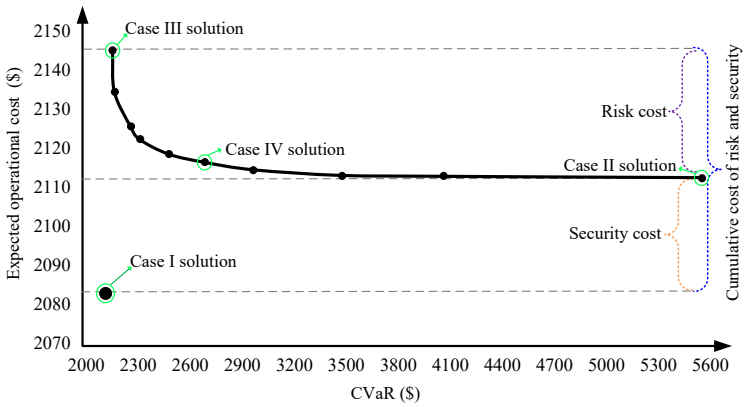

FIGURE 6.7: Value of cost and CVaR in different case studies.

trade-off between RN and RA solutions, the best compromise solution is obtained in *Case IV*, as shown in Fig. 6.7.

In order to analyse the performance of CVaR measure in handling the risk of uncertainty scenarios in the real-time energy scheduling, the energy procurement cost of each scenario in *Case II*, and *Case III* along with that of *Case IV* is depicted and compared with the expected cost of each strategy in Fig. 6.8. The red bars show the scenarios in which the energy procurement cost exceeded the expected cost (i.e. blue bar), while the green bars stand for the scenarios with lower/equal energy procurement cost than/to the expected value. These figures show how risk of uncertainty can influence the real-time energy scheduling over different scenarios. For the RN solution (i.e. *Case II*), it is shown that the energy procurement cost in all scenarios is higher than

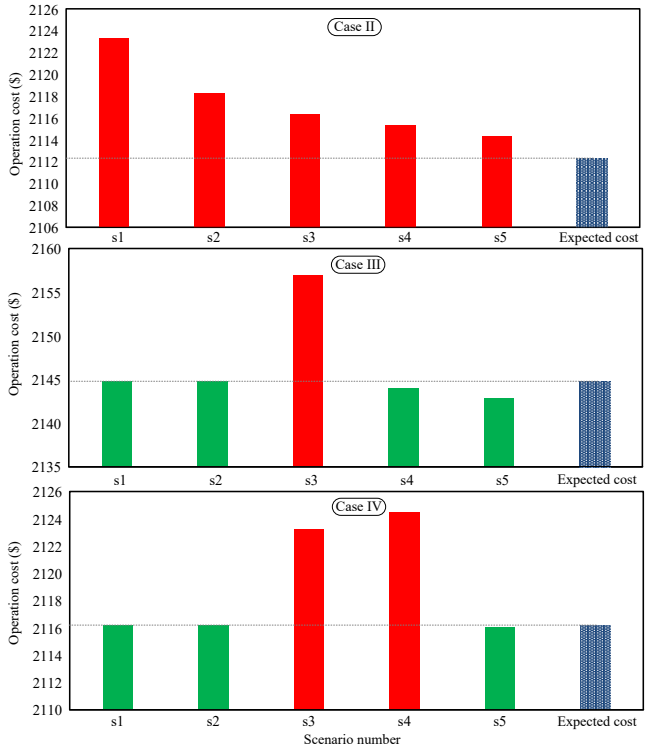

FIGURE 6.8: Application of CVaR in decreasing the energy procurement cost in different case studies.

the expected cost. However, the CVaR measure decreased such a gap between solutions of different scenarios in the RA strategy (i.e. *Case III*). Consequently, the expected cost is increased by \$32.50. Finally, the compromise solution (i.e. *Case IV*), made a trade-off between these two cases, as shown in Fig. 6.8. The security constraints and risk measures are compensated by the energy procurement cost of \$62.12 compared to *Case I*.

Figure 6.9 shows the result of worst-case line contingency conditions based on the proposed method in equations (6.36)-(6.42), for each zone of the microgrid in different uncertainty scenarios. The repair time is considered to be two hours. Therefore, a failed line at time-period t remained out-of-service until time period $t+2$. The vulnerable lines are mainly recognised around the DERs; especially WTs as their output power change in each scenario. The changes in the uncertainty scenarios affected the classification of worst-case scenarios.

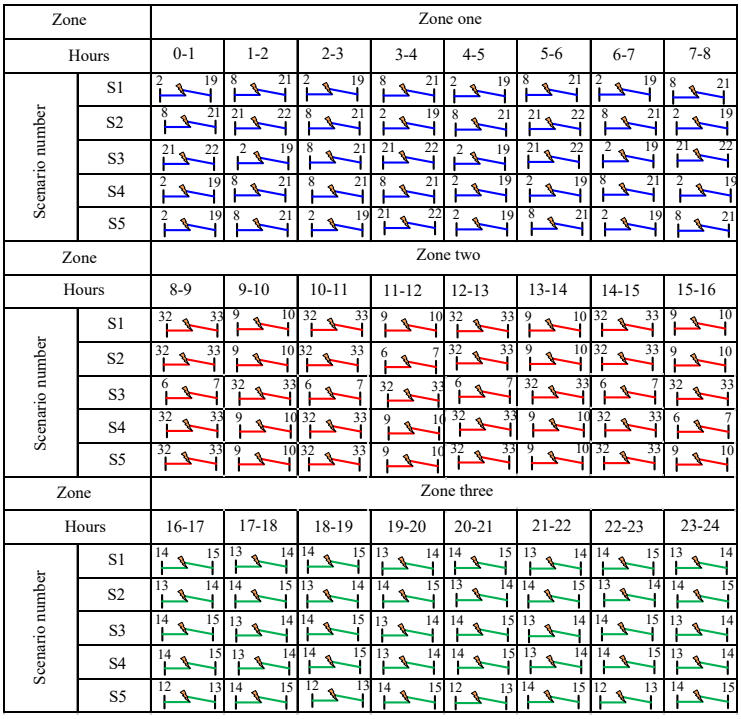

FIGURE 6.9: Variation of real-time contingency conditions in different uncertainty scenarios.

Considering the fact that high winds can increase the WT's generation, the worst-case line outages in Scenario s_5 (i.e. high wind power generation) should be considered as the most critical lines for the MG.

However, the corrective flexibility measures taken in the third layer prevented load curtailment by employing topology reconfiguration on a real-time basis. Variation in the hourly status of the line between buses 8 and 9 in different real-time uncertainty scenarios over system zones is depicted in Fig. 6.10. Knowing that this line is one of the longest lines in the network (i.e. with a high resistance), in the RN strategy (i.e. *Case II*), it is mostly open while it has been changed to closed status in the RA strategy *Case III*. Opening this line decreases the power loss, and consequently the energy procurement cost. However, in the latter case, this line is a strategic connection between two buses that direct the flow of power to different parts of the network and can comply with the deviation of WT power output (Fig. 6.6). Similar to the energy procurement cost, the compromise solution in *Case IV* considered a trade-off between RN and RA strategies. Generally, if the economic issues are important to the FIMG operators, the compromise solution can be a case with a lower cost and some degree of risk aversion.

The decisions made by the microgrid operator regarding the inclusion of risk and security measures can affect the optimal scheduling of energy resources, as shown in Fig. 6.11. The optimal scheduling of available energy resources in scenarios with no wind power generation (i.e. s_1) and high wind power

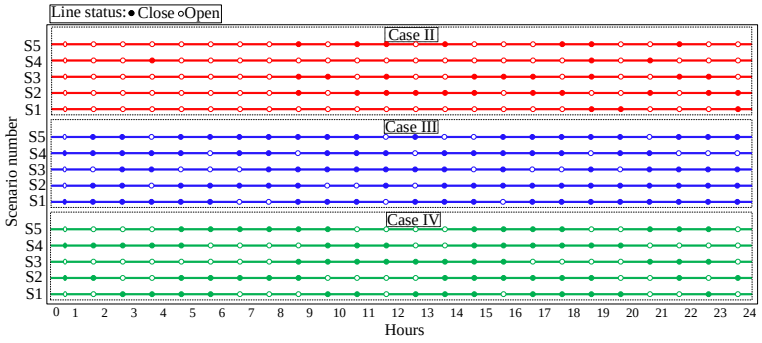

FIGURE 6.10: The corrective configuration of line between buses 8 and 9 in different case studies.

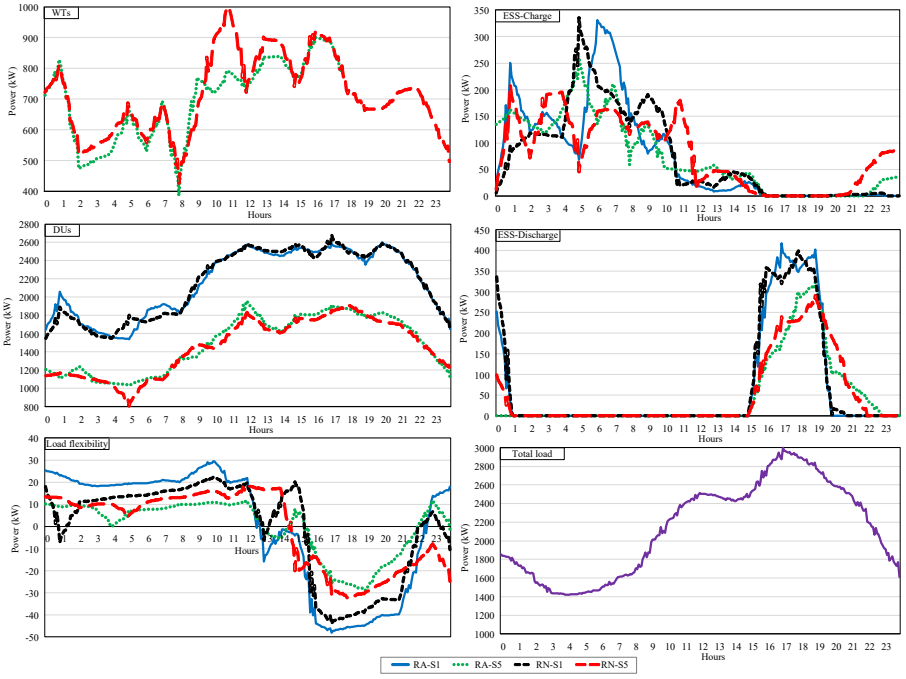

FIGURE 6.11: Optimal scheduling of different DERs in different cases.

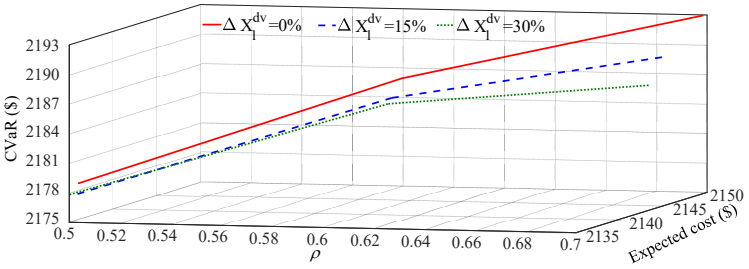

FIGURE 6.12: Variation of CVaR and expected cost over the changes in the risk aversion degree.

generation (i.e. s_5) is depicted in this figure. It can be seen that the injected power of WT in RN strategy is more than that of RA. This means that the decision maker needs to decrease the WT output power to deal with the risk of uncertainty. On the other hand, to deal with such a risk, there is a need to use more reliable units such as DUs. Therefore, the power output of DUs in scenario s_5 for the RA strategy is more than that of the RN. Besides, in

the scenarios with no wind (i.e. s_1), the participation of DUs in load supply is more obvious, which shows the importance of these units in boosting the system security. To deal with variation of load, the BES played its part by charging in off-peak periods and discharging during peak hours. Finally, the responsive loads consumption pattern is adjusted accordingly to deal with load variation and electricity price signals.

In order to show the effect of higher layer decisions on the final solutions of the inner layer optimisation, a freedom level (e.g. ΔX_l^{dv}) is introduced to the decision variables transferred from each layer to another. ΔX_l^{dv} indicates the level of freedom between the linking decision variables transferred between the layers. For example $\Delta X_l^{dv} = 15\%$ means that the linking decision variables have 15% degree of freedom, i.e. $(1-0.15) \times \Delta X_l^{dv^H} \leq \Delta X_l^{dv^L} \leq (1+0.15) \times \Delta X_l^{dv^H}$; where $\Delta X_l^{dv^H}$ stands for decision variables of higher layers (i.e. layer one) and $\Delta X_l^{dv^L}$ shows the inner layer decision variables (i.e. second layer). Figure 6.12 demonstrates the variation of CVaR and expected cost in RA strategy over risk aversion degree (i.e. ρ) for different values of freedom in the linking decision variables. It is shown that increasing the risk aversion degree raises the cost of dealing with the risk of uncertainty. Besides, it can be seen that the optimal values of CVaR and expected cost have not experienced a dramatic change when the degree of freedom is increased. For example, introducing 15% degree of freedom for $\rho = 0.5$ resulted in 0.01% and 0.05% changes in the values of expected cost and CVaR respectively, while it brought about 0.22% and 0.14% for $\rho = 0.7$ in latter and former respectively.

Finally, the computational performance of the proposed RSC-MPC in each time interval for *Case IV* is summarised in Table 6.3. This table shows the efficiency of the proposed method in terms of processing time. Besides, the considerably small value of relative gap shows the optimality and accuracy of the model.

TABLE 6.3: Computational data of the proposed MICP model.

Parameter	Value
Number of single variables	1,404,506
Number of iterations	22,239
Execution time [s]	1,893.6
Relative gap	0.002

6.6 Conclusions

This chapter proposed a hierarchical tri-layer min-max-min MPC framework for real-time energy scheduling of FIMGs under the influence of uncertainty and real-time time-varying contingency conditions. A mathematical model is developed for inclusion of convex security constraints, allowing the real-time tracking of contingency conditions based on the geographical structure of microgrid. The risk associated with the uncertainty of predicted data is also added to the proposed RSC-MPC through adapting the CVaR method in the control mechanism. The proposed method benefits from DER, demand, and network flexibilities to supply FIMG demand under different conditions. Different forms of preventive and corrective flexibilities are used in this model. A convex network reconfiguration is adopted as a corrective flexibility measure to deal with critical line outages and risk of uncertainty on a real-time basis. The optimisation problem investigates the role of risk and time-varying security constraints in the optimal operation of FIMGs. The multi-objective economic analysis of the model shows the necessity of additional budget to be considered for dealing with risk and security measures. The results show the variation of contingency condition over different zones and for various scenarios of RES uncertainty, demonstrating the necessity of a real-time approach that accounts for these measures. Furthermore, the efficiency of the proposed corrective network reconfiguration is evident in the results, such that the configuration of the system has been changed to satisfy different economic and security goals. Sensitivity analysis of risk measures and economic targets shows a considerable rise in the energy procurement cost to achieve a higher layer of risk aversion degree. Finally, the

computational efficiency of the model is demonstrated by a considerably small value of relative gap.

7

Conclusions and Future Work

This thesis investigated the methods for enabling flexibility in the energy networks. The main objective of the thesis was to enable higher levels of flexibility in the demand-side through disaggregating the demand response to its sources. Another primary goal of the thesis was to investigate the application of flexibility in providing system security and stability. The outcomes of this thesis can be useful in achieving the net-zero targets. More sophisticated, grid-aware control of flexibility can delay generation investment for the system managers and can increase the penetration level of renewable energy sources. This thesis is in line with decarbonisation goals and its outcome can be a guideline for researchers and industry stakeholders.

This chapter covers the conclusions and summarises the achievements of this PhD research followed by suggested opportunities for continuation of this research as future work.

7.1 Conclusions and Key-findings

The main conclusions of this research based on chapters 3-6 are summarised here.

7.1.1 Activating building flexibility

Based on the literature review, the gaps in the literature were identified as below:

Enabling energy exchange between buildings to unlock higher levels of flexibility, while considering the occupants preferences. Also, the effect of uncertainty on the real-time building energy management system (BEMS) is another critical aspect which should be studied in more depth.

These gaps were covered in Chapter 3 by proposing a multi-level real-time energy management for a community of buildings which can actively co-operate to unlock flexibility. A rolling horizon based method is adopted to receive real-time weather and energy price data, while the robustness in each consecutive dispatch time interval is increased using the notion of information gap decision theory. The proposed controller exploits flexibility in active building (AB) loads (through interruptible loads and building inertia) and shared distributed energy resources to introduce building to building (B2B) and building for grid (B4G) strategies as advanced methods of flexibility.

The key-findings based on the highlighted gaps are:

- The B2B and B4G strategies are viable flexibility approaches which exploit differences in timing and extent of occupant thermo-visual comfort to deliver an optimal comfort solution at community level while providing techno-economic advantages for the main grid.
- Utilising the B2B and B4G strategies in a local market level can create potential energy transaction between dwellings, which can bring about cost saving for the community. This can also delay the generation investment in a higher level.

- The residential microgrid (RMG) controller can be an efficient solution for the conventional thermostats. This controller can achieve desirable comfort zones while decreasing the energy bill.
- If the controller has the autonomy to decrease comfort expectation of AB occupants by 1.3%, the control robustness is improved by 10%. This shows the considerable role of building occupants in improving system robustness in face of uncertainty.
- Building occupants can play a critical role in energy exchange between dwellings. Increasing the occupants expectation in terms of comfort level can have a direct influence on the building participation in the local market.
- The robust rolling horizon (RRH) approach reduced the total computation time by approximately 76% when compared with the conventional controllers that for similar comfort and cost optimisation need to shorten simulation intervals from 30min to 5min leading to high computational penalties.

These results demonstrate that B2B and B4G are practical building flexibility measures that concern building characteristics and unlock higher levels of flexibility in the dwellings.

7.1.2 Effects of EVs on building flexibility

Based on the literature, the following gaps were identified.

Electrification of transport sector can influence the energy network and consequently flexibility. Therefore, it is necessary to investigate the effect of multiple-energy vector optimisation on the AB flexibility.

These gaps were covered by Chapter 4 by adding corresponding electric vehicle (EV) model to the energy balance model studied in Chapter 3.

The key-findings based on the highlighted gaps are:.

- Energy management of ABs requires consideration of multiple goals which often pivots around a compromise arrived at by solving techno-economic constraints assuming that social willingness of occupant is secured..
- EVs can decrease the operational cost of RMGs by 44% while they can increase the energy exchange between ABs' community and and consequently the value of flexibility.
- An AB can be considered as a virtual thermal storage, by optimal energy scheduling of heat pumps and other similar primary energy conversation assets.

These results show that considering the EVs as a part of BEMS can bring about higher levels of flexibility to the demand side.

7.1.3 Role of flexibility in preserving the system stability

The gap observed in the literature were:

The study of distribution system flexibility focuses mainly on the potential of distributed generation to provide services for the upper network in a normal situation. Nevertheless, there are other practical methods that should be studied for evaluating the distribution level flexibility under different circumstances including an emergency condition. Such circumstances can threaten the stability of the network. Therefore, the role of different practical flexibility methods in preserving the system stability is lacking in the literature.

These gaps were covered in Chapter 5 by introducing a decentralised security-constrained TSO-DSO coordination framework. The proposed method investigates the practical flexibility options at the distribution level for preventing load curtailment in an emergency condition. A decentralised control architecture is proposed for optimising the critical components of the power flow model (i.e. active/reactive power, and voltage magnitude) in the interface between transmission and distribution networks. Rather than consider models of coordination, this method is designed to achieve optimal

values in the boundary points connecting the transmission and distribution networks. To ensure secure coordination, the proposed model considers the loading margin as the security measure. This measure should be satisfied under different circumstances.

The key-findings of this chapter are:

- The coordinated utilisation of conservation voltage reduction (CVR) and feeder reconfiguration is a promising option for the reduction of physical load curtailment in the TSO-DSO coordination process. Joint utilisation of CVR and feeder reconfiguration reduced the need for curtailing the active and reactive load in each individual distribution network by 3.8% and 19% respectively. These methods can be utilised along with distributed energy resources (DER) flexibility options in the future studies to guarantee system security.
- Increasing the security margin raises the required load curtailment by the TSO and consequently the actual load curtailment by DSOs. Increasing the security margin by 2.5% resulted in a twofold increase in the required load curtailment by the TSO. This criteria is important in the coordination schemes that require a higher level of security. Under such paradigm, the system operators need to curtail load to preserve higher security margins.
- A 2.5% increase in the security margin requires 5% change in the tap settings of voltage regulators installed in the distribution networks. This shows the effect of security margin in the transmission level on the flexibility measures taken by DSOs. It also highlights the active role of distributed flexibilities in preserving the whole system security.

These results indicated that the practical flexibility measures can provide specific levels of security for the whole system coordination while preserving the system stability.

7.1.4 Application of flexibility in preserving system security

The following gaps were identified.

Importance of security in real-time energy scheduling and influence of uncertainty on the real-time flexibility of system. Also, economic factors associated with risk of uncertainty and real-time flexibility measures created by the energy grid.

These gaps were covered in Chapter 6 by a proposing tri-layer min-max-min joint risk and security constrained model predictive control (RSC-MPC) framework for real-time energy scheduling of flexible microgrids under the influence of uncertainty and real-time time-varying contingency conditions. The control philosophy starts from first layer cost optimisation, which applies the preventive measures based on the predicted data. The preventive flexibility measures in this layer are adopted through optimal pre-scheduling of DERs, and applying the demand flexibility program. The second layer aims at identifying the worst-case contingency conditions by maximising the load curtailment and the mismatch between the pre-scheduling energy procurement cost (i.e. first layer) and that of real-time (i.e. second layer). Finally, in the third layer, the controller develops a convex real-time network reconfiguration as a corrective flexibility measure against the contingency conditions, while re-scheduling the flexible islanded microgrid (FIMG) with a trade-off decision making (i.e. making compromise between energy procurement cost and risk of uncertainty in the predicted data).

The following key-findings are obtained in this chapter.

- The multi-objective economic analysis of the model shows the necessity of additional budget to be considered for dealing with risk and security measures.
- The results show the variation of contingency condition over different zones and for various scenarios of RES uncertainty, demonstrating the necessity of a real-time approach that accounts for these measures.

- The network reconfiguration is a practical corrective flexibility measure, such that the configuration of the system can be changed to satisfy different economic and security goals.

These results show that different flexibility measures can be adopted as preventive and/or corrective actions to preserve system security.

7.2 Fulfilment of the Main Research Questions

All five main chapters of this thesis shed a different light on the topic of flexibility in the energy networks. While chapter 2 investigated the challenges and opportunities in enabling flexibility in the buildings, Chapters 3 and 4 highlighted the importance of buildings flexibility through developing new methods for unlocking flexibility. Chapter 5 showed how the combination of DER, demand and network flexibility can be utilised to prevent disconnection of distribution grids from the main network. Finally, Chapter 6 demonstrated the role of flexibility measures as preventive and corrective actions for preserving system security.

The main research questions arising from the main topic of the thesis were fulfilled as below:

1. How to enable higher levels of building flexibility in the distribution networks?

This research question has been addressed in the first part of the thesis, where Section 2 introduced challenges and opportunities in enabling building flexibility while chapters 3 and 4 introduced new approaches for enabling higher levels of building flexibility. The main challenges in enabling AB flexibility were identified as possibility of energy exchange between buildings, consideration for occupants comfort, uncertainty of input data and the role of EVs in improving flexibility of the ABs. The challenges arising from this research question have been answered by proposing a robust multi-level MILP optimisation model for AB flexibility, with consideration for occupant comfort

and appliance/task constraints. These control method implies that in order to have a higher level of AB flexibility:

1. The operation of building appliances should be controlled optimally to shift the demand consumption of shiftable appliances such as washing machine while exploiting the use of building-scale generating and storage capacities.
2. The possibility of energy exchange between buildings can provide a higher level of building flexibility.
3. Optimal control of EVs' charge and discharge in the buildings can have a considerable effect on the energy bill of ABs while improving flexibility.
4. It is important to consider occupants comfort while achieving 1)-3) since building users play a crucial role in optimal operation of dwellings and slight changes in the expectation of building occupants can have a considerable effect on the flexibility of ABs.

2. To what extent flexibility can improve the electricity distribution network characteristics?

This research question has been addressed in the second part of the thesis, where Chapter 5 investigated the application of demand, DER, and network flexibility in preserving voltage stability of TSO-DSO coordination while Chapter 6 investigated the application of such flexibility in preserving system security after line outage disruption. Chapter 5 answered this research question by investigating the application of flexibility in the distribution network through a decentralised control framework for TSO-DSO coordination. In this method, DSOs use their available flexibility measures or/and load curtailment to comply with the requirements of the TSO. Distributed optimal DER scheduling, conservation voltage reduction and network reconfiguration were adopted as the flexibility measures preserving the security of TSO-DSO coordination with minimum physical load curtailment. Chapter 6 answered this research question by investigating the role of flexibility in islanded microgrids. A hierarchical joint risk- and security-constrained model predictive control framework is proposed for

real-time energy scheduling of flexible islanded microgrids. This chapter introduced DER scheduling and demand flexibility as precautionary flexibility measures and network reconfiguration as the corrective flexibility methods. Both chapters clearly highlighted the importance of different flexibility methods in achieving important security and stability challenges in distribution networks.

7.2.1 Fulfilment of sub-research questions

The sub-research question arising from the main topic of the thesis were fulfilled as below:

1. Chapter 3: How to optimise energy transaction between buildings together as well as with the main grid so as to unlock their flexibility in a real-time multi-objective problem while accounting for uncertainty?

This research question has been answered in Chapter 3 by proposing a real-time multi-objective optimisation problem for enabling B2B and B4G as the advanced building flexibility techniques. The uncertainty in the market price and weather forecast were taken into account and a robust control technique was proposed to deal with uncertainty in enabling building flexibility. The main contributions of this Chapter based on the research question were:

- A multi-level MILP optimisation model was proposed for AB flexibility, with consideration for occupant comfort and appliance/task constraints. Compared to current MILP models, the proposed solution allowed greater asset/building participation using a linear robust controller that did not require excessive processing power (as opposed to the MINLP) predecessors). It also pursued multiple goals in achieving an optimal energy management.
- Introducing an RRH controller to maximise the robustness of real-time energy management systems against prediction uncertainties at a lower computational time (compared to conventional controllers) while accounting for partial knowledge of input parameters.

- Proposing B2B and B4G strategies to oversee the peer-to-peer energy trading in RMG level while valuing the occupants comfort, and appliance settings under an uncertain environment. The former strategy facilitates the power exchange between dwellings using flexibility in in-site generation capacity, while the latter deconstructs the DR response to its sources of sensitivity to alterations of comfort level and timing- ON/OFF status – or load adjustment of home appliances.
- Taking into account the effect of multiple sources of uncertainty on the local energy markets, while exploring the role of building occupants in improving AB flexibility robustness.

2. Chapter 4: How can electric vehicles enable more flexibility in the buildings?

This research question has been answered in Chapter 4 by proposing a model for EVs which takes into account their driving pattern, while adding their charge/discharge model to the power balance equation of the BMES controller. This chapter tried to show the role of home-charging EVs in increasing the value of building flexibility. Generally, the main contributions of this chapter based on the research question were:

- The effect of electrification of transport on the building flexibility was studied through adding corresponding EV model to the energy balance model studied in Chapter 3. Furthermore, the effect of EVs on the occupant comfort was studied.
- The model investigated the effect of EVs on the B2B. Therefore, this chapter was the continuation of the previous chapter by adding the EVs as a mobile storage that can be effected by occupants decisions.

3. Chapter 5: To what extent can distributed flexibilities be used to preserve system stability?

This research question has been fulfilled in Chapter 5 by proposing a coordination scheme for the transmission and distribution network while focusing on the role of flexibility in preserving voltage stability. At the

distribution level, the DSOs utilise their available distributed flexibilities, such as DER, CVR, and feeder reconfiguration, to provide the required set-points received from TSO and preserve the system stability margin. Generally, the main contributions of this chapter were:

- A decentralised control framework was introduced for TSO-DSO coordination with the least information exchange between them. In this method, DSOs use their available flexibility measures or/and load curtailment to comply with the requirements of the TSO. This proposed method benefited from short computational time spans and achieves the required convergence degree with a small number of iterations.
- Distributed optimal DER scheduling, conservation voltage reduction and network reconfiguration were adopted as the flexibility measures preserving the security of TSO-DSO coordination with minimum physical load curtailment. In the upper level, the TSO ensured the minimum loading margin for the transmission network considering the critical components of the power flow model. In the lower-level distributed optimisation models, DSOs aimed at minimising the actual load curtailment, using the available flexibility options. Each DSO provided a different level of flexibility in the proposed distributed framework. However, the total flexibility provided complied with the requirements of the TSO.
- The transmission network's loadability constraint was considered as the main security margin influencing the TSO-DSO coordination. This index can be utilised as a measure for evaluating the degree of security of TSO-DSO coordination.

4. Chapter 6: To what extent can flexibility methods preserve security of an islanded microgrid?

Chapter 6 aimed at answering this question by introducing a hierarchical tri-layer min-max-min joint risk- and security-constrained model predictive control framework for real-time energy scheduling of FIMGs under the influence of uncertainty and real-time time-varying contingency conditions. The proposed

method benefited from DER, demand, and network flexibilities to supply FIMG demand under different conditions. Different forms of preventive and corrective flexibilities were used in this model. Generally the main contributions of this chapter were:

- Proposing a multi-layer MICP model for multi-objective energy scheduling of FIMGs. The introduced model was computationally efficient and can provide an accurate representation of the flexibility in the power flow model for inclusion in the RSC-MPC.
- Developing a min-max-min RSC-MPC framework which considered the uncertainty of predicted data and the risk associated with them. The introduced control model allowed the inclusion of uncertainties in real-time energy scheduling of FIMGs while accounting for structural changes in the network topology.
- Building time-varying security constraints based on a MICP power flow model. The proposed framework took into account the real-time disruptions which change over the grid zones. This framework allowed the inclusion of more realistic contingency conditions.
- Developing a corrective real-time network reconfiguration model which improved system security, while guaranteeing the network radiality over uncertainty scenarios (i.e. stochastic network reconfiguration). This framework enabled the system controller to change the system configuration so as to prevent load curtailment caused by real-time contingency, while considering the uncertainty.

Altogether this work provided a framework for enabling flexibility in the energy networks and benefiting from them in securing the energy systems. The scalable methods considered in this work are an important step toward decarbonisation of the energy grids. Energy system flexibility is a critical step for utilising higher share of renewable energy sources while concerning the stability and the security if the system.

7.3 Future Work

Based on the research work carried out in this thesis, five research directions are suggested as the final section.

7.3.1 Flexible building communities

Future research studies can examine the role of flexibility in the building communities. The interconnection between different communities could bring about more flexibility for the network and users. This interconnection can be challenged by different security measures. For example, the idea of stable islands can be investigated for the the building communities.

7.3.2 Environmental objectives in the control models

This thesis has shown the importance of flexibility in improving the system characteristics. In the meantime, the use of different RESs and storage devices can bring about the reduction in the carbon emission. As a future research direction, the environmental objectives can be considered as an objective function or a constraint in the control mechanisms. The application of flexibility in improving such environmental indicators can be investigated.

7.3.3 Public health measures

The integration of issues arising from public health measures in the operation of flexibility can be another research direction which can study the effect of pandemic issues on the application of flexibility and the way they can contribute in emergency conditions.

7.3.4 Flexibility in the market

This thesis demonstrated the importance of flexibility. Increasing the levels of flexibility requires designing the practical markets that consider the viewpoint of different stakeholders. For example, a fair flexibility market for the demand flexibility is essential so as to encourage buildings as the end-users to the network to participate in the grid operation.

7.3.5 Other applications of flexibility

This thesis investigated the effect of flexibility on the security and stability of the network as a whole considered economic goals as the objective function. Different applications of flexibility in improving system characteristics (e.g. reliability, voltage support, etc.) can be investigated in the future works.

Bibliography

[1] Department for Business, Energy and Industrial Strategy. 'energy white paper: Powering our net zero future'. (Dec 2020). [Online]. Available: https://www.gov.uk/government/publications/energy-white-paper-powering-our-net-zero-future

[2] Department for Transport, Office for Low Emission Vehicles, Department for Business, Energy and Industrial Strategy, The Rt Hon Alok Sharma MP, and The Rt Hon Grant Shapps MP. 'government takes historic step towards net-zero with end of sale of new petrol and diesel cars by 2030'. (Nov 2020). [Online]. Available: https://www.gov.uk/government/news/government-takes-historic-step-towards-net-zero-with-end-of-sale-of-new\petrol-and-diesel-cars-by-2030

[3] Department for Business, Energy and Industrial Strategy. 'heat and building strategy (accessible webpage)'. (Oct 2021). [Online]. Available: https://www.gov.uk/government/publications/heat-and-buildings-strategy/heat-and-building-strategy-accessible-webpage

[4] Department for Business, Energy and Industrial Strategy, Office of Gas and Electricity Markets. 'transitioning to a net zero energy system: smart systems and flexibility plan 2021'. (July 2021). [Online]. Available: https://www.gov.uk/government/publications/transitioning-to-a-net-zero-energy-system-smart-systems-and-flexibility-plan-2021

[5] S. Karagiannopoulos, C. Mylonas, P. Aristidou, and G. Hug, "Active distribution grids providing voltage support: The swiss case," *IEEE Transactions on Smart Grid*, vol. 12, no. 1, pp. 268–278, 2020.

[6] M. H. Albadi and E. F. El-Saadany, "Demand response in electricity markets: An overview," in *2007 IEEE power engineering society general meeting*, pp. 1–5. IEEE, 2007.

[7] NationalGrid ESO. 'future energy scenarios 2021'. (July 2021). [Online]. Available: https://www.nationalgrideso.com/future-energy/future-energy-scenarios/archive

[8] M. Royapoor, M. Pazhoohesh, P. J. Davison, C. Patsios, and S. Walker, "Building as a virtual power plant, magnitude and persistence of deferrable loads and human comfort implications," *Energy and Buildings*, p. 109794, 2020.

[9] S. Nikkhah, A. Allahham, M. Royapoor, J. W. Bialek, and D. Giaouris, "A community-based building-to-building strategy for multi-objective energy management of residential microgrids," in *2021 12th International Renewable Engineering Conference (IREC)*, pp. 1–6. IEEE, 2021.

[10] J. A. Pinzon, P. P. Vergara, L. C. Da Silva, and M. J. Rider, "An milp model for optimal management of energy consumption and comfort in smart buildings," in *2017 IEEE Power & Energy Society Innovative Smart Grid Technologies Conference (ISGT)*, pp. 1–5. IEEE, 2017.

[11] The US Department of Energy, "Buildings-to-grid technical opportunities: introduction and vision," https://www.energy.gov/eere/buildings/downloads/buildings-grid-technical-opportunities-introduction-and-vision, 2014.

[12] G. C. Kryonidis, M. E. Tsampouri, K.-N. D. Malamaki, and C. S. Demoulias, "Distributed methodology for reactive power support of transmission system," *Sustainable Energy, Grids and Networks*, p. 100753, 2022.

[13] S. Lefebvre, G. Gaba, A. Ba, D. Asber, A. Ricard, C. Perreault, and D. Chartrand, "Measuring the efficiency of voltage reduction at

hydro-québec distribution," in *2008 IEEE Power and Energy Society General Meeting-Conversion and Delivery of Electrical Energy in the 21st Century*, pp. 1–7. IEEE, 2008.

[14] P. Harsh and D. Das, "Energy management in microgrid using incentive-based demand response and reconfigured network considering uncertainties in renewable energy sources," *Sustainable Energy Technologies and Assessments*, vol. 46, p. 101225, 2021.

[15] B. Kitchenham, O. P. Brereton, D. Budgen, M. Turner, J. Bailey, and S. Linkman, "Systematic literature reviews in software engineering–a systematic literature review," *Information and software technology*, vol. 51, no. 1, pp. 7–15, 2009.

[16] B. Kitchenham, "Procedures for performing systematic reviews," *Keele, UK, Keele University*, vol. 33, no. 2004, pp. 1–26, 2004.

[17] M. Ban, M. Shahidehpour, J. Yu, and Z. Li, "A cyber-physical energy management system for optimal sizing and operation of networked nanogrids with battery swapping stations," *IEEE Transactions on Sustainable Energy*, vol. 10, no. 1, pp. 491–502, 2017.

[18] B. Dong, Z. Li, A. Taha, and N. Gatsis, "Occupancy-based buildings-to-grid integration framework for smart and connected communities," *Applied energy*, vol. 219, pp. 123–137, 2018.

[19] M. Razmara, G. R. Bharati, M. Shahbakhti, S. Paudyal, and R. D. Robinett, "Bilevel optimization framework for smart building-to-grid systems," *IEEE transactions on Smart Grid*, vol. 9, no. 2, pp. 582–593, 2016.

[20] A. Najafi-Ghalelou, S. Nojavan, and K. Zare, "Heating and power hub models for robust performance of smart building using information gap decision theory," *International Journal of Electrical Power & Energy Systems*, vol. 98, pp. 23–35, 2018.

[21] D. Buoro, M. Casisi, P. Pinamonti, and M. Reini, "Optimal synthesis and operation of advanced energy supply systems for standard and domotic home," *Energy conversion and management*, vol. 60, pp. 96–105, 2012.

[22] Q. Wu, M. Shahidehpour, C. Li, S. Huang, W. Wei *et al.*, "Transactive real-time electric vehicle charging management for commercial buildings with pv on-site generation," *IEEE Transactions on Smart Grid*, vol. 10, no. 5, pp. 4939–4950, 2018.

[23] D. Wu, H. Zeng, C. Lu, and B. Boulet, "Two-stage energy management for office buildings with workplace ev charging and renewable energy," *IEEE Transactions on Transportation Electrification*, vol. 3, no. 1, pp. 225–237, 2017.

[24] L. Hurtado, P. Nguyen, and W. Kling, "Smart grid and smart building inter-operation using agent-based particle swarm optimization," *Sustainable Energy, Grids and Networks*, vol. 2, pp. 32–40, 2015.

[25] Z. Wang and L. Wang, "Adaptive negotiation agent for facilitating bi-directional energy trading between smart building and utility grid," *IEEE Transactions on Smart Grid*, vol. 4, no. 2, pp. 702–710, 2013.

[26] H. Mehrjerdi and R. Hemmati, "Energy and uncertainty management through domestic demand response in the residential building," *Energy*, vol. 192, p. 116647, 2020.

[27] J. A. Pinzon, P. P. Vergara, L. C. Da Silva, and M. J. Rider, "Optimal management of energy consumption and comfort for smart buildings operating in a microgrid," *IEEE Transactions on Smart Grid*, vol. 10, no. 3, pp. 3236–3247, 2018.

[28] A. F. Taha, N. Gatsis, B. Dong, A. Pipri, and Z. Li, "Buildings-to-grid integration framework," *IEEE Transactions on Smart Grid*, vol. 10, no. 2, pp. 1237–1249, 2017.

[29] Y. Lu, X. Yu, X. Jin, H. Jia, and Y. Mu, "Bi-level optimization framework for buildings to heating grid integration in integrated community energy systems," *IEEE Transactions on Sustainable Energy*, 2020.

[30] D. Thomas, O. Deblecker, and C. S. Ioakimidis, "Optimal operation of an energy management system for a grid-connected smart building considering photovoltaics' uncertainty and stochastic electric vehicles' driving schedule," *Applied Energy*, vol. 210, pp. 1188–1206, 2018.

[31] F. Luo, W. Kong, G. Ranzi, and Z. Y. Dong, "Optimal home energy management system with demand charge tariff and appliance operational dependencies," *IEEE Transactions on Smart Grid*, vol. 11, no. 1, pp. 4–14, 2019.

[32] F. Wang, L. Zhou, H. Ren, X. Liu, S. Talari, M. Shafie-khah, and J. P. Catalao, "Multi-objective optimization model of source–load–storage synergetic dispatch for a building energy management system based on tou price demand response," *IEEE Transactions on Industry Applications*, vol. 54, no. 2, pp. 1017–1028, 2017.

[33] S. Arun and M. Selvan, "Intelligent residential energy management system for dynamic demand response in smart buildings," *IEEE Systems Journal*, vol. 12, no. 2, pp. 1329–1340, 2017.

[34] J. Guo and S. Yin, "The optimization of household and apartment energy management system," in *2018 2nd IEEE Conference on Energy Internet and Energy System Integration (EI2)*, pp. 1–6. IEEE, 2018.

[35] S. Duerr, C. Ababei, and D. M. Ionel, "Load balancing with energy storage systems based on co-simulation of multiple smart buildings and distribution networks," in *2017 IEEE 6th International Conference on Renewable Energy Research and Applications (ICRERA)*, pp. 175–180. IEEE, 2017.

[36] A. Ahmad and J. Y. Khan, "Real-time load scheduling, energy storage control and comfort management for grid-connected solar integrated smart buildings," *Applied Energy*, vol. 259, p. 114208, 2020.

[37] S. Paul and N. P. Padhy, "Real time bi-level energy management of smart residential apartment building," *IEEE Transactions on Industrial Informatics*, 2019.

[38] M. Di Piazza, G. La Tona, M. Luna, and A. Di Piazza, "A two-stage energy management system for smart buildings reducing the impact of demand uncertainty," *Energy and Buildings*, vol. 139, pp. 1–9, 2017.

[39] M. Shakeri, M. Shayestegan, H. Abunima, S. S. Reza, M. Akhtaruzzaman, A. Alamoud, K. Sopian, and N. Amin, "An intelligent system architecture

in home energy management systems (hems) for efficient demand response in smart grid," *Energy and Buildings*, vol. 138, pp. 154–164, 2017.

[40] P. Rocha, A. Siddiqui, and M. Stadler, "Improving energy efficiency via smart building energy management systems: A comparison with policy measures," *Energy and Buildings*, vol. 88, pp. 203–213, 2015.

[41] O. Van Cutsem, D. H. Dac, P. Boudou, and M. Kayal, "Cooperative energy management of a community of smart-buildings: A blockchain approach," *International Journal of Electrical Power & Energy Systems*, vol. 117, p. 105643, 2020.

[42] M. Sechilariu, B. Wang, and F. Locment, "Building integrated photovoltaic system with energy storage and smart grid communication," *IEEE Transactions on Industrial Electronics*, vol. 60, no. 4, pp. 1607–1618, 2012.

[43] A. Aldegheishem, R. Bukhsh, N. Alrajeh, and N. Javaid, "Faavpp: Fog as a virtual power plant service for community energy management," *Future Generation Computer Systems*, vol. 105, pp. 675–683, 2020.

[44] M. Tasdighi, P. J. Salamati, A. Rahimikian, and H. Ghasemi, "Energy management in a smart residential building," in *2012 11th International Conference on Environment and Electrical Engineering*, pp. 128–133. IEEE, 2012.

[45] A. Fleischhacker, H. Auer, G. Lettner, and A. Botterud, "Sharing solar pv and energy storage in apartment buildings: resource allocation and pricing," *IEEE Transactions on Smart Grid*, vol. 10, no. 4, pp. 3963–3973, 2018.

[46] W. Gorman, S. Jarvis, and D. Callaway, "Should i stay or should i go? the importance of electricity rate design for household defection from the power grid," *Applied Energy*, vol. 262, p. 114494, 2020.

[47] M. A. F. Ghazvini, D. Steen *et al.*, "A close-to-real-time energy management system for smart residential buildings," in *2019 IEEE Milan PowerTech*, pp. 1–6. IEEE, 2019.

[48] Z. Pooranian, J. H. Abawajy, M. Conti *et al.*, "Scheduling distributed energy resource operation and daily power consumption for a smart building to optimize economic and environmental parameters," *Energies*, vol. 11, no. 6, p. 1348, 2018.

[49] C. A. Correa-Florez, A. Gerossier, A. Michiorri, and G. Kariniotakis, "Stochastic operation of home energy management systems including battery cycling," *Applied energy*, vol. 225, pp. 1205–1218, 2018.

[50] A. Akbari-Dibavar, S. Nojavan, B. Mohammadi-Ivatloo, and K. Zare, "Smart home energy management using hybrid robust-stochastic optimization," *Computers & Industrial Engineering*, p. 106425, 2020.

[51] M. S. H. Nizami, J. Hossain, and E. Fernandez, "Multi-agent based transactive energy management systems for residential buildings with distributed energy resources," *IEEE Transactions on Industrial Informatics*, 2019.

[52] B. Kim and O. Lavrova, "Optimal power flow and energy-sharing among multi-agent smart buildings in the smart grid," in *2013 IEEE Energytech*, pp. 1–5. IEEE, 2013.

[53] D. Yu, T. Zhang, G. He, S. Nojavan, K. Jermsittiparsert, and N. Ghadimi, "Energy management of wind-pv-storage-grid based large electricity consumer using robust optimization technique," *Journal of Energy Storage*, vol. 27, p. 101054, 2020.

[54] H. Golpîra and S. A. R. Khan, "A multi-objective risk-based robust optimization approach to energy management in smart residential buildings under combined demand and supply uncertainty," *Energy*, vol. 170, pp. 1113–1129, 2019.

[55] C. Keles, A. Karabiber, M. Akcin, A. Kaygusuz, B. B. Alagoz, and O. Gul, "A smart building power management concept: Smart socket applications with dc distribution," *International Journal of Electrical Power & Energy Systems*, vol. 64, pp. 679–688, 2015.

[56] E. Shirazi and S. Jadid, "Optimal residential appliance scheduling under dynamic pricing scheme via hemdas," *Energy and Buildings*, vol. 93, pp. 40–49, 2015.

[57] D. Zhang, S. Liu, and L. G. Papageorgiou, "Fair cost distribution among smart homes with microgrid," *Energy Conversion and Management*, vol. 80, pp. 498–508, 2014.

[58] H. Wolisz, T. M. Kull, D. Müller, and J. Kurnitski, "Self-learning model predictive control for dynamic activation of structural thermal mass in residential buildings," *Energy and Buildings*, vol. 207, p. 109542, 2020.

[59] J. Gasser, H. Cai, S. Karagiannopoulos, P. Heer, and G. Hug, "Predictive energy management of residential buildings while self-reporting flexibility envelope," *Applied Energy*, vol. 288, p. 116653, 2021.

[60] M. Tavakoli, F. Shokridehaki, M. Marzband, R. Godina, and E. Pouresmaeil, "A two stage hierarchical control approach for the optimal energy management in commercial building microgrids based on local wind power and pevs," *Sustainable Cities and Society*, vol. 41, pp. 332–340, 2018.

[61] A. Baniasadi, D. Habibi, O. Bass, and M. A. Masoum, "Optimal real-time residential thermal energy management for peak-load shifting with experimental verification," *IEEE Transactions on Smart Grid*, vol. 10, no. 5, pp. 5587–5599, 2018.

[62] R. Missaoui, H. Joumaa, S. Ploix, and S. Bacha, "Managing energy smart homes according to energy prices: analysis of a building energy management system," *Energy and Buildings*, vol. 71, pp. 155–167, 2014.

[63] S. S. Barhagh, M. Abapour, and B. Mohammadi-Ivatloo, "Optimal scheduling of electric vehicles and photovoltaic systems in residential complexes under real-time pricing mechanism," *Journal of Cleaner Production*, vol. 246, p. 119041, 2020.

[64] H. O. Alwan, H. Sadeghian, and S. Abdelwahed, "Energy management optimization and voltage evaluation for residential and commercial areas," *Energies*, vol. 12, no. 9, p. 1811, 2019.

[65] S. Bracco, G. Dentici, and S. Siri, "Economic and environmental optimization model for the design and the operation of a combined heat and power distributed generation system in an urban area," *Energy*, vol. 55, pp. 1014–1024, 2013.

[66] A. Keshtkar and S. Arzanpour, "An adaptive fuzzy logic system for residential energy management in smart grid environments," *Applied Energy*, vol. 186, pp. 68–81, 2017.

[67] S. C. Dhulipala, R. V. A. Monteiro, R. F. da Silva Teixeira, C. Ruben, A. S. Bretas, and G. C. Guimarães, "Distributed model-predictive control strategy for distribution network volt/var control: A smart-building-based approach," *IEEE Transactions on Industry Applications*, vol. 55, no. 6, pp. 7041–7051, 2019.

[68] K. An, S. Zhang, H. Huang, Y. Liu, W. Cai, and C. Wang, "Socioeconomic impacts of household participation in emission trading scheme: A computable general equilibrium-based case study," *Applied Energy*, vol. 288, p. 116647, 2021.

[69] H. Hao, Y. Lin, A. S. Kowli, P. Barooah, and S. Meyn, "Ancillary service to the grid through control of fans in commercial building hvac systems," *IEEE Transactions on smart grid*, vol. 5, no. 4, pp. 2066–2074, 2014.

[70] Y. Wang, Y. Xu, and Y. Tang, "Distributed aggregation control of grid-interactive smart buildings for power system frequency support," *Applied Energy*, vol. 251, p. 113371, 2019.

[71] International Energy Agency. Global ev outlook 2021. [Online]. Available: https://iea.blob.core.windows.net/assets/ed5f4484-f556-4110-8c5c-4ede8bcba637/GlobalEVOutlook2021.pdf

[72] International Energy Agency. Electric car deployment in selected countries, 2013-2018, iea, paris. [Online]. Available: https://www.iea.org/data-and-statistics/charts/electric-car-deployment-in-selected-countries\-2013-2018

[73] T. Sousa, T. Soares, P. Pinson, F. Moret, T. Baroche, and E. Sorin, "Peer-to-peer and community-based markets: A comprehensive review," *Renewable and Sustainable Energy Reviews*, vol. 104, pp. 367–378, 2019.

[74] M.-A. Nasr, S. Nikkhah, G. B. Gharehpetian, E. Nasr-Azadani, and S. H. Hosseinian, "A multi-objective voltage stability constrained energy management system for isolated microgrids," *International Journal of Electrical Power & Energy Systems*, vol. 117, p. 105646, 2020.

[75] O. Sadeghian, A. Oshnoei, S. Nikkhah, and B. Mohammadi-Ivatloo, "Multi-objective optimisation of generation maintenance scheduling in restructured power systems based on global criterion method," *IET Smart Grid*, vol. 2, no. 2, pp. 203–213, 2019.

[76] Y. Yang, S. Zhang, and Y. Xiao, "An milp (mixed integer linear programming) model for optimal design of district-scale distributed energy resource systems," *Energy*, vol. 90, pp. 1901–1915, 2015.

[77] D. Tenfen and E. C. Finardi, "A mixed integer linear programming model for the energy management problem of microgrids," *Electric Power Systems Research*, vol. 122, pp. 19–28, 2015.

[78] S. Pazouki, A. Mohsenzadeh, S. Ardalan, and M.-R. Haghifam, "Optimal place, size, and operation of combined heat and power in multi carrier energy networks considering network reliability, power loss, and voltage profile," *IET Generation, Transmission & Distribution*, vol. 10, no. 7, pp. 1615–1621, 2016.

[79] S. Walker, W. Khan, K. Katic, W. Maassen, and W. Zeiler, "Accuracy of different machine learning algorithms and added-value of predicting aggregated-level energy performance of commercial buildings," *Energy and Buildings*, vol. 209, p. 109705, 2020.

[80] M. Hu and F. Xiao, "Quantifying uncertainty in the aggregate energy flexibility of high-rise residential building clusters considering stochastic occupancy and occupant behavior," *Energy*, vol. 194, p. 116838, 2020.

[81] B. L. R. Stojkoska and K. V. Trivodaliev, "A review of internet of things for smart home: Challenges and solutions," *Journal of Cleaner Production*, vol. 140, pp. 1454–1464, 2017.

[82] B. Qolomany, A. Al-Fuqaha, A. Gupta, D. Benhaddou, S. Alwajidi, J. Qadir, and A. C. Fong, "Leveraging machine learning and big data for smart buildings: A comprehensive survey," *IEEE Access*, vol. 7, pp. 90 316–90 356, 2019.

[83] M. Bastian, S. Heymann, and M. Jacomy, "Gephi: an open source software for exploring and manipulating networks," in *Third international AAAI conference on weblogs and social media*, 2009.

[84] M. Jacomy, T. Venturini, S. Heymann, and M. Bastian, "Forceatlas2, a continuous graph layout algorithm for handy network visualization designed for the gephi software," *PloS one*, vol. 9, no. 6, 2014.

[85] Y. Hu, "Efficient, high-quality force-directed graph drawing," *Mathematica Journal*, vol. 10, no. 1, pp. 37–71, 2005.

[86] M. Schmidt and C. Åhlund, "Smart buildings as cyber-physical systems: Data-driven predictive control strategies for energy efficiency," *Renewable and Sustainable Energy Reviews*, vol. 90, pp. 742–756, 2018.

[87] U. R. Nair and R. Costa-Castelló, "A model predictive control-based energy management scheme for hybrid storage system in islanded microgrids," *IEEE access*, vol. 8, pp. 97 809–97 822, 2020.

[88] Active Building Centre. What is an active building? [Online]. Available: https://www.activebuildingcentre.com

[89] Kroposki, Benjamin and Bernstein, Andrey and King, Jennifer and Ding, Fei . Tomorrow's Power Grid Will Be Autonomous. (November 2020). [Online]. Available: https://spectrum.ieee.org/energy/the-smarter-grid/tomorrows-power-grid-will-be-autonomous

[90] J. Bialek, "What does the GB power outage on 9 August 2019 tell us about the current state of decarbonised power systems?" *Energy Policy*, vol. 146, p. 111821, 2020.

[91] A. Soroudi and T. Amraee, "Decision making under uncertainty in energy systems: State of the art," *Renewable and Sustainable Energy Reviews*, vol. 28, pp. 376–384, 2013.

[92] T. Morstyn, N. Farrell, S. J. Darby, and M. D. McCulloch, "Using peer-to-peer energy-trading platforms to incentivize prosumers to form federated power plants," *Nature Energy*, vol. 3, no. 2, pp. 94–101, 2018.

[93] C. Long, J. Wu, C. Zhang, L. Thomas, M. Cheng, and N. Jenkins, "Peer-to-peer energy trading in a community microgrid," in *2017 IEEE power & energy society general meeting*, pp. 1–5. IEEE, 2017.

[94] A. Soroudi, A. Rabiee, and A. Keane, "Information gap decision theory approach to deal with wind power uncertainty in unit commitment," *Electric Power Systems Research*, vol. 145, pp. 137–148, 2017.

[95] Y. Ben-Haim, *Info-gap decision theory: decisions under severe uncertainty*. Elsevier, 2006.

[96] A. Soroudi, *Power system optimization modeling in GAMS*, vol. 78. Springer, 2017.

[97] Chartered Institution of Building Services Engineers. Test Reference Year for Newcastle upon Tyne. (May 2020). [Online]. Available: https://www.cibse.org/weatherdata

[98] Nikkhah, Saman and Giaouris, Damian and Bialek, Janusz and Allahham, Adib and Royapoor Mohammad , " Active Building Data," December 2020. [Online]. Available: https://data.ncl.ac.uk/articles/dataset/Energy_scheduling/13387280/1

[99] K. Chen, W. Wu, B. Zhang, S. Djokic, and G. P. Harrison, "A method to evaluate total supply capability of distribution systems considering network reconfiguration and daily load curves," *IEEE Transactions on Power systems*, vol. 31, no. 3, pp. 2096–2104, 2015.

[100] IEA, "Global ev outlook 2022," https://www.iea.org/reports/global-ev-outlook-2022, 2022.

[101] E. Kianmehr, S. Nikkhah, V. Vahidinasab, D. Giaouris, and P. C. Taylor, "A resilience-based architecture for joint distributed energy resources allocation and hourly network reconfiguration," *IEEE Transactions on Industrial Informatics*, vol. 15, no. 10, pp. 5444–5455, 2019.

[102] H. Mehrjerdi and R. Hemmati, "Coordination of vehicle-to-home and renewable capacity resources for energy management in resilience and self-healing building," *Renewable Energy*, vol. 146, pp. 568–579, 2020.

[103] G. Barone, A. Buonomano, F. Calise, C. Forzano, and A. Palombo, "Building to vehicle to building concept toward a novel zero energy paradigm: Modelling and case studies," *Renewable and Sustainable Energy Reviews*, vol. 101, pp. 625–648, 2019.

[104] A. Soroudi and A. Keane, "Risk averse energy hub management considering plug-in electric vehicles using information gap decision theory," in *Plug in electric vehicles in smart grids*, pp. 107–127. Springer, 2015.

[105] D. Qiu, Y. Ye, D. Papadaskalopoulos, and G. Strbac, "Scalable coordinated management of peer-to-peer energy trading: A multi-cluster deep reinforcement learning approach," *Applied Energy*, vol. 292, p. 116940, 2021.

[106] H. Sun, Q. Guo, J. Qi, V. Ajjarapu, R. Bravo, J. Chow, Z. Li, R. Moghe, E. Nasr-Azadani, U. Tamrakar *et al.*, "Review of challenges and research opportunities for voltage control in smart grids," *IEEE Transactions on Power Systems*, vol. 34, no. 4, pp. 2790–2801, 2019.

[107] H. Brunner, and A. Zegers,, "An overview of current interaction between transmission and distribution system operators and an assessment of their cooperation in smart grids." [Online]. Available: http://smartgrids.no/wp-content/uploads/sites/4/2016/01/ISGAN-TSO-DSO-interaction.pdf

[108] A. G. Givisiez, K. Petrou, and L. F. Ochoa, "A review on tso-dso coordination models and solution techniques," *Electric Power Systems Research*, vol. 189, p. 106659, 2020.

[109] Global Power System Transformation, "Inaugural research agenda." [Online]. Available: https://globalpst.org/

[110] M. Kalantar-Neyestanaki, F. Sossan, M. Bozorg, and R. Cherkaoui, "Characterizing the reserve provision capability area of active distribution networks: A linear robust optimization method," *IEEE Transactions on Smart Grid*, vol. 11, no. 3, pp. 2464–2475, 2019.

[111] S. Stanković and L. Söder, "Probabilistic reactive power capability charts at dso/tso interface," *IEEE Transactions on Smart Grid*, vol. 11, no. 5, pp. 3860–3870, 2020.

[112] P. Sheikhahmadi, S. Bahramara, A. Mazza, G. Chicco, and J. P. Catalão, "Bi-level optimization model for the coordination between transmission and distribution systems interacting with local energy markets," *International Journal of Electrical Power & Energy Systems*, vol. 124, p. 106392, 2021.

[113] V. A. Evangelopoulos, I. I. Avramidis, and P. S. Georgilakis, "Flexibility services management under uncertainties for power distribution systems: Stochastic scheduling and predictive real-time dispatch," *IEEE Access*, vol. 8, pp. 38 855–38 871, 2020.

[114] C. Lin, W. Wu, and M. Shahidehpour, "Decentralized ac optimal power flow for integrated transmission and distribution grids," *IEEE Transactions on Smart Grid*, vol. 11, no. 3, pp. 2531–2540, 2019.

[115] T. Jiang, C. Wu, R. Zhang, X. Li, H. Chen, and G. Li, "Flexibility clearing in joint energy and flexibility markets considering tso-dso coordination," *IEEE Transactions on Smart Grid*, 2022.

[116] F. Marten, L. Löwer, J.-C. Töbermann, and M. Braun, "Optimizing the reactive power balance between a distribution and transmission grid through iteratively updated grid equivalents," in *2014 Power Systems Computation Conference*, pp. 1–7. IEEE, 2014.

[117] L. Kristov, P. De Martini, and J. D. Taft, "A tale of two visions: Designing a decentralized transactive electric system," *IEEE Power and Energy Magazine*, vol. 14, no. 3, pp. 63–69, 2016.

[118] Z. Yuan and M. R. Hesamzadeh, "Hierarchical coordination of tso-dso economic dispatch considering large-scale integration of distributed energy resources," *Applied energy*, vol. 195, pp. 600–615, 2017.

[119] K. Purchala, L. Meeus, D. Van Dommelen, and R. Belmans, "Usefulness of dc power flow for active power flow analysis," in *IEEE Power Engineering Society General Meeting, 2005*, pp. 454–459. IEEE, 2005.

[120] A. Mohammadi, M. Mehrtash, and A. Kargarian, "Diagonal quadratic approximation for decentralized collaborative tso+ dso optimal power flow," *IEEE Transactions on Smart Grid*, vol. 10, no. 3, pp. 2358–2370, 2018.

[121] J. Silva, J. Sumaili, R. J. Bessa, L. Seca, M. A. Matos, V. Miranda, M. Caujolle, B. Goncer, and M. Sebastian-Viana, "Estimating the active and reactive power flexibility area at the tso-dso interface," *IEEE Transactions on Power Systems*, vol. 33, no. 5, pp. 4741–4750, 2018.

[122] S. Nikkhah, M. A. Nasr, and A. Rabiee, "A stochastic voltage stability constrained ems for isolated microgrids in the presence of pevs using a coordinated uc-opf framework," *IEEE Transactions on Industrial Electronics*, 2020.

[123] A. Sarhan, V. K. Ramachandaramurthy, T. S. Kiong, and J. Ekanayake, "Definitions and dimensions for electricity security assessment: A review," *Sustainable Energy Technologies and Assessments*, vol. 48, p. 101626, 2021.

[124] Z. Li, Q. Guo, H. Sun, J. Wang, Y. Xu, and M. Fan, "A distributed transmission-distribution-coupled static voltage stability assessment method considering distributed generation," *IEEE Transactions on Power Systems*, vol. 33, no. 3, pp. 2621–2632, 2017.

[125] A. O. Rousis, D. Tzelepis, Y. Pipelzadeh, G. Strbac, C. D. Booth, and T. C. Green, "Provision of voltage ancillary services through enhanced tso-dso interaction and aggregated distributed energy resources," *IEEE Transactions on Sustainable Energy*, vol. 12, no. 2, pp. 897–908, 2020.

[126] K. Tang, M. Ge, S. Dong, J. Cui, and X. Ma, "Transmission contingency analysis based on data-driven equivalencing of radial distribution networks considering uncertainties," *IEEE Access*, vol. 8, pp. 227 247–227 254, 2020.

[127] A. Bachoumis, C. Kaskouras, G. Papaioannou, and M. Sousounis, "Tso/dso coordination for voltage regulation on transmission level: A greek case study," in *2021 IEEE Madrid PowerTech*, pp. 1–7. IEEE, 2021.

[128] F. Escobar, J. M. Víquez, J. García, P. Aristidou, and G. Valverde, "Coordination of ders and flexible loads to support transmission voltages in emergency conditions," *IEEE Transactions on Sustainable Energy*, vol. 13, no. 3, pp. 1344–1355, 2022.

[129] A. Nawaz, H. Wang, Q. Wu, and M. Kumar Ochani, "Tso and dso with large-scale distributed energy resources: A security constrained unit commitment coordinated solution," *International Transactions on Electrical Energy Systems*, vol. 30, no. 3, p. e12233, 2020.

[130] E. Leonidaki, D. Georgiadis, and N. Hatziargyriou, "Decision trees for determination of optimal location and rate of series compensation to increase power system loading margin," *IEEE Transactions on Power Systems*, vol. 21, no. 3, pp. 1303–1310, 2006.

[131] M. E. Baran and F. F. Wu, "Network reconfiguration in distribution systems for loss reduction and load balancing," *IEEE Power Engineering Review*, vol. 9, no. 4, pp. 101–102, 1989.

[132] M. Lavorato, J. F. Franco, M. J. Rider, and R. Romero, "Imposing radiality constraints in distribution system optimization problems," *IEEE Transactions on Power Systems*, vol. 27, no. 1, pp. 172–180, 2011.

[133] R. D. Zimmerman, C. E. Murillo-Sánchez, and R. J. Thomas, "Matpower: Steady-state operations, planning, and analysis tools for power systems research and education," *IEEE Transactions on power systems*, vol. 26, no. 1, pp. 12–19, 2010.

[134] C.-T. Su, C.-F. Chang, and J.-P. Chiou, "Distribution network reconfiguration for loss reduction by ant colony search algorithm," *Electric power systems research*, vol. 75, no. 2-3, pp. 190–199, 2005.

[135] S. Nikkhah, I. Sarantakos, N.-M. Zografou-Barredo, A. Rabiee, A. Allahham, and D. Giaouris, "A joint risk and security constrained control framework for real-time energy scheduling of islanded microgrids," *IEEE Transactions on Smart Grid*, 2022.

[136] M.-A. Nasr, E. Nasr-Azadani, H. Nafisi, S. H. Hosseinian, and P. Siano, "Assessing the effectiveness of weighted information gap decision theory integrated with energy management systems for isolated microgrids," *IEEE Transactions on Industrial Informatics*, 2019.

[137] S. Nikkhah, A. Allahham, M. Royapoor, J. W. Bialek, and D. Giaouris, "Optimising building-to-building and building-for-grid services under uncertainty: A robust rolling horizon approach," *IEEE Transactions on Smart Grid*, 2021.

[138] M. Falahi, K. Butler-Purry, and M. Ehsani, "Dynamic reactive power control of islanded microgrids," *IEEE Transactions on Power Systems*, vol. 28, no. 4, pp. 3649–3657, 2013.

[139] D. R. Prathapaneni and K. P. Detroja, "An integrated framework for optimal planning and operation schedule of microgrid under uncertainty," *Sustainable Energy, Grids and Networks*, vol. 19, p. 100232, 2019.

[140] A. Khodaei, "Resiliency-oriented microgrid optimal scheduling," *IEEE Transactions on Smart Grid*, vol. 5, no. 4, pp. 1584–1591, 2014.

[141] P. M. de Quevedo, J. Contreras, A. Mazza, G. Chicco, and R. Porumb, "Reliability assessment of microgrids with local and mobile generation, time-dependent profiles, and intraday reconfiguration," *IEEE Transactions on Industry Applications*, vol. 54, no. 1, pp. 61–72, 2017.

[142] N.-M. Zografou-Barredo, C. Patsios, I. Sarantakos, P. Davison, S. L. Walker, and P. C. Taylor, "Microgrid resilience-oriented scheduling: A robust misocp model," *IEEE Transactions on Smart Grid*, vol. 12, no. 3, pp. 1867–1879, 2020.

[143] J. D. Lara, D. E. Olivares, and C. A. Canizares, "Robust energy management of isolated microgrids," *IEEE Systems Journal*, vol. 13, no. 1, pp. 680–691, 2018.

[144] M. Singh. 'california and texas are warnings': blackouts show us deeply unprepared for the climate crisis'. (Feb 2021). [Online]. Available: https://www.theguardian.com/environment/2021/feb/19/power-outages-texas-california-climate-crisis

[145] K. A. Saleh, H. H. Zeineldin, and E. F. El-Saadany, "Optimal protection coordination for microgrids considering n −1 contingency," *IEEE Transactions on Industrial Informatics*, vol. 13, no. 5, pp. 2270–2278, 2017.

[146] M. Amirioun, F. Aminifar, and H. Lesani, "Resilience-oriented proactive management of microgrids against windstorms," *IEEE Transactions on Power Systems*, vol. 33, no. 4, pp. 4275–4284, 2017.

[147] W. Sun, S. Ma, I. Alvarez-Fernandez, A. Golshani *et al.*, "Optimal self-healing strategy for microgrid islanding," *IET Smart Grid*, vol. 1, no. 4, pp. 143–150, 2018.

[148] A. A. Eajal, A. H. Yazdavar, E. F. El-Saadany, and K. Ponnambalam, "On the loadability and voltage stability of islanded ac–dc hybrid microgrids during contingencies," *IEEE Systems Journal*, vol. 13, no. 4, pp. 4248–4259, 2019.

[149] F. H. Aghdam, J. Salehi, and S. Ghaemi, "Contingency based energy management of multi-microgrid based distribution network," *Sustainable Cities and Society*, vol. 41, pp. 265–274, 2018.

[150] S. Córdova, C. Cañizares, Á. Lorca, and D. E. Olivares, "An energy management system with short-term fluctuation reserves and battery degradation for isolated microgrids," *IEEE Transactions on Smart Grid*, 2021.

[151] W. Mendieta and C. A. Cañizares, "Primary frequency control in isolated microgrids using thermostatically controllable loads," *IEEE Transactions on Smart Grid*, vol. 12, no. 1, pp. 93–105, 2020.

[152] D. K. Dheer, O. V. Kulkarni, S. Doolla, and A. K. Rathore, "Effect of reconfiguration and meshed networks on the small-signal stability margin of droop-based islanded microgrids," *IEEE Transactions on Industry Applications*, vol. 54, no. 3, pp. 2821–2833, 2018.

[153] S. Nikkhah, K. Jalilpoor, E. Kianmehr, and G. B. Gharehpetian, "Optimal wind turbine allocation and network reconfiguration for enhancing resiliency of system after major faults caused by natural disaster considering uncertainty," *IET Renewable Power Generation*, vol. 12, no. 12, pp. 1413–1423, 2018.

[154] E. Dall'Anese and G. B. Giannakis, "Risk-constrained microgrid reconfiguration using group sparsity," *IEEE Transactions on Sustainable Energy*, vol. 5, no. 4, pp. 1415–1425, 2014.

[155] M. Dabbaghjamanesh, A. Kavousi-Fard, and S. Mehraeen, "Effective scheduling of reconfigurable microgrids with dynamic thermal line rating," *IEEE Transactions on Industrial Electronics*, vol. 66, no. 2, pp. 1552–1564, 2018.

[156] P. Akaber, B. Moussa, M. Debbabi, and C. Assi, "Automated post-failure service restoration in smart grid through network reconfiguration in the presence of energy storage systems," *IEEE Systems Journal*, vol. 13, no. 3, pp. 3358–3367, 2019.

[157] A. Arif, Z. Wang, J. Wang, and C. Chen, "Power distribution system outage management with co-optimization of repairs, reconfiguration, and dg dispatch," *IEEE Transactions on Smart Grid*, vol. 9, no. 5, pp. 4109–4118, 2017.

[158] B. V. Solanki, A. Raghurajan, K. Bhattacharya, and C. A. Cañizares, "Including smart loads for optimal demand response in integrated energy management systems for isolated microgrids," *IEEE Transactions on Smart Grid*, vol. 8, no. 4, pp. 1739–1748, 2015.

[159] A. C. Luna, N. L. Diaz, M. Graells, J. C. Vasquez, and J. M. Guerrero, "Mixed-integer-linear-programming-based energy management system for hybrid pv-wind-battery microgrids: Modeling, design, and

experimental verification," *IEEE Transactions on Power Electronics*, vol. 32, no. 4, pp. 2769–2783, 2016.

[160] I. Sarantakos, D. M. Greenwood, J. Yi, S. R. Blake, and P. C. Taylor, "A method to include component condition and substation reliability into distribution system reconfiguration," *International Journal of Electrical Power & Energy Systems*, vol. 109, pp. 122–138, 2019.

[161] D. E. Olivares, A. Mehrizi-Sani, A. H. Etemadi, C. A. Cañizares, R. Iravani, M. Kazerani, A. H. Hajimiragha, O. Gomis-Bellmunt, M. Saeedifard, R. Palma-Behnke *et al.*, "Trends in microgrid control," *IEEE Transactions on smart grid*, vol. 5, no. 4, pp. 1905–1919, 2014.

[162] D. E. Olivares, C. A. Cañizares, and M. Kazerani, "A centralized energy management system for isolated microgrids," *IEEE Transactions on smart grid*, vol. 5, no. 4, pp. 1864–1875, 2014.

[163] A. Rabiee, A. Soroudi, and A. Keane, "Risk-averse preventive voltage control of ac/dc power systems including wind power generation," *IEEE Transactions on Sustainable Energy*, vol. 6, no. 4, pp. 1494–1505, 2015.

[164] G. S. Georgiou, P. Christodoulides, and S. A. Kalogirou, "Real-time energy convex optimization, via electrical storage, in buildings–a review," *Renewable energy*, 2019.

[165] R. A. Jabr, R. Singh, and B. C. Pal, "Minimum loss network reconfiguration using mixed-integer convex programming," *IEEE Transactions on Power systems*, vol. 27, no. 2, pp. 1106–1115, 2012.

[166] M. Chakravorty and D. Das, "Voltage stability analysis of radial distribution networks," *International Journal of Electrical Power & Energy Systems*, vol. 23, no. 2, pp. 129–135, 2001.

[167] MOSEK, "The mosek optimization tools version 10," https://www.mosek.com/.

[168] R. A. Jabr, "Radial distribution load flow using conic programming," *IEEE transactions on power systems*, vol. 21, no. 3, pp. 1458–1459, 2006.

[169] S. Tripathy, G. D. Prasad, O. Malik, and G. Hope, "Load-flow solutions for ill-conditioned power systems by a newton-like method," *IEEE Transactions on Power apparatus and Systems*, no. 10, pp. 3648–3657, 1982.

[170] R. Cespedes, "New method for the analysis of distribution networks," *IEEE Transactions on Power Delivery*, vol. 5, no. 1, pp. 391–396, 1990.

[171] M. Farrokhabadi, C. A. Cañizares, and K. Bhattacharya, "Unit commitment for isolated microgrids considering frequency control," *IEEE Transactions on Smart Grid*, vol. 9, no. 4, pp. 3270–3280, 2016.

[172] D. M. Ward, "The effect of weather on grid systems and the reliability of electricity supply," *Climatic Change*, vol. 121, no. 1, pp. 103–113, 2013.

[173] M. Kendon, "Storm malik and storm corrie, january 2022," https://www.metoffice.gov.uk/binaries/content/assets/metofficegovuk/pdf/weather/learn-about/uk-past-events/interesting/2022/2022_01_storms_malik_corrie.pdf, 2022.

[174] G. McClure, S. Langlois, and J. Rogier, "Understanding how overhead lines respond to localized high intensity wind storms," in *Structures Congress 2008: Crossing Borders*, pp. 1–10, 2008.

[175] Z. Li, S. Jazebi, and F. De Leon, "Determination of the optimal switching frequency for distribution system reconfiguration," *IEEE Transactions on Power Delivery*, vol. 32, no. 4, pp. 2060–2069, 2016.

[176] A. Kavousi-Fard, A. Zare, and A. Khodaei, "Effective dynamic scheduling of reconfigurable microgrids," *IEEE Transactions on Power Systems*, vol. 33, no. 5, pp. 5519–5530, 2018.

[177] N. G. Paterakis, A. Mazza, S. F. Santos, O. Erdinç, G. Chicco, A. G. Bakirtzis, and J. P. Catalão, "Multi-objective reconfiguration of radial distribution systems using reliability indices," *IEEE Transactions on Power Systems*, vol. 31, no. 2, pp. 1048–1062, 2015.